2011

Role of Vascular Endothelial Growth Factor, Placental Growth Factor and Cytokines on Outer Blood Retinal Barrier Breakdown.

Sangeetha Sukumaran
Technological University Dublin

Role of Vascular Endothelial Growth Factor, Placental Growth Factor and Cytokines on outer Blood Retinal Barrier breakdown

Sangeetha V Sukumaran

BSc. (Hons) Biochemistry, Molecular Biology and Biotechnology

School of Biological Sciences

Dublin Institute of Technology

Republic of Ireland

Thesis submitted in fulfilment of the requirements for the degree of

MPhil in Biochemistry

Supervisors

Dr. Brenda Brankin, Dr. Gwilym Williams

Submitted: July 2011

Declaration

I certify that this thesis, which I now submit for examination for the award of M.Phil is entirely my own work and has not been taken from the work of others save and to the extent that such work has been cited and acknowledged within the text of my work.

This thesis was prepared according to the regulations for postgraduate study by research of the Dublin Institute of Technology and has not been submitted in whole or in part for an award in any other Institute or University.

The work reported on in this thesis confirms to the principles and requirements of the Institute's guidelines for ethics in research.

The Institute has permission to keep, to lend or to copy this thesis in whole or in part, on condition that any such use of the material of the thesis be duly acknowledged.

Signature: Date:

Abstract

The Blood Retinal Barrier is composed of an inner BRB (iBRB) and outer BRB (oBRB). The iBRB is formed by retinal microvascular endothelial cells. The oBRB is formed by a monolayer of Retinal Pigment Epithelial (RPE) cells which lines and supports the functions of the photoreceptor layer. The tight junctions in the oBRB regulate ion and macromolecular transport along the paracellular layer. Neovascular Age Related Macular Degeneration (ARMD) is associated with alterations of the oBRB. Vascular Endothelial Growth Factor (VEGF) levels are high in neovascular ARMD and may promote oBRB breakdown. Low grade inflammation also plays a role in ARMD with infiltration of the BRB by macrophages and lymphocytes. Inflammation induced accumulation of macrophages, followed by secretion of pro-inflammatory cytokines Tumour necrosis factor – α (TNF- α) or Interleukin-1β (IL-1β), may affect oBRB function.

The aim of this thesis was to investigate the effect of the VEGF family of growth factors and cytokines TNF- α and IL-1β on oBRB function. The human RPE line ARPE-19 was employed as an *in vitro* model of the oBRB. Two-Dimensional gel electrophoresis was employed to study the effect of growth factors on the RPE proteome. The barrier properties of the oBRB were evaluated by expression of the TJ proteins occludin or Zo-1, or claudins-1, 2, 3 and 4, determined by western blotting analysis. Claudins 2, 3 and 4 were found to be significantly up-regulated by TNF-α, while interleukin 1 β-treated RPE showed increased expression of Claudins 1 and 3.

Immunoflourescence imaging showed junctional loss of occludin and ZO-1 in VEGF, TNF-α and IL-1β treated RPE. Placental growth factor (PlGF), a member of the VEGF family, has been found to be produced by hypoxia-stimulated RPE, and treatment with PlGF was shown to cause a disruption of junctional integrity of occludin in RPE. Cytokine induced regulation of Zo-1, occludin and claudins may lead to oBRB breakdown in ARMD, affecting photoreceptor function and leading to vision loss.

These findings will help in identifying inflammatory mediators important in the pathogenesis of ARMD, and molecular targets for control of ARMD related inflammation and disease progression.

Acknowledgement

Many people helped me in completing this degree. First and foremost, I would like to express my profound gratitude to Dr. Brenda Brankin for all her invaluable support, supervision and timely feedbacks she gave me, which enabled me to progress in my research and successfully complete this project and Dr. Gwilym Williams for his feedbacks and comments on this research work. My heartfelt thanks to both my supervisors for their patience and helping me write my thesis.

I would like to thank Dr. Mary Hunt, assistant Department head (School of Biological Sciences) for her continuous encouragement and advice. I specially thank Dr. John Kearney for his help with statistical analysis of data collected for this project. I would also like to thank Dr. Louis Armstrong, Head of Dept. (School of Biological Sciences) for this research opportunity.

I thank Fighting Blindness for funding this project.

To all the technicians and staff in School of Biological Sciences and School of Chemistry.

To all my colleagues at Lab 230 and my friends outside of DIT for their support and continued encouragement.

To my family

1-D	One Dimensional
2-D	Two Dimensional
AGE	Advanced Glycation End-products
AJ	Adherens Junction
AMD / ARMD	Age Related Macular Degeneration
ANOVA	Analysis of Variations
BBB	Blood Brain Barrier
BCIP / NBT	5-bromo 4-chloro 3'-indoyl phosphate / nitro-blue tetrazolium
BRB	Blood Retinal Barrier
BRMEC	Bovine Retinal Micro-vascular Endothelial Cells
BSA	Bovine Serum Albumin
CLDN	Claudin
Da	Daltons
DAPI	4',6-di amidino-2-phenyl indole
DR	Diabetic Retinopathy
DTT	Dithiothreitol
FITC	Flourescein iso-thio cyanate
GuK	Guanylate Kinase
HaCaT	Human keratinocytes
HRP	Horse Radish Peroxidase
iBRB	Inner Blood Retinal Barrier
IFN-γ	Interferon gamma
IL-1β	Interleukin – one Beta
IPG	Immobilized pH gradients

KDa	Kilo Daltons
MAGUK	Membrane Associated Guanylate Kinase
MCP-1	Monocyte Chemotactic protein one
MDCK	Madine Darby Canine Kidney
MHC	Major Histocompatibility Complex
mRNA	Messenger Ribo nucleic acid
NPDR	Non-proliferative Diabetic Retinopathy
NRK	Normal Rat Kidney
oBRB	Outer Blood Retinal Barrier
PBS	Phosphate Buffered Saline
PDGF	Platelet Derived Growth Factor
PDR	Proliferative Diabetic Retinopathy
PEDF	Pigment Epithelium Derived Factor
PlGF	Placental Growth Factor
PVR	Proliferative Vitreo Retinopathy
RAGE	Receptor for AGEs
RMEC	Retinal Microvascular Endothelial Cells
RP	Retinitis Pigmentosa
RPE	Retinal Pigment Epithelium
SDS-PAGE	Sodium Dodecyl Sulphate Poly Acrylamide Gel Electrophoresis
SEM	Standard Error of Mean
TBS	Tris Buffered Saline
TEER	Trans Epithelial Electrical Resistance
TJ	Tight Junction

TNF-α	Tumour Necrosis Factor – Alpha
TRITC	Tetramethyl Rhodamine Iso-thio cyanate
VEGF	Vasculo Endothelial Growth Factor
WHO	World Health Organization
ZO	Zonula Occludens

Chapter 1

Introduction

The Blood Retinal barrier (BRB) located in the eye provides a selective barrier for regulation of the retinal milieu and for maintaining the specialised environment of the neural retina. The concept of a retinal barrier impermeable to dyes, with possible structural similarity to the Blood Brain Barrier (BBB), was proposed as early as 1913 by Schnaudigal (Cunha-Vaz *et al* 1966, Schnaudigal O.V 1913). Unlike BBB, the BRB is comprised of two layers – inner and outer. The inner layer (iBRB) is composed of the Retinal Microvascular Endothelial cells (RMECs) and the outer layer (oBRB) comprises the Retinal Pigment Epithelial (RPE) cells. Together, the BRB layers regulate the passage of ions, water and protein in and out of the retina, in response to the varying metabolic demands of the retina (Cunha-Vaz *et al*., 2010). The barrier property of the BRB is due to the presence of 'tight junctions' (TJs) which seal the paracellular space from the outer environment. The TJs are formed by interaction between membrane proteins in the adjacent cells in the BRB.

The oBRB regulates permeability of molecules from choroid into the retinal microenvironment. RMEC and RPE cells secrete cytokines, growth factors and other key molecules essential for maintenance of retinal homeostasis (Holtkamp *et al.* 1999). The integrity of the BRB is critical to normal visual function (Gardner *et al*, 1999). Abnormal permeability change or breakdown of BRB is the hallmark of several pathological conditions that affect the neural retina.

1.1. Inner Blood Retinal Barrier

The iBRB is structurally similar to the Blood Brain Barrier (BBB) with the RMECs surrounded by retinal pericytes and macroglial cells (Hosoya and Tomi, 2005). The RMECs

form complex TJs which functions to prevent the free diffusion of substances between circulating blood and neural retina (Hosoya and Tachikawa, 2009). The selectively permeable TJs in RMECs ensure correctly regulated hemodynamics and delivery of oxygen and metabolites (Pournaras *et al*, 2008). Breakdown of the iBRB is the major cause of vision loss in ocular disorders such as diabetic retinopathy, sickle cell disease and cystoid macular edema (Brankin *et al*. 2005, Vinores *et al*. 1999). Retinal vascular changes resulting in increased retinal vascular permeability represent a major pathological change in diabetic retinopathy (Ma *et al.* 2005).

1.2 Outer Blood Retinal Barrier

The Outer Blood Retinal Barrier (oBRB) is formed by a monolayer of RPE cells which lies between the neural retina and Bruch's membrane, separating it from the choroid. The oBRB faces the photoreceptor layer of the eye on its apical side. The Bruch's membrane separates the RPE from the chorio-capillaries on the basolateral side. The long apical microvilli of RPE cells surround the light sensitive outer segments of the photoreceptor cells establishing a complex of close structural interaction (Strauss, 2005). The oBRB regulates passage of ions and macromolecules into the photoreceptor layer and transports water and metabolic end products from the sub-retinal space to blood. The RPE layer also assists in development of retinal structures by secreting a host of growth factors required for endothelial and photoreceptor cell differentiation (Strauss, 2005, Adamis *et al*. 1993). Breakdown of the oBRB in conditions such as Age Related Macular Degeneration (ARMD) and Retinitis Pigmentosa leads to degradation of the photoreceptor cell layer (Cunha-Vaz *et al*. 2010, Vinores *et al*. 1995).

1.3 Retinal Pigment Epithelium

The Retinal Pigment Epithelium (RPE) is a highly specialized tissue that serves an indispensable and multifunctional role within the eye (Strauss 2005). It comprises a monolayer of pigmented cells lining the basal surface of the photoreceptor layer of the neural retina (Fig. 1.1). Apart from forming the oBRB, the RPE cells also regulate the functioning of the neural retina. RPE is required for transportation of nutrients and ions between the retina and choriocapillaries (Kevany and Palczewski, 2010, Rizzolo *et al* 2007(a)). The RPE cells play an important role in the visual cycle by regenerating 11-cis-retinal from trans-retinal (Strauss 2005). The reduction in delivery of retinal to photoreceptors has been found to cause photoreceptor dystrophy (Seeliger *et al*, 1999). The photoreceptor cells require a delicate balance of proteins, lipids and metabolites in order to function properly. Disturbance of this balance leads to retinal degeneration (Strauss 2005). The photoreceptor cells undergo a daily renewal process in order to prevent the toxic effects of accumulated photo-oxidative products, by shedding 10% of their volume in the form of discs (Kevany and Palczewski, 2010). These discs are phagocytosed by RPE cells. Breakdown in the ability of the RPE to degrade the photo-oxidative products is believed to be the underlining cause for degenerative disorders such as ARMD (Nandrot *et al*, 2004) and Usher's syndrome (Fig 1.1).

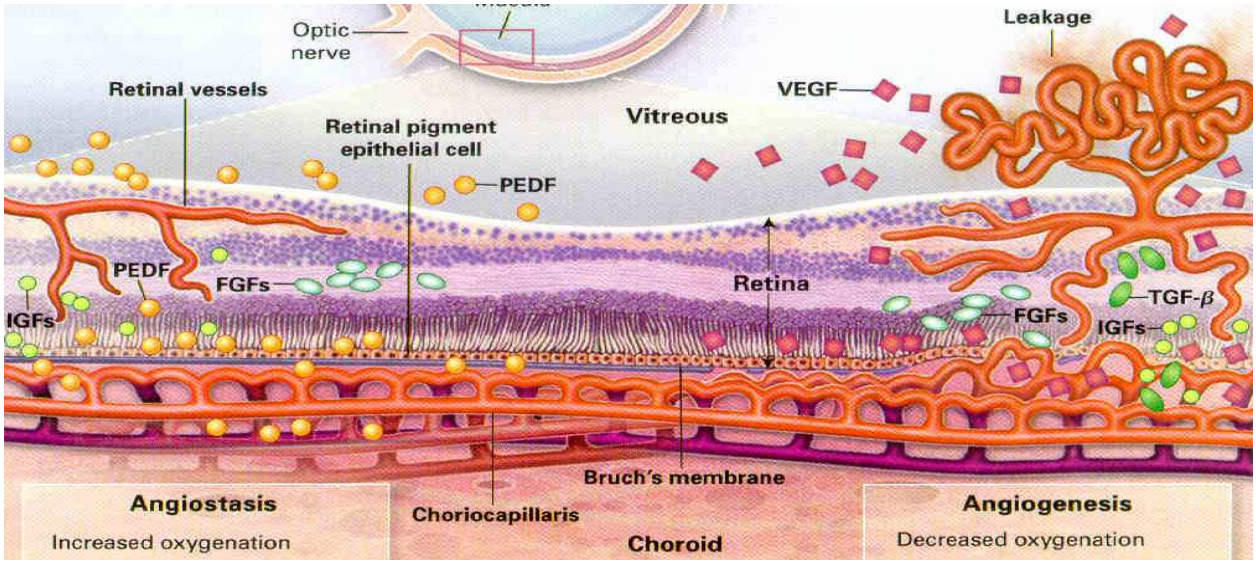

Fig: 1.1 Photoegulatory function of RPE barrier (Image provided by Dr. Brenda Brankin)

1.4 Tight Junctions

The interaction between protein complexes of adjacent cells gives rise to two types of membrane barrier junctions – Tight Junctions (TJ) and Adherens Junctions (AJ). Among other components, TJs are required in the oBRB to regulate the trans-epithelial movement of ions and other molecules into the paracellular space (Balda and Matter, 2000). TJs provide a continuous seal around the apical region of the lateral membranes of adjacent cells (Citi, 1993). When viewed under the microscope using freeze fracture electron microscopy, TJs appear as a 'necklace' of strands encircling the cells (Rizzolo *et al*, 2007(b)). The TJs lie on the apical side of the cells, close to AJs which bind the adjacent cells in the monolayer (Rizzolo *et al*., 2007 (a)). TJs constitute a barrier both to the passage of molecules and ions through the epithelium, and also to the free movement of proteins and lipids between the apical and basolateral domains of the epithelium (González-Mariscal *et al*., 2003). A decrease in epithelial transport of chloride ions has been reported to cause retinal degeneration (Jentsch *et al*, 2002). However, their function is not merely limited to their barrier properties. TJs play an important role in vesicle targeting, cytoskeletal dynamics proliferation and

transcription signalling while also defining cell polarity (Anderson *et al*., 2004, Tsukita *et al*., 2001).

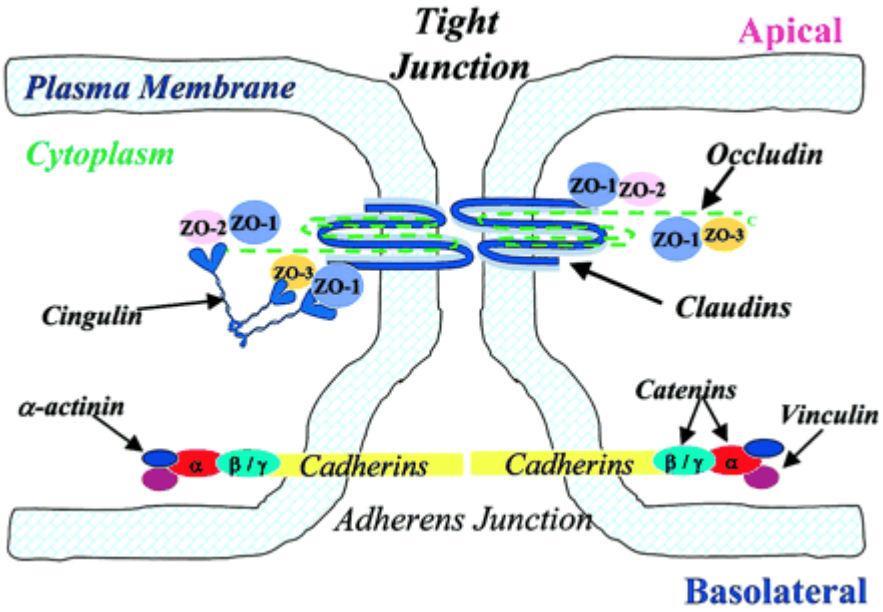

Fig 1.2 Illustration showing positioning of tight junctions and adherens junctions (Source: Mark and Davis, 2002)

Paracellular transport can be achieved through TJs either through membrane pores formed by transmembrane proteins, or via breakdown of TJs, as in the case of pathological conditions (Anderson and Van Itallie, 2008). The charge-selective claudin-based pores in TJs are about 0.4nm in radius and a second non charge selective transport mechanism is achieved through the large discontinuities in the barrier (Anderson and Van Itallie, 2009).

1.5 Tight junction proteins

TJ barriers in the RPE layer are formed by interaction between several key membrane proteins. The TJs have a surprisingly complex protein composition compared to other cell – cell junctions and nearly 40 different proteins associated with TJs have been identified so far

(Anderson and Van Itallie 2009; Yamazaki *et al*., 2008, González-Mariscal *et al*. 2003). The earliest TJ associated proteins discovered were the Zonula Occludens (Zo) proteins (Franke, 2009, Balda and Matter 1998). They were later identified as proteins associated with the cytoplasmic domain of claudins (CLDN) and occludin. Occludin was discovered later by Furuse *et al* (1993) and was shown to be able to create tight junction-like assemblies in normal rat kidney cells (Van Itallie and Anderson 1997). However, it was later discovered that there are other tight junction molecules apart from occludin, as intact TJs have been discovered in occludin -/- mice (Franke 2009, Saitou *et al* 2000). These mice survived to adulthood, although with several abnormalities (Saitou *et al*, 2000). Further research led to the identification of two 22kDa proteins which immuno-localized at TJs of living cells. These proteins were later named claudin 1 and 2. Claudins were able to form new TJs when the cDNA was transfected into mouse L fibroblast cells which lacked TJs completely (Franke 2009, Furuse and Tsukita 2006, Furuse *et al*, 1998).

With the discovery of more members of the claudin family, it was clear that the TJs were more complex structures than they initially appeared to be. Co-culture of mouse L fibroblast cells expressing claudin 1, 2 or 3 revealed that heterotypic TJs were formed by binding of claudin 1/3 or claudin 2/3, but not claudin 1/2 (Furuse, 1999). Occludin and Tricellulin are closely associated with claudins and modulate TJ strand formation (Furuse, 2010).

1.6 Occludin

Occludin was the first TJ protein to be identified and was isolated from chick liver tissue (Furuse *et al*, 1993). It is a 65kDa tetraspannin protein found localized almost exclusively in

tight junctions (Feldman *et al*. 2005, Tsukita and Furuse 1998). The tertiary structure of Occludin is made up of four transmembrane domains - a long C-terminal cytoplasmic domain; a short N-terminal cytoplasmic domain; two extracellular loops; and one intracellular turn (Harhaj and Antonetti 2004, Saitou *et al*, 2000) (Fig 1.2). The first extracellular loop, consisting of a high percentage of 60% tyrosine and glycine, residues is characteristic of occludin, although the exact physiological function remains to be elucidated (Furuse, 2010). The cytoplasmic carboxy-terminal of occludin interacts with Zo-1, establishing a link with the actin cytoskeleton (Fanning *et al*, 1998).

Through immunoflourescence and immunoelectron microscopy techniques it was established that Occludin is exclusively located at the TJs of epithelial and endothelial cells (Blasig *et al* 2011, McCarthy *et al* 1996, *Furuse et al* 1993). The expression of occludin correlates with barrier properties of the tissue (Harhaj and Antonetti, 2004). Very high expression of occludin in tissues such as brain endothelium and RPE results in formation of a very tight barrier. Over-expression of occludin in mouse L fibroblasts which lack TJs and AJs, caused localization of occludin into cell-cell contacts between adjacent cells, although it did not form fully developed strand-like TJs as observed in wild type (Furuse *et al*, 1998).

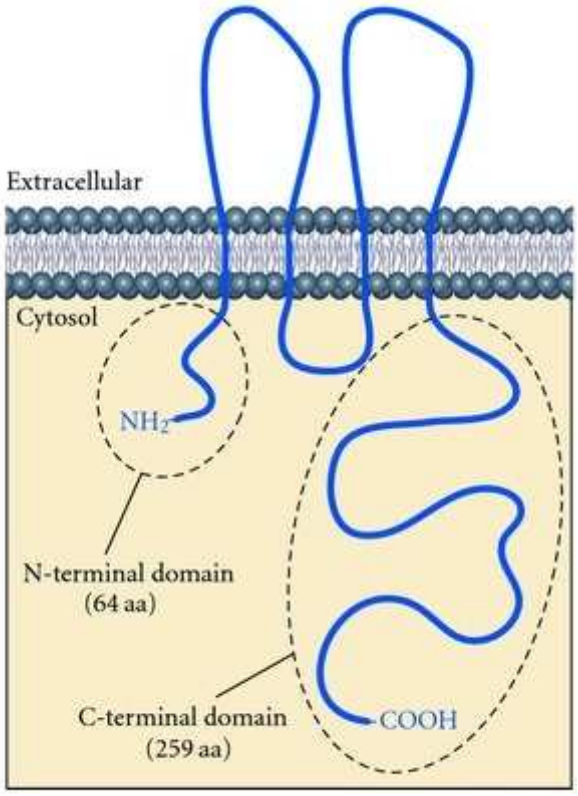

Fig: 1.3 – Schematic diagram of transmembrane protein Occludin (Dörfel and Huber, 2012)

Sequencing studies have shown that the membrane topology of Occludin is well conserved across species (Ando-Akatsuka *et al*, 1996). Occludin spans the plasma membrane of endothelial cells of the BRB. The extracellular domain of Occludin binds to another occludin molecule on the adjacent cell to form the tight junction responsible for permeability barrier (Jin *et al* 2002). The cytoplasmic terminal of Occludin associates with Zo-1 and helps in membrane localization of the protein while the second extracellular domain helps in stabilizing Occludin in the tight junction (Medina *et al* 2000)

Occludin is naturally present in TJs in multicellular organisms and plays a role in maintaining the structural integrity of TJs. Over-expression of occludin in MDCK cells has been found to increase the trans-epithelial electrical resistance (TEER) (Tsukita and Furuse 1998, Balda *et*

al. 1996). An Occludin knock-out study performed by Saitou *et al* (1998) on embryonic stem cells showed the presence of intact tight junctions, structurally similar to that seen in wild type embryonic stem cells. This indicated that Occludin was not indispensable for maintenance of TJ integrity, and that other tight junction membrane proteins were able to compensate for lack of Occludin expression in tight junctions. However, Occludin -/- mice displayed several abnormalities, including testicular atrophy, gastric hyperplasia, thinning of compact bone and calcium deposits in the brain (Saitou *et al*., 2000). This suggested that the role of Occludin and TJs cannot be defined as being merely of structural nature. A knock-out study performed by Schulzke *et al* (2005) showed that the permeability of intestinal epithelia, measured using TEER and tests of barrier function, did not significantly alter from that of the wild type. However, the glandular structure of gastric corpus mucosa in occludin -/- mice exhibited a complete loss of parietal cells, and also mucus cell hyperplasia, resulting in a loss of ability to secrete acid. This demonstrated that occludin was essential for differentiation of gastric epithelia.

The role of Occludin in the formation of tight junctions has been investigated widely. When occludin expression was induced in NRK (Normal Rat Kidney) cells and Rat-1 fibroblasts, which lack endogenous occludin and tight junctions, it co-localized with Zo-1 to form cell-cell adherens-like junctions (Van Itallie and Anderson, 1997).

1.7 The Claudin Family of Tight Junction Proteins

Among the several molecular components of TJs now identified, the claudins, a family of at least 24 different proteins, are now believed to comprise the backbone of TJs (Overgaard *et al*

2011, Lal-Nag and Morin, 2009, Furuse and Tsukita, 2006, Firth 2002). Claudins are tetra-spanning transmembrane proteins of molecular weight range between 20-25kDa, with two extracellular and one intracellular loop. They have been broadly classified into two groups based on the degree of sequence similarity – "classic claudins" which include claudins 1 to 10, 14, 15, 17 and 19 and "non-classic claudins" which include claudins 11 to 13, 16, 18 and 20 to 24 (Krause *et al*, 2009). Of these, 23 have been identified to have functional significance in humans (Katoh and Katoh, 2003). Occludin was the first protein identified to localize at TJs (Tsukita *et al*., 2008). Until the discovery of Claudins, occludin was considered to be solely involved in TJ formation. However, targeted disruption of the occludin gene in embryonic stem cells did not prevent formation of intact TJs (Saitou *et al*., 1998), which indicated involvement of other proteins in barrier formation. This led to the discovery of two membrane proteins of ~22kDa weight, which bore no sequence similarity to Occludin. The first two Claudins identified - Claudin-1 and Claudin-2 - were isolated from fractions of chick liver (Harhaj and Antonetti 2004, Furuse *et al*., 1998). The intrinsic ability of Claudins to form TJs was observed when their expression in fibroblasts was found to induce the formation of singular TJ strands in the otherwise non-adherent cell line (Furuse *et al*., 1998 (a)).

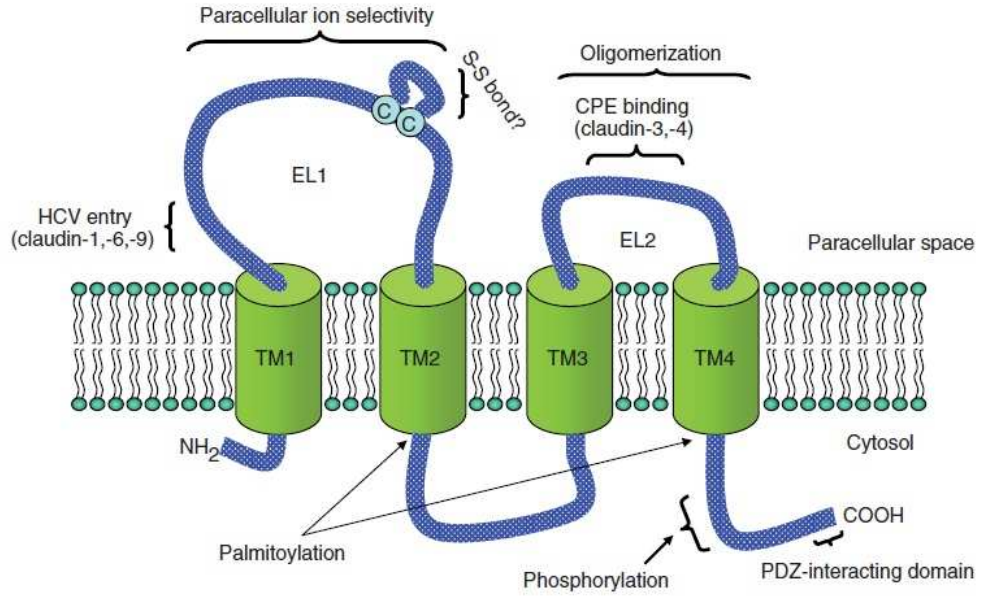

Fig 1.4 Schematic representation of Claudin Monomer showing four transmembrane domains (TM1, 2, 3 and 4), two extracellular loops and one intracellular turn. (Source: Lal-Nag and Morin 2009)

Claudins are integral membrane proteins containing four hydrophobic transmembrane domains and two extracellular loops (Fig 1.3) (Gupta and Ryan 2010). The carboxy- and amino- terminal domains are cytoplasmic and interact with Zo-1 in the cytoplasm. The amino terminus is relatively short while the carboxy-terminus is variable in length in claudins (Lal-Nag and Morin, 2009). The first extracellular loop has several charged amino acids and is thought to influence paracellular charge selectivity (Lal-Nag and Morin 2009, Colegio *et al* 2002). Two highly conserved cysteine residues in the first extracellular loop (Fig 1.3) are thought to play an important role in protein stability by forming intramolecular disulphide bonds (Angelow and Yu 2009, Angelow, Ahlstrom and Yu, 2008). Phosphorylation of serine or threonine residues in the carboxy- terminal of claudins may play a role in membrane localization of claudins to form TJs (Furuse, 2010).

Claudins 1 and 2 have been identified as being most crucial for formation of the tight junctional barrier (Furuse *et al.* 1998(b)). Introduction of claudin-1 and claudin-2 genes into TJ-lacking fibroblasts caused the formation of a network of TJ like strands very similar to epithelial and endothelial TJs (Furuse M *et al* 1998). Co-expression of different claudins into fibroblasts revealed that TJ strands are comprised of mosaics of different claudins, forming homotypic and heterotypic interactions between cells and homomeric and heteromeric complexes in individual cells, although their compatibility is dependant on the right combination of claudins (Furuse, 2010).

Other *in vivo* functions of claudins are being studied using gene knock-outs, over- or under-expression in epithelial cells, and by the study of human disease phenotypes resulting from claudin mutations (Turksen and Troy 2011, Angelow *et al.* 2008). Other members of the claudin family have been identified to have several other functions including paracellular transport (Will *et al* 2008). For instance, claudin-16, also known as paracellin-1, is important for electrolyte handling in kidney, apart from playing a structural role in the organ (Weber *et al.* 2001, Simon *et al*. 1999). Key functions of claudins identified to date, along with their functions are shown in Table 1.1.

Table 1.1 – Overview of properties, distribution, function and pathologies of claudins

Claudin	Size (Da)	Key Points
Claudin - 1	22744	Plays a key role in epidermal TJ barrier formation along with claudin-2. Co-localizes with occludin to forms a permeability barrier. Important in BBB and BRB formation.
Claudin – 2	24549	Forms discontinuous strands when expressed individually. Co-expressed with claudin-1 and plays an important role in embryonic development and TJ formation. Also functions as cationic pore protein and decreases TEER when over-expressed in SMIE cells.
Claudin – 3	23319	Over-expressed in ovarian cancers along with claudin-4.
Claudin – 4	22077	Directly interacts with TJ proteins Zo-1, 2 and 3. Expressed in many foetal and adult tissues, predominantly in intestine, kidney and lung. Claudin-4 is an integral membrane protein and forms an important component of TJs. Over-expression leads to increase in TEER. Over-expressed in several carcinomas, except in pancreas. Cardiovascular and cytoskeletal abnormalities implicated due to claudin-4 gene deletion in Williams-Beuren Syndrome.
Claudin – 5	23147	Primarily found in human endothelial TJs and colonic epithelium. Co-localizes with occludin and assists in TJ sealing. Plays a significant role in BBB formation.
Claudin – 6	23292	Present in embryonic kidney, but disappears in adult kidney. Identified as a biomarker for abnormal skin conditions.
Claudin – 7	22390	Biomarker for breast and neck carcinomas. Acts as a channel protein for paracellular Na^+ ion transport. Found in nephrons, colonic and tonsillar epithelia.
Claudin – 8	24845	Found in colonic epithelia and kidney. Found to reduce paracellular cation permeability. Claudin-8 is down-regulated in Crohn's disease.
Claudin – 9	22848	Found in inner ear and embryonic kidney. Thought to play a role in paracellular permeability changes in embryonic epithelia.
Claudin – 10	24251 (a) 24488 (b)	Two claudin-10 variants transcribed from different start sites. Different amino termini. Preferential paracellular permeation of anions (a) or cations (b)
Claudin – 11	21993	Endocochlear potential regulation. Found to reduce paracellular cation permeability in MDCK. Down-regulation found to cause deafness, male sterility and hind limb weakness in mice.
Claudin – 12	27110	Found in inner ear, brain endothelium and colon
Claudin – 13	Absent in humans.	

Claudin – 14	25699	Found in inner ear and sensory epithelium of organ of corti in mammalian ear. Down-regulation causes non-syndromic deafness and degeneration of cochleal hair cells.
Claudin – 15	24356	Found in kidney endothelial cells and intestine. Found to increase cation permeability.
Claudin – 16	33836	Primarily found in kidneys. N terminal is 73 amino acids long.
Claudin – 17	24603	mRNA identified in human kidney and taste receptor cells.
Claudin – 18	27856 27720	Two variants formed by alternate transcription start sites. Different amino termini. Down-regulated in gastric cancer.
Claudin – 19	23229 22076	Two variants formed by alternative splicing. Different carboxy termini. Found in kidney and retinal cells. Up-regulation increases TEER, reduces cation permeability. Adversely affects nerve conduction when down-regulated.
Claudin – 20	23515	Found in skin.
Claudin – 21	25393	Down-regulated in chondrosarcoma, liver cancer.
Claudin – 22	25509	Found in human trachea. Down-regulated in breast cancer.
Claudin – 23	31915	The C-terminus is 111 amino acid long. Down-regulated in intestinal type gastric carcinomas.
Claudin – 24	22802	Gene identified. No expression or knockout studies found.

(Source: Gupta and Ryan 2010, Findley and Koval, 2009, Lal-Nag and Morin 2009, Furuse 2009, Florian *et al* 2003)

Biochemical diversity among members of the Claudin family underlies differences in TJ structure and function in different tissues and cell types (Van Itallie and Anderson, 2004). Individual cells express more than one Claudin protein. Studies show that claudins form the functional backbone of TJ pores and play a very active role in paracellular transport (Table 1.1). These properties may provide a route to therapeutic manipulation of TJ structure for delivery of pharmacological agents.

1.8 Zonula occludens (Zo) proteins

The Zo proteins are a group of high density proteins which interact with the cytoplasmic terminals of occludin and claudins (Anderson and Van itallie, 1995). Zo proteins are best characterized among the "cytoplasmic plaque proteins" in the tight junctional complex. Three Zo proteins have been identified and named as Zo-1, Zo-2 and Zo-3. They belong to a family of Membrane Associated Guanylate Kinases (MAGUKs) (Mitic and Anderson 1998, Anderson *et al*, 1995). In addition to the core domain structure consisting of PDZ, SH3 and GuK domains characteristic of MAGUKs, the Zo proteins have a distinctive carboxy-terminal with splicing domains, acidic- and proline-rich regions (González-Mariscal *et al*. 2000).

Among the Zo proteins, Zo-1 exists in two isoforms, formed by alternative splicing, depending on the presence or absence of an 80 amino acid domain termed **α**. Zo-1(**α**+) is found in most epithelial cells and Zo-1(**α**-) is found in endothelial cells and certain highly specialized epithelial cells (Van Itallie and Anderson, 1998). Although this helps in molecular distinction in TJs, the actual function of the **α** domain remains unclear.

Zo-1 and Zo-2 proteins play a pivotal role in the final establishment of belt-like adherens and tight junctions (Ikenouchi *et al*, 2007). The N-terminus of Zo proteins associate with cytoplasmic termini of occludin (Fanning *et al*., 1998) and Claudins, stabilizing their positioning in the tight junctions. The C-terminus of Zo proteins bind to actin, and thus act as scaffolds binding the tight junction proteins to the cytoskeleton (Umeda *et al*., 2006, Fanning

et al., 1998). Zo-3 shows epithelial-specific tight junction localization in a Zo-1/2-dependant fashion (Tsukita *et al*., 2009, Inoko *et al*, 2003).

Functional significance of Zo-1 in TJ formation was analyzed by ablating Zo-1 expression through RNA interference or deletion of the gene by homologous recombination. Absence of Zo-1 did not prevent formation of the TJ barrier, although it delayed its formation (McNeil *et al*., 2006, Umeda *et al*., 2004). Complete absence of Zo-1, 2 and 3 proteins in mouse EpH4 cells resulted in complete elimination of TJs on confluence (Umeda *et al*., 2006) although the cells were well polarized.

1.9 Adherens junctions

The classical cadherins mediate specific adhesion at intercellular adherens junctions. The adherens junctions (AJ) are formed by homophilic cadherin interactions in adjacent cells. AJs play a significant role in cell polarization and differentiation of epithelial cells, and calcium-dependent cadherin-based adherens junctions organise microfilaments to the plasma membrane in polarized cells (Green 2010). The carboxy-terminal of cadherins in AJs binds cytoplasmically to P120 and β-catenin (Shapiro and Weis, 2009) which in turn bind to the actin cytoskeleton through α-catenin (Meng and Takeichi, 2009).

1.10 Ocular diseases and abnormal RPE

The TJ, which is the most apical component of the junctional complex, represents the anatomic substrate of the outer blood retinal barrier (Jin *et al*., 2002). Disruption of transport

mechanisms of the RPE leads to photoreceptor degeneration. For instance, disruption of epithelial chloride ion transport leads to loss of transepithelial potential in RPE. This results in an inability to extrude lactic acid from photoreceptors, leading to metabolic stress and eventual breakdown of the photoreceptor layer (Bosl *et al*., 2001). The RPE layer plays a major supportive role in maintaining the delicate metabolic balance required for functioning of photoreceptor cells (Strauss, 2005).

1.10.1 Age Related Macular Degeneration (AMD)

AMD is the leading cause of blindness worldwide, in the population above 50 years of age (Chappelow and Kaiser 2008, Friedman *et al* 2004, Klein *et al*, 2004). A recent report by WHO in 2009 lists AMD as one of the primary causes for vision loss worldwide. AMD is a multifactorial disease which affects the RPE-choroid interface in the macula (Strunnikova *et al* 2010).

The ocular structures involved in AMD are photoreceptor cells, neurons in the outer retina, the RPE, Bruch's membrane and choriocapillaries (Bird 2010). Metabolic interdependency of these tissues increases the risk of vision loss if any one of these structures is affected. AMD is characterized by degenerative changes in the macula, therefore leading to central vision loss and loss of visual acuity. A reduced capability to absorb light energy leads to the cascade of events leading to AMD (Strauss, 2005).

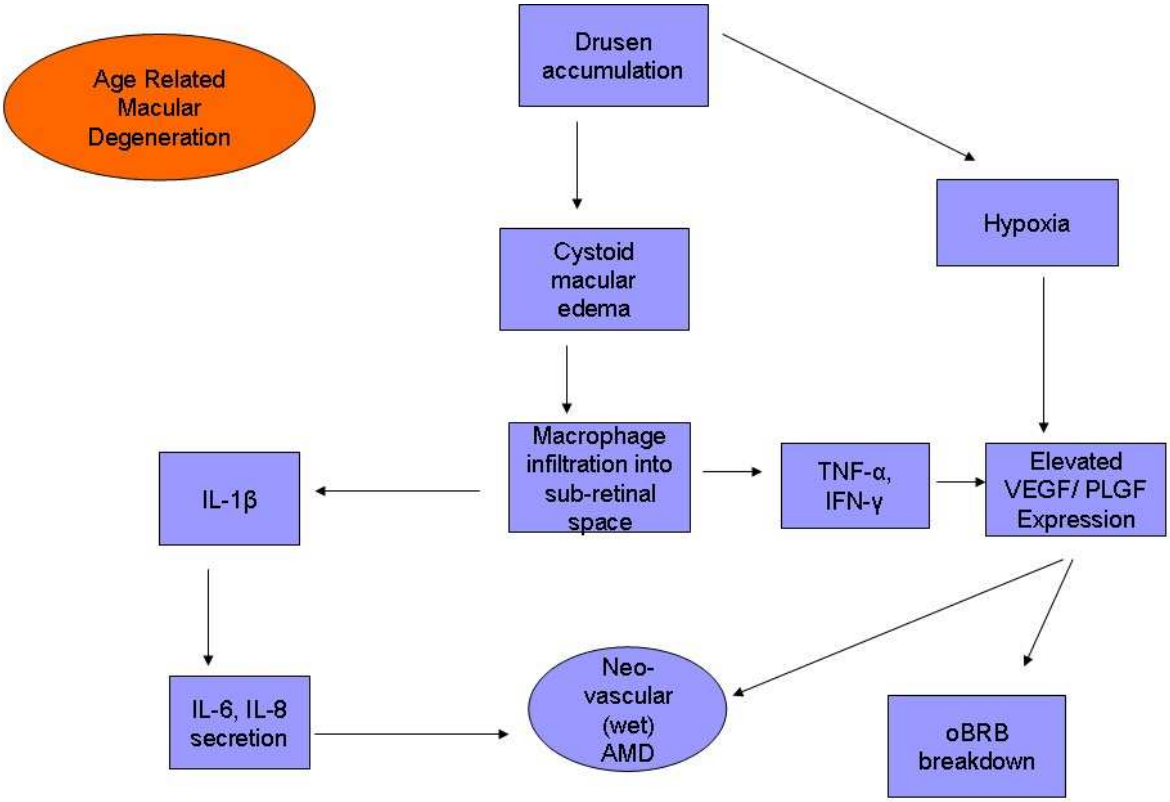

Fig 1.5 Development and Progression Pathway of AMD

Based on the progression of disease, AMD has been divided into 'dry' and 'wet' types (Fig 1.5). The earliest symptom and pathological feature of dry AMD is accumulation of photo-oxidative residue (drusen) beneath the RPE layer and inside the Bruch's membrane (Strauss 2005, Handa *et al* 1999, Docchio *et al*. 1991). A small amount of drusen is found in healthy individuals over the age of 50, but the presence of large or numerous drusen confers significant risk for AMD (Patel and Chan, 2008).

The presence of large and confluent drusen leads to inflammatory condition known as Cystoid Macular Edema (Fig 1.4). It also paves way for the establishment of large diffusion barriers between the RPE and choroid. This may lead to development of areas with reduced supply of oxygen and glucose (Strauss 2005, Frank 1997). Hypoxic stress thus induced leads to degeneration of photoreceptors in drusen-covered areas (Coleman *et al*, 2008). In a more

severe case, this stimulates hypoxia-induced secretion of VEGF, and suppression of PEDF secretion, leading to choroidal neovascularisation (Klein *et al*, 2004). Choroidal neovascularisation is the hallmark of wet AMD (Chappelow and Kaiser, 2008) and leads to an increase in intraocular pressure and may cause the newly formed capillaries to break (Fig 1.6). Intra-ocular bleeding is a major cause for vision loss in wet AMD (Strauss, 2005). Wet AMD is also known as 'exudative' or 'neovascular' AMD.

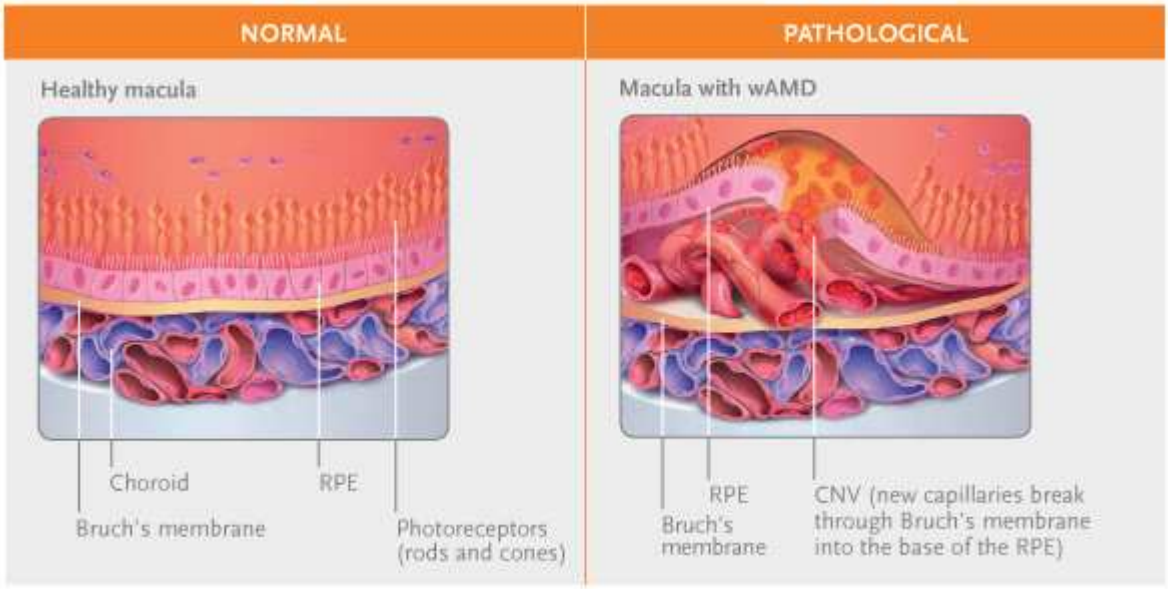

Fig 1.6 Healthy Macula versus macula with wet AMD (Source: Genentech)

VEGF-A over-expression is important for progression and development of AMD (Witmer *et al*., 2003). Therefore, control of VEGF and its receptors is looked at as an important therapeutic target for control of AMD.

1.10.2 Retinitis Pigmentosa

Retinitis Pigmentosa (RP) is a group of inherited genetic eye diseases characterized by gradual degeneration of the outer retinal layer leading to vision loss (Hamel 2007). It generally affects the peripheral vision with other complications such as macular edema

affecting central visual acuity (Sahel *et al*, 2010). RP may be inherited as an autosomal dominant, autosomal recessive, X-linked recessive or digenic traits (Wang *et al*. 2001, Humphries *et al*. 1990). RP is characterized by primary degeneration of rod photoreceptors and secondary degeneration of cone cells in the retina (Campbell *et al*, 2006(a)). The photoreceptor layer undergoes a constant renewal and sheds cytoskeletal protein, photo-oxidative residue and rhodopsin-rich 'discs' which are phagocytosed by the underlying RPE layer (Strauss, 2005). RP may involve gene mutations in RPE leading to impairment of its photoregulatory function, or mutations which cause dysfunction of rod cells (Farrar *et al*. 2002). Degeneration of rod outer segments leads to the presence of deposits of pigmented granules in the outer retina (Hamel 2009, Hamel 2007). A gene knockout study in mice involving targeted disruption of the Rhodopsin gene Rho (-/-) showed disruption of AJs in the outer retina, in 6 week old Rho (-/-) mice (Campbell *et al*. 2007).

Key therapeutic approaches for Retinitis Pigmentosa include using pluripotent stem cells to differentiate into functional ocular cells that can replace damaged RPE and/or photoreceptor cells (Rowland *et al*. 2011).

1.11 Diseases of iBRB – Diabetic Retinopathy (DR)

Diabetes leads to a wide array of complications including kidney failure, vascular disease, peripheral nerve degeneration and vision loss (Antonetti *et al* 1999). Diabetic retinopathy is the leading cause of blindness in the working age population in the USA causing 12000 to 24000 new cases of blindness every year (Whitmire *et al*. 2011, Klein *et al*. 2009). Increased vascular permeability leading to macular edema and endothelial cell proliferation is the

hallmark of DR (Mitamura *et al*, 2005). The underlying metabolic pathways leading to development of DR is not completely understood. However, causes attributed to the pathogenesis and progression of DR include chronic hyperglycemia (Whitmire *et al*, 2011), formation and accumulation of AGEs (Takeuchi *et al* 2010, Stitt, 2003) and oxidative stress (Frey and Antonetti, 2011).

The two stages of progression of DR are classified into "Non-Proliferative" (NPDR) and "Proliferative" (PDR). Microaneurysms develop in the retinal vasculature leading to retinal haemorrhages and fluid leakage in the retina. Development of macular edema leads to a reduction in functionality of RPE cells to remove fluid from the retina. NPDR is prevalent in patients suffering from type – II diabetes (Caldwell *et al*, 2005).

PDR is a more severe form of DR. Oxidative stress and increase in photo-oxidative reactive species leads to expression of Advanced Glycation End products (AGEs). RPE cells express active receptors (RAGE) for AGEs (Hammes *et al*, 1999) and express Vasculo Endothelial Growth Factor (VEGF) in response to AGE exposure (Lu *et al*, 1998). Retinal pericytes are reported to accumulate AGEs during diabetes (Stitt *et al*, 1997) which blocks retinal vessels thereby leading to hypoxic stress and apoptosis of retinal pericytes. Hypoxic stress and AGE-stimulated release of VEGF and related growth factors into the retina leads to angiogenesis and neovascularization in the retina (Okamoto *et al*, 2002). Neo-vascularisation progresses into the vitreous cavity towards the later stages of PDR. Newly formed blood vessels are weak and may break, allowing blood to leak out and cloud the vitreous and impair vision (Caldwell *et al*. 2005). Formation of fibrovascular tissue in advanced stages of PDR leads to retinal detachment and loss of vision in patients.

VEGF has been identified as a critical stimulus in the pathogenesis of macular edema in NPDR (Wolfensberger and Gregor, 2010, Karim and Tang, 2010). VEGF antagonists have hence received a great deal of interest in the treatment of DR.

Aims and Hypothesis

The blood brain barrier and the blood retinal barrier are immunologically privileged and depend on intact barriers to partition them from the systemic circulation (Padden *et al*., 2007, Brankin *et al*., 1995, Allen and Brankin, 1993). It has been previously reported that VEGF165 has a synergistic effect on iBRB permeability, both *in vitro* and *in vivo* (Brankin *et al*., 2005). VEGF165 significantly increased BRMEC paracellular permeability, and induced iBRB breakdown in C57/Bl6 mice which was demonstrated by an increase in Evans blue/albumin permeation at the BRB (Campbell *et al*., 2006, Brankin *et al*., 2005).

These findings of an increase in permeability of the iBRB by VEGF led us to speculate that VEGF may also modify the oBRB permeability properties. The oBRB is formed by the RPE cells which separate the outer layer of the neural retina from the capillaries of the choroid. The cardinal function of the RPE is to prevent fluid from choroidal vessels from entering the retina, and to control the flow of solutes and fluid from the choroidal vasculature into the outer retina. This strict control of fluid and solutes that cross the outer barrier is achieved by TJs at the RPE. Thus a breakdown in the oBRB may lead to an accumulation of fluid in the sub-retinal space, and to macular edema.

Studies carried out in conjunction with the iBRB, showed modulation of Zo-1 expression in an animal model of retinal degeneration, the Rho (-/-) knock-out mouse (Humphries *et al*, 1977). In this work, Brankin and colleagues found an up-regulation of Zo-1 in neural retinas of C-129 Rho(-/-) knockout mice compared to C-129 WT mice, associated with the retinal vasculature, and a loss of expression of Zo-1 at the Outer Limiting Membrane of the photoreceptors in Rho(-/-) (Campbell *et al*., 2007). In view of these previous reports, we wished to further extend the work in this project by investigating the effects of the VEGF family of growth factors on BRB function. PLGF is a member of the VEGF family and potentiates the activity of VEGF (Hollborn *et al*., 2006). Brankin and Stitt, have reported that PLGF induced phosphorylation of occludin on serine and tyrosine residues, and may modify the capacity of occludin to associate with Zo-1 at the BRB (Brankin and Stitt, 2003).

The proinflammatory cytokines, TNF-α and IL-1β have been found to affect BBB and iBRB permeability, and may promote choroid neovascularisation (Oh *et al*., 1999), which is a sight-threatening complication of macular diseases, including ARMD. Previously, it has been shown that IL-1β and TNF-α affected the TJ expression and that these cytokines increased phosphorylation of occludin on threonine residues in balb/c microvascular endothelial cells, and caused a down-regulation of occludin expression (Brankin and Padden, 2004). Thus, in this project, we wished to further investigate whether IL-1β and TNF-α would have an effect on the oBRB.

Hypotheses

1. Overall it is hypothesised that key components of the TJ and AJ of the RPE may become compromised following treatment with growth factors and cytokines, facilitating breakdown of the oBRB and retinal dysfunction.

2. VEGF165, produced in high amounts by cells in the neural retina, may affect Zo-1 or occludin expression and localisation at the oBRB, leading to oBRB dysfunction.

3. PLGF is a member of the VEGF family and may modify expression levels of TJs which will affect RPE function.

4. Chronic, low-grade inflammatory processes such as cystoid macular edema may contribute to the pathogenesis of ARMD. It is hypothesised that TNF-α produced locally at the RPE by infiltrating macrophages in ARMD may modulate TJ expression and disrupt the oBRB. Changes in expression or localisation of TJs may affect RPE polarity as the TJs of RPE are anchored to the actin cytoskeleton of RPE, and interact with signalling molecules and are important in establishment of cellular polarity

5. It is hypothesised that IL-1β affects expression and distribution of the TJ junctional proteins occludin, Zo-1 and the claudin family. This may lead to loss of RPE function, breakdown in the ability to degrade the photo-oxidative products, retinal edema and oBRB breakdown. Claudins regulate diffusion across the paracellular pathway by determining ion selectivity and electrical resistance of the junction, and they may be modulated by Il-1β, giving rise to oBRB breakdown.

Project Aims

The research presented in this thesis will focus on the BRB in health and disease and the effects of growth factors and cytokines on oBRB function which will be investigated using an *in vitro* model, human retinal pigment epithelial cells. Specifically the following will be determined:

I. Tight/adherens junction expression at the oBRB, including occludin, Zo-1, beta catenin, claudins 1, 2, 3 and 4.

II. Effects of vitreal growth factors VEGF and PLGF on oBRB integrity

III. Effects of pro-inflammatory cytokines, which are elevated in ocular disorders, on RPE function as determined by TJ expression and localisation at the oBRB.

Chapter 2

Materials and Methods

2.1 Materials

2.1.1 Materials for cell culture and cell treatment

2.1.1.1. Cell types used:

Human Retinal Pigment Epithelial Cells (ARPE-19) were obtained from American Type Culture Collection (ATCC, Manassas, VA, USA)

Human Brain Endothelial Cells (Endo Balbc) – were a gift from Dr. Brenda Brankin, School of Biological Sciences, Dublin Institute of Technology, Dublin, Ireland.

2.1.1.2. Materials

Nunc cell culture flasks 25cm^2 (Cat no: TKT-130-170F) and 75cm^2 (Cat no: TKT-130-210T) (Fischer scientific, Dublin – 2)

Cell Star cell culture plates (6 well) Greiner Bio-One (Cat no: 657160, Lot no: E1008003)

Nunc Lab-Tek Chamber Slide System and Lab-Tek chambered coverglass (Cat no: 177429)

Dulbecco's Modified Eagle's Medium (DMEM): Sigma Aldrich (Wicklow, Dublin – 24) Nutrient Mixture F12- Ham (DMEM / F12 1:1) with L- glutamine (Cat no: D8437, Lot No: 048K2413, 097K2406, RNBB0033)

Sigma Aldrich Protease inhibitor cocktail (Cat no: P8340)

Adult Bovine Serum – Sigma Aldrich (Wicklow, Dublin) (Cat no: B9433, Lot No: 018K8413)

Trypsin-EDTA [0.25% (w/v) Trypsin 0.02% (w/v) EDTA] Sigma Aldrich (Wicklow, Dublin) (Cat no: T4049, Lot no: 10A725, 097K2336)

Insulin Transferrin Selenium (ITS) media supplement – Sigma Aldrich (Cat no: I3146, Lot no: 069K8409)

Penicillin Streptomycin solution – Sigma Aldrich (Wicklow) (Cat no: P4458)

Amphotericin – B Sigma Aldrich (Wicklow, Ireland) (Cat no: A4888, Lot no:117K4016)

Dimethyl Sulphoxide (DMSO) – Sigma Aldrich (Cat no: D2650)

Vascular Endothelial Growth Factor (VEGF) Sigma Aldrich (Wicklow, Ireland) (Cat no: V7259, Lot: 075K1601)

Placental Growth Factor – Invitrogen (Biosciences, Ireland), Cat no: PHG0296

Interleukin 1-beta (IL-1β) – Sigma Aldrich (Wicklow, Ireland) (Cat no: I2393)

Tumor Necrosis Factor – Alpha (TNF - α) Sigma Aldrich (Wicklow, Ireland) (Cat no: T0157, Lot: 114K1429)

Endostatin – Sigma Aldrich (Wicklow, Ireland) (Cat no: E8154)

Disposable Cell Scraper – Fisherbrand – Fischer Scientific (Dublin 2) (Cat no: 08-773-2)

BD Plastipak Green needle and Syringe – Becton Dickinson (Spain) (Lot: 0512006)

2.1.1.3. Solutions used:

Phosphate Buffered Saline (PBS) – 8.1mM di-sodium hydrogen phosphate (Na_2HPO_4), 1.7mM sodium di-hydrogen phosphate (NaH_2PO_4), 27.4mM sodium chloride (NaCl) per litre, adjusted to pH 7.4 and sterilized by autoclaving.

2.1.2. Materials for Protein Analysis

96 well flat bottom ELISA plates – Nunc – Fischer Scientific Ireland (Cat No: TKT-180-070U)

Bradford Reagent – Sigma Aldrich (Wicklow) (Cat no: B6916, Lot no: 033K9279)

ELISA plate reader - Labsystems Multiscan Plus

Bovine Serum Albumin – Sigma Aldrich (Wicklow) (Cat no: A7030, Lot No. 038K0704). Protein standards ranging from 100µg/ml to 1000µg/ml made up using distilled de-ionized water.

2.1.3 Materials for SDS PAGE

Protein Samples prepared from cell extracts as detailed in section 2.1.2

Sigma Aldrich acrylamide / bis acrylamide 30% (w/v) solution (Cat no: A3699, Lot no: 097K6067)

N,N,N',N' Tetramethylethylenediamine (TEMED) – Sigma Aldrich (Wicklow) (Cat no: T9281, Lot no: 93H0857)

Ammonium persulphate – Sigma Aldrich (Wicklow) (Cat no: A3698, Lot No: 022K1258)

Trizma base SigmaUltra - Sigma Aldrich (Wicklow) (Cat no: T6791, Lot no: 083K5417)

Sodium Dodecyl Sulphate – BDH Laboratory supplies (Poole, England) (Cat no: 301754L, Lot no: ZA2003410-649)

Glycine (Molekula) (Cat no: M10760576, Lot no: 51613)

Bromophenol blue – Sigma Aldrich (Cat no: B5525, Lot no: 124H3631)

Glycerol – (Riedel-de Haen) – Lennox Chemical Supplies (Dublin) (Cat no: 33224, Lot no: 72610)

3-[(3-Cholamidopropyl)dimethylammonio]-1-propanesulfonate (CHAPS) – GE Life sciences (United Kingdom) (Cat no: 17-1314-01)

2.1.3.1 Solutions used

Resolving Gel Stock – 1.5 M Tris containing 0.4% (w/v) SDS adjusted to pH 8.8

Stacking Gel Stock – 0.5M Tris, 0.4% (w/v) SDS adjusted to pH 6.8

Running Buffer (10-fold concentrate) 1L: 248mM Tris, 1.92M Glycine, 10g SDS adjusted to pH 8.6

4x Sample buffer (100ml): 0.5M Tris (pH 6.6), 16g SDS, 20% (v/v) Glycerol, 16mg Bromophenol Blue, 10% (w/v) CHAPS.

Butanol 95% (v/v)

Ammonium persulphate 0.1% (w/v)

2.1.4. Materials for Western blotting

Semi-dry blotting apparatus – Appolo Laboratories, Sweden

Alpha Imager FC™ 1-D digital analysis software (Alpha Innotech)

AlphaImager HP™ Gel imaging system (Alpha Innotech) – Cell Biosciences

Whatman Protran BA83 Nitrocellulose membrane – Sigma Aldrich (Wicklow, Ireland) (Cat no: Z670960, Lot No: 8558862)

Ponceau S Solution – Sigma Aldrich (Wicklow) (Cat no: P7170, Lot no: 093K4356)

Albumin Bovine Serum, Fraction V – Sigma Aldrich (Wicklow) (Cat no: A9647, Lot no: 038K0704)

Tween 20 for electrophoresis – Sigma Aldrich (Cat no: P5927, Lot no: 043K01541)

Western Super Signal West Pico Chemiluminescent Substrate - Pierce

Western Super Signal West Pico Chromogenic Substrate BCIP / NBT – Pierce

Novex AP Chromogenic Substrate (BCIP / NBT) Invitrogen (Biosciences, Ireland) (Cat no: WP20001, Lot no: 622918)

Methanol (Riedel-de Haen) – Lennox Laboratories Ltd. (Dublin)

MagicMark™ XP Western Standard – Invitrogen (Biosciences, Ireland) (Cat no: LC5602, Lot no: 462876).

2.1.4.1. Antibodies used

Sigma Aldrich – Monoclonal anti β-Actin antibody produced in mouse (Cat No: A1978, Lot No: 016K4817)

Zymed Labs –Monoclonal anti Zo-1 antibody produced in mouse 100ug (Cat No: 33-9100, Lot No: 60605689)

Sigma Aldrich – anti rabbit IgG (whole molecule) – peroxidase-conjugated antibody developed in goat (Cat No: A6154, Lot No: 055K6015)

2.1.4.2. Solutions Used

Transfer Buffer – 25mM Tris, 20% (v/v) methanol, 20% (w/v) glycine; adjusted to pH 7.0.

Tris Buffered Saline (TBS) – 50mM Tris, 0.15M Sodium Chloride, adjusted to pH 7.0

Blocking Solution – 5% (w/v) Bovine Serum Albumin (BSA) dissolved in TBS

Wash Buffer – 0.2% (v/v) Tween20 in TBS (pH 7.0)

Western Blot Stripping solution – 0.01mM Tris, 10% SDS, 0.001% (v/v) β-mercaptoethanol.

2.1.4.3. SDS PAGE Resolving Gel preparation

Percentage	**7.5%**	**12%**	**14%**
Gel stock	5 ml	5 ml	5ml
Water	10 ml	8.4 ml	5.7ml
Bis-Acrylamide (30%)	5 ml	6.6 ml	9.3ml
Ammonium Persulphate (0.1%)	200µl	200µl	200µl
TEMED	20µl	20µl	20µl

2.1.4.4. 4% Stacking Gel preparation

Stacking Gel Stock – 1.5ml

Water – 3.6ml

30% (w/v) Bis acrylamide – (0.9%) - 900µl

Ammonium persulphate 0.1% (w/v) – 100µl

TEMED – 20µl

2.1.5. Materials for Immunoflourescence

Occludin and Zo-1 primary antibodies, as outlined in section 2.1.4.1

Biotinylated mouse immunoglobulin (Vector Labs) provided with Vectastain universal ABC kit (Cat no: PK6200)

Vectastain Flourescein Streptavidin – Vector Labs (Cat no: SA-1200)

Vectastain Texas Red Streptavidin – Vector Labs (Cat no: SA-5006)

Vectastain Flourescence mounting medium with DAPI – Vector Labs (Cat no: H-1200)

Lab-Tek 2 well chamber slides with coverglass – Nunc – (Cat no: 177380)

Blocking solution – 3% (w/v) BSA in PBS

Wash solution – 0.2% (v/v) Tween20 in Phosphate buffered saline

100% Methanol

2.1.6 Materials for immunohistochemistry

Paraffin-embedded tissue sections – gift from Dr. Helen Lambkin, School of Biological Sciences, Dublin Institute of Technology, Dublin, Ireland.

Histolab Xylene – (Cat no 02080)

Histolab 99.5% Ethanol, Histolab 95% Ethanol and Histolab 80% Ethanol (all v/v)

Sodium Citrate – Fischer Scientific (Dublin, Ireland) (Cat no: BP327-1)

Vector Labs VECTASTAIN Universal ABC staining kit: Mouse IgG (Cat no: PK6200)

Vector Labs DAB Peroxidase substrate kit (Cat no: SK 4100)

DPX and coverslips

2.1.6.1 Solutions used

Citrate buffer – 10mM Sodium Citrate in 1.0 L of double distilled water adjusted to pH 6.0

Blocking reagent – 5% (v/v) normal horse / goat serum in PBS

3% (v/v) hydrogen peroxide prepared by diluting 1ml of 30% (v/v) hydrogen peroxide in 9mls of distilled water.

ABC reagent – prepared according to manufacturer's instructions

DAB reagent – prepared according to manufacturer's instructions.

2.1.7. Materials for 2-D Electrophoresis

IPG Buffer – pH 3.0 – 10.0 (GE Healthcare LifeSciences, UK) (Cat no: 17-6000-87) Storage: $4^{o}C$

Immobiline Dry Strip IPG Gel strips – pH 3-10, Length 13cm (GE Healthcare LifeSciences, UK) (Cat no: 17-6001-14) storage: $-20^{o}C$

PlusOne Dry Strip cover fluid – 1L (GE Healthcare LifeSciences, UK) (Cat no: 17-1335-01)

PlusOne CHAPS – 1g (GE Healthcare LifeSciences, UK) (Cat no: 17-1314-01) – Storage: $4^{o}C$

PlusOne Dithiothreitol (DTT) – 1g (GE Healthcare LifeSciences, UK) (Cat no: 17-1318-01) – Storage: 4^{o}C

Coomassie brilliant blue R250 (Sigma Aldrich, Wicklow) (Cat no: 27816)

Bromophenol Blue – Sigma Aldrich (Cat no: B5525, Lot no: 124H3631)

DeStreak Rehydration Solution – pH 3-10 (GE Healthcare LifeSciences, UK) (Cat no: 17-6003-19) storage: -20^{o}C

Sigma ProteoSilver™ Silver Staining Kit – Sigma Aldrich (Wicklow) (Cat: PROTSIL1)

Refrigerated centrifuge (Eppendorf 5417R)

pH meter (Hanna instruments pH 210 microprocessor)

Balance (Mettler Toledo, AB204)

Vortex (Rotamix Hoock and Tucker Instruments Ltd)

Immobiline drystrip reswelling tray (GE Life sciences, UK)

Ettan IPGphor II Isoelectric Focusing System, Ettan IPGphor Manifold, Electrodes and paperwicks (GE Lifesciences, UK)

Gel apparatus consisting of – Gel electrophoresis box (ATTO - MSC), Glass plates 16x14 cm and 2mm thick, rubber gaskets, bulldog clips and combs

Power pack (0-400V, 0-200mA) (Vokam SAE 2761)

Staining and destaining trays

Orbital mixer (KS 125 basic IKA Labortechnik)

Tissue culture hood (EHRET Reinraumtechnik)

Scanjet 5300C (Hewlett Packard)

Imaxia Gelfox™ 3.0 (Alpha Innotech)

2.1.7.1 Solutions Used

Bromophenol blue stock solution – 1% (w/v) bromophenol blue and 0.6% (w/v) Trizma base in double distilled water.

Rehydration stock – 7M Urea, 2M Thiourea, 15mM DTT, 1% Pharmalytes, 4% Triton-X 100, 0.002% (v/v) bromophenol blue stock solution in distilled water. Divided into 2.5ml aliquots and stored at -20^{o}C.

Equilibration solution – 0.05M Trizma base, 6M Urea, 30% (v/v) glycerol, 1% (w/v) SDS, 32mM DTT (Buffer – I), 0.002% (v/v) bromophenol blue stock solution.

Coomassie blue stain – 0.025% (w/v) Coomassie brilliant blue R250 (Sigma Aldrich), 40% (v/v) methanol, 7% (v/v) acetic acid made up to 2L using double distilled water and filtered through filter paper. Stored at room temperature.

Destain solution 1 – 40% (v/v) methanol and 7% (v/v) acetic acid made up to 1L using double distilled water. Stored at room temperature.

Destain solution 2 – 5% (v/v) methanol and 7% (v/v) acetic acid made up to 1L using double distilled water. Stored at room temperature.

2.2. Methods

2.2.1. Cell Culture

ARPE-19 is a spontaneously arising retinal pigment epithelia (RPE) cell line derived in 1986 from the normal eyes of a 19-year-old male. These cells form stable monolayers, which exhibit morphological and functional polarity. ARPE-19 expresses the RPE-specific markers CRALBP and RPE-65. The cells are diploid and can be carried for over 30 passages. Progeny were found to undergo an additional 48 population doublings in longevity trials performed during characterization at ATCC. The ARPE-19 cells were bought from ATCC and used at passage numbers less than 30.

The ARPE-19 cells were removed from liquid nitrogen storage and thawed quickly to retain viability. They were cultured in Dulbecco's Modified Eagle's Medium F12 HAM (Sigma Aldrich) containing 10% (v/v) Adult Bovine Serum (Sigma Aldrich), 1% (w/v) penicillin-Streptomycin(Sigma Aldrich) and 250µl ITS media supplement (Sigma Aldrich). Cells were propagated in T25 cell culture flasks (Corning) with 5ml of 10% (v/v) complete medium and incubated at 37^{o}C with 5% carbon dioxide. The medium was changed every 3-4 days until cells achieved desired confluence.

A flask of confluent cells was taken from the incubator. The cells were washed 3 times with sterile PBS and then 1ml of 0.25% (v/v) Trypsin EDTA (Sigma Aldrich) was added to the flask. The flask was then incubated at 37^{o}C for 10 minutes to allow trypsinisation. The cells were observed under the microscope to check whether trypsinisation was complete and 2.0 mls of complete medium was added to the flask to stop the reaction. The cells were then pipetted into a sterile 15ml centrifuge tube

and pelleted at 1000rpm for 10minutes. The supernatant was aspirated from the tube and the pellet re-suspended in 1.0 ml of fresh medium. The cells were then distributed evenly into 3x T25 flasks, each containing 5.0 ml of 10% (v/v) complete medium. This process was repeated until the required amount of cells were obtained

2.2.2. Growth factor treatment and extraction

Confluent cultures were washed 3 times with sterile PBS and incubated in serum free medium for 6 hours. Following this, appropriate amounts of growth factors were added to the flasks in serum free medium and incubated for a further 24 hours at 37^{o}C.

Growth factor treated RPE cells were washed 3 times with PBS to remove any traces of media. The cells were scraped from the flask and homogenized using a 21-gauge needle in extraction buffer containing 62.5mM Tris, 2% (w/v) SDS, 10mM DTT and 10% (v/v) protease inhibitor cocktail (Brankin B *et al*. 2005). The cell lysate was then centrifuged at 14,000 rpm for 20 minutes at 4^{o}C. The supernatant was removed and used for protein analysis.

2.2.3. Protein Analysis

Six different BSA protein standards ranging from 0.1 – 1mg/ml were prepared. To perform the assay, 10µl of each BSA standards and test samples were pipetted in duplicate into a 96-well flat bottom ELISA plate followed by addition of 200µl of Bradford Reagent (Sigma). The samples were allowed to mix on a shaker for 20 minutes. It was then read using a spectrophotometer (Labsystems Multiskan plus) at 595nm. If the samples were highly concentrated, then a 1:10 or 1:20 dilution of the sample was prepared as required.

2.2.4. 1-D Electrophoresis

Equal amounts of protein were loaded on to SDS-PAGE minigels along with loading buffer. Resolving gel strengths used were 12% (Occludin analysis), 7.5% (Zo-1) and 14% (claudins). Resolving gel recipes are given in Table 3.1

After the resolving gel had set, the butanol was poured off. The resolving gel was then topped with stacking gel with a Teflon comb was placed into the gel. The gel was allowed to set. The gel rigs were filled with 1x running buffer. The rubber lining was removed from the plates after the gel had set. The plates were then gently placed into the rigs, avoiding any bubbles from forming under the gel.

The gap between glass plates in the gel rig was then filled with 1x running buffer to immerse the gels completely in buffer. 30ug protein sample was added to 10µl of 4x sample buffer. The protein samples were then boiled for 3 minutes. Equal amounts of protein per sample were loaded on to each well after loading 5µl of the molecular weight marker in the first well. The electrophoresis was then run at 150V and 100mA for 1.5 hours (or 2 hours for Zo-1). When the dye from the loading buffer reached the bottom of the gel, the electrophoresis was stopped and the plates removed. The stacking gel was cut and removed from the gel.

2.2.5. Western Blotting Protocol

The Bio-Rad semi-dry electroblot apparatus was prepared by placing 2 sheets of blotting paper, cut to the size of the gel and soaked in transfer buffer, on the ceramic transfer platform. One sheet of nitrocellulose membrane cut to the exact size of the gel, was placed on top of the wet blotting paper followed by the resolving gel

and two further sheets of blotting paper (also soaked in transfer buffer). The lid was placed on top of this and securely closed. The electroblot was run at a current of 0.9mA per gel for 1.5 hours (3.0 hours for Zo-1). The proteins should move from the gel to the nitrocellulose membrane due to the negative charge imparted by SDS. They are attracted towards the positively charged nitrocellulose membrane.

After transfer, the membrane is briefly rinsed in TBS. Efficiency of transfer was determined using Ponceau S solution (Sigma Aldrich). The membrane was rinsed again to wash off the Ponceau S dye. It was then incubated in a blocking solution of 5% (w/v) Bovine Serum Albumin (BSA) in TBS for one hour at room temperature on the shaker. After incubation, the membrane was rinsed briefly with TBS and incubated in blocking solution containing a 1:5000 dilution of the antibody for the protein of interest. The membrane was incubated at 4^{o}C overnight on the shaker.

Post incubation, the blocking solution containing the antibody was removed and stored at 4^{o}C for re-use. The membrane was washed thrice for 5 minute in TBS containing 0.2% (v/v) Tween-20. It was then re-incubated in blocking solution containing a 1:5000 dilution of the secondary antibody for 3.0 hours at room temperature. The secondary antibody used was species-specific IgG conjugated with horse radish peroxidase (HRP) or alkaline phosphatase (AP). The diluted antibody was removed and stored at 4^{o}C for reuse. The membrane was washed 3x in TBS containing 0.2% (v/v) Tween-20 for 5 minutes.

2.2.5.1. Chromogenic detection

Chromogenic detection of protein was done using the Invitrogen Western-breeze Chromogenic kit – (anti-mouse). Membrane blocking and wash steps were carried out as per instructions in the manual. The membrane was incubated overnight with the primary antibody at 4^{o}C on a shaking platform. It was then washed 3x in diluted wash buffer provided with the kit and then incubated with alkaline phosphatase-conjugated mouse anti-IgG at a concentration of 1:5000 for 2.0 hours at room temperature. The blot was rinsed post incubation and developed using the chromogenic substrate provided with the kit. The developed blot was scanned and densitometric analysis performed using Alpha Imager FC.

2.2.5.2. Enhanced Chemiluminescence

Post-transfer, the nitrocellulose membrane was incubated in a blocking solution [5% (w/v) BSA in TBS] for 2.0 hours. Membranes were washed quickly in TBS and incubated with the polyclonal rabbit anti-claudin2 or anti-claudin3 antibodies (1:5000) overnight at 4^{o}C. The membranes were washed 3 times with 0.1% (v/v) Tween20 in TBS and incubated with secondary anti-rabbit IgG with HRP-conjugate (1:5000) for 3.0 hours at room temperature. Immune complexes were detected using enhanced chemiluminescence. The film was scanned and densitometric analysis performed using Alpha Imager FC software.

2.2.5.3 Densitometric analysis

The finished blot was placed over the platform inside Alpha Imager under white light only option. The blot was positioned to get a clear view for the camera and the focus was adjusted using Imaxia Gelfox software. A photograph was taken and the image

was saved in tiff format. The protein bands on the blot was selected using Gelfox and the total pixel density per band was calculated and saved to file.

Experiments were performed in duplicates or triplicates. Mean density of all repeats were used for statistical analysis.

2.2.6. Viability Assay:

ARPE-19 cells were propagated in 6-well cell culture plates in 10% (v/v) growth medium, until confluent. The medium was changed to the serum-free composition, 6 hours prior to growth factor treatment. Cells were incubated for 24 hours with growth factors as described earlier. The culture was then washed 3 times with PBS and trypsinized by adding 200µl of 0.25% (v/v) Trypsin-EDTA solution. Trypsinisation was stopped by adding 200µl of complete medium. A 20µl aliquot was removed from this and an equal volume of 0.4% (w/v) Trypan Blue (Sigma Aldrich) was added. This was allowed to stand for 5 minutes. Cell suspension (10µl) mixed with Trypan blue was applied to a haemocytometer, and the ratio of viable to non-viable cells determined. The plasma membranes of non-viable cells are permeable to Trypan blue and hence take up the dye and appear blue while observed under the microscope

2.2.7. Statistical analysis

Statistical analysis of data obtained was done using single parametric Analysis of Variations (ANOVA) method. The data was compared and a P value <= 0.05 at 95% accuracy was considered statistically significant. A minimum of two sets of values were used for comparison of results.

2.2.8. Immunofluorescence

Cells grown to confluence in T25 flasks were washed 3 times with sterile PBS to remove any traces of serum, followed by trypsinization and centrifugation. The pellet was dissolved in 1.0 ml of fresh medium. Sterile $1cm^2$ coverslips were placed in 6 well tissue culture plates and 100µl of cell suspension aseptically placed on top. The plates were then incubated at 37^oC for 2.0 hours to allow the cells to settle. After 2.0 hours, 2 ml of 10% (v/v) complete medium was added to each well, and the cells were reincubated at 37^oC until the desired degree of confluence was achieved. Coverslip-immobilized cells were treated with growth factors as explained previously. The treated cells were then washed 3 times in sterile PBS and fixed for 10minutes in ice-cold methanol. The methanol was then aspirated to waste and the cells washed quickly in 2.0 ml PBS to avoid drying.

The coverslips were then blocked in 3% (w/v) BSA in PBS for one hour at room temperature. Following this, the cells were rinsed briefly with PBS and incubated with the primary antibody at 4^oC overnight. After incubation, the cells were washed 3 times with PBS for 10 minutes each. The cells were then incubated with the appropriate biotinylated secondary antibody for 2.0 hours at room temperature. The cells were washed again with PBS. They were then incubated with 1:200 dilution of flourescein streptavidin (Vector Labs) for 15 minutes in the dark. Following a further wash with PBS, the coverslips were mounted on a glass slide using a fluorescence mounting medium containing DAPI (Vector Labs). The cells were then observed under the flourescence microscope and images captured using Cell™ software.

2.2.9. Immunohistochemistry (IHC)

2.2.9.1. Tissue Rehydration

Paraffin-embedded tissue sections were gifted by Dr. Helen Lambkin. The tissue specimens were cut into 5.0 µM sections using a microtome and mounted on silanized charged slides. They were allowed to dry for 15 minutes, followed by one hour incubation at 58^{o}C.

2.2.9.2. Dewaxing and antigen retrieval

The slides were submerged in two changes of xylene (5 min), followed by two changes of absolute alcohol (5 min). The slides were then submerged in spirit for 1 minute followed by rinsing with tap water for 2 minutes to remove the alcohol. The slides were then allowed to sit in citrate buffer preheated to 95^{o}C for 45 minutes. They were then treated with 3% (v/v) methyl hydrogen peroxide for 5 minutes to inactivate endogenous peroxidases.

2.2.9.3. ABC staining method

The ABC staining was done using a Vectastain kit as per manufacturer's instructions. The slides were washed in PBS (5 min), blocked using Normal Horse Serum (10 min) and then washed again with PBS (1 min). They were then incubated in the primary antibody for either 2 hours at room temperature or 4oC overnight. The slides were then washed three times with PBS (5 min) and secondary antibody added and incubated for 1 hour. The sections were washed thrice with PBS (5 min) and then the ABC peroxidase (Vector Labs) was added and incubated for 15 minutes. After the wash step, the slides were incubated in DAB peroxidase (10 min). When sufficient colour had developed, the slides were washed using tap water and counter-stained

using Meyer's Haematoxylin for 1 minute. They were then blued in warm running water for a minute.

2.2.9.4. Rehydration

Slides were rehydrated by immersion in spirit for 1 minute, followed by two changes of absolute alcohol for 3 and 10 minutes respectively. They were then submerged in xylene (5 min) followed by a second change of xylene (2 min). DPX was added and a coverslip applied.

2.2.10 2-D Electrophoresis

2.2.10.1. Acetone precipitation

Samples were extracted using extraction buffer as described in section 2.2.2. A specific volume of test sample containing approximately 500µg protein was pipetted into a 1 ml tube and diluted five-fold with ice cold acetone. This was then mixed by vortexing and left at -20^{o}C for 2.0 hours. The sample was then removed and spun at 10000 rpm for 20 minutes at 4^{o}C. The acetone was aspirated to waste and the protein pellet dried at room temperature.

2.2.10.2 IPG Strip rehydration

IPG strips in the pI range pH 3-10 were used. A 2.5ml aliquot of rehydration stock solution was slowly thawed at 4^{o}C prior to use. IPG buffer (12.5µl) and DTT (7mg) was added per 2.5ml of rehydration solution. The solution was inverted slowly and 250µl aliquots added to each protein pellet. Proteins were dissolved by gently mixing for 15 minutes at room temperature.

The protective lid was removed from the re-swelling tray and 250µl of re-hydration solution containing the protein pellet was pipetted into the central point of each tray slot. The protective foil cover lining the IPG strip was gently removed, starting at the acidic end marked (+). Each strip was gently laid down on the solution, with the gel side facing down. The strip was gently lifted and lowered back-and-forth so that the fluid covered the entire strip. Care was taken to avoid air bubbles forming in the solution. The strips were then covered with 2 ml of dry strip cover fluid to prevent evaporation. The re-swelling tray lid was replaced and the strips allowed to hydrate overnight at room temperature.

2.2.10.3 Isoelectric focusing (IEF)

The ceramic manifold was placed on the Ettan IPGphor Isoelectric focusing system platform. Drystrip cover fluid was added to each of the manifold channels. The hydrated strips were gently removed and placed, gel-side-up, on filter paper to remove excess cover fluid. The strips were then placed gel-side-up on the manifold, with the anode (+) end aligned with the 13cm mark on the IEF platform. An appropriate number of paper wicks were counted and 150µl of double distilled water added to each wick. A wick was placed at each end of the strip in such a way that one end of the strip overlapped the end of the gel. The electrodes were placed on top of all wicks, ensuring that the electrodes were in contact with the wicks, and the electrode cams were swivelled into closed position.

The IPGphor lid was programmed with parameters shown in table below and the lid was closed.

Voltage -mode	Voltage	Volt-hours	Duration (hours)
Step and hold	500	500	1
Step and hold	1000	1000	1
Step and hold	8000	14500	2
			4

2.2.10.4 IPG strip equilibration

Following IEF, the IPG strips were taken from the manifold and placed on a filter paper to remove excess cover fluid. The SDS equilibration solution was thawed at 4^{o}C and 10ml added to a clean test tube. DTT was then added to this just before use. IPG strips were gently placed into these test tubes with the support film towards the wall. The test tube mouth was closed using Parafilm® and placed on Spiramix rotating mixer for 15 minutes. Equilibration saturates the IPG strips with the SDS buffer system required for the second dimension separation of proteins.

2.2.10.5. Electrophoresis

Buffers and reagents were prepared as previously described (Section 2.3). A 12% SDS PAGE gel was prepared as previously described in section 2.1.4.2. Resolving gel was poured between plates, leaving approximately 0.5cm gap from the top. A layer of butanol was added to ensure a level surface for the gel. The resolving gel was allowed to set for 30 minutes. Butanol was poured off after the gel had set and excess butanol was rinsed off with distilled water. The IPG strip was removed from the equilibration solution and rinsed carefully in running buffer. It was then placed carefully on top of

the SDS-PAGE gel, face-side-up, with the plastic side in contact with the glass plate. The gel was then pushed down gently with a forceps until the strip was in contact with the gel. Care was taken to ensure that no air bubbles were present between contact surfaces. A small plastic spacer was placed beside the strip, and 1% agarose poured into the glass plates to hold the strip in place during electrophoresis. The plastic spacer was removed after the agarose had set, leaving a well for applying the molecular weight marker.

The gel was run at 150V per gel for 3.5 hours. At the end of this run, the bromophenol blue dye had reached the bottom of the gel. The gel was then removed from the glass chamber and the IPG strip and agarose discarded.

2.2.10.6 – Coomassie blue staining

The gel was placed on plastic trays and a sufficient volume of Coomassie blue stain was poured to cover the gel. The tray was placed on a shaker and the gel was stained using Coomassie brilliant blue overnight. The stain was discarded and the gel was then destained in destain-1 for 1.0 hour followed by destain-2 overnight or until the background was clear. The destained gels were scanned using a scanner for further analysis. The optimized time scale for 2-D electrophoresis is provided in the table 2.3 below, as used in all subsequent experiments.

Step	Temperature	Time
Day 1		
Protein sample (1000µg) + 4x Acetone Incubation	-20C	2 hours
Centrifuge – 10,000 rpm	4C	10 min
Pipette off Acetone. Airdry	Room temp	5 min
Heat Samples	100C	3 min
Cool on bench	Room temp	5 min
Add 250ul rehydration stock (DTT+Buffer) per pellet	-	5 min
Mix	Room temp	15 min

Place on reswelling tray. Add IPG strip face down. Cover with oil and allow to rehydrate	Room temp	8-12 hours

Step	Temperature	Time
Day 2		
Set Manifold on IEF. Cover with oil	-	5 min
Transfer strips to manifold	-	20 min
Place wet paperwicks on both sides of gel	-	20 min
Place electrode cams. Lock into position	-	10 min
Run IEF	Room temp	4-5 hours

Step	Temperature	Time
Day 3		
Blot excess oil from gel	-	5 min
Equilibrate gel in Equilibration solution	-	20 min
Prepare resolving gel (leave 0.5cm space)	-	30 min
Resolving gel set time	-	30 min
Add IPG strip to resolving gel	-	10 min
Add 1% agarose (+bromophenol blue) – Allow to set	-	5 min
Setup SDS system. Add m.w marker	-	10 min
Run 2D	-	4-5 hours

Step	Temperature	Time
Day4		
Transfer gel to Coomassie blue	-	30 min
Stain	-	8-12 hours

Step	Temperature	Time
Day 5		
Destain 1	Room temp	1-1.5 hour
Destain 2	Room temp	8-12 hours

Table 2.3: Optimized time scale for 2 dimensional electrophoresis of RPE samples.
Processing time from sample preparation until the stage of obtaining the final destained gel was five days.

2.2.10.7 – Silver Staining

Silver staining and destaining was done using ProteoSilver kit (Sigma Aldrich) as per manufacturer's instructions. All steps require constant agitation and hence were performed at room temperature on a shaker. The steps are outlined below.

a) Fixation

The gel was fixed in a solution containing 50% (v/v) ethanol and 10% (v/v) acetic acid for 20 min., followed by 30% (v/v) ethanol for 10 minutes. The gel was then washed in distilled water (10 min.).

b) Sensitisation

The gel was sensitized in sensitizing solution provided for 10 minutes. It was then washed twice in distilled water for 10 minutes each.

c) Silver equilibration

Silver solution was added to the gel for 10 minutes, after which it was washed with water.

d) Development

Developer solution was added and the gel agitated until spots became visible. After the desired stain intensity had been achieved, colour development was halted by stopping solution, followed by washing (15 min.) and the result archived using a flat-bed scanner.

Chapter 3

Standardisation of techniques for detection of protein expression

Investigation of the effects of selected modulators on regulation of tight junction protein expression within this study was carried out by electrophoretic and cytochemical techniques, in conjunction with immuno-localization of target proteins. To permit reproducible comparative analysis of protein expression over the entire study period, it was necessary to perform standardization experiments to identify optimal assay conditions and to characterize the robustness of the detection methods. Variations in global protein expression in response to treatment challenges utilized 2-dimensional gel electrophoresis, and this was complemented by SDS-PAGE and western blotting to study the expression of specific biomarkers. Bio-distribution studies to localize the expression of a selection of target biomarkers within cells utilized fluorescent-labelled antibodies.

3.1 Two-Dimensional (2-D) Electrophoresis

The technique of 2-D gel electrophoresis was selected to study the effect of growth factors on the RPE proteome, comparing the resultant fingerprint (generated on the basis of molecular mass and isoelectric point) with in-house data and previously published reports. An integral aspect of deploying this technique is ensuring adequate amounts of protein which can be reproducibly detected after separation in both dimensions. Using the method previously described by Brankin and colleagues (2006), it was found that it was only possible to reproducibly prepare cell homogenates with a maximum protein concentration of 0.8–1mg/ml; previous studies have also reported extensive protein loss at almost every stage of sample preparation and transfer (Zhou *et al*, 2005), citing proteolysis, the presence of unspecified contaminants or uncontrolled insolubilization of proteins as reasons. This loss of protein also contributes to experimental variations, reducing chances of reproducing

the 2-D gel pattern (Zhou *et al*., 2005). On the basis of such reports, and given that further optimization of homogenate preparation was beyond the scope of this work (on the grounds of limited time available), it was decided to try to compensate for this limitation by incorporation of a protein precipitation step into the sample preparation protocol, in conjunction with deployment of enhanced sensitivity detection methodology during the final band detection steps in the electrophoresis.

Initial investigation of untreated RPE protein extracts by SDS-PAGE revealed densely staining bands in the regions of 30 kDa and 116 kDa (data not shown). Initial range-finding experiments with the 2-D gel system revealed problems of run-to-run variation and a low number of (sometimes faintly stained) protein spots on gels (Fig 3.1, a); the sub-optimal performance of the method was judged on the basis of comparison with previous in-house work on similar systems. A number of approaches were pursued to remedy this problem.

Incorporation of an organic solvent (acetone) precipitation step into the sample preparation protocol allowed an approximate 50% increase in amounts of protein available for application to the gel, and thereby assuring that low abundance protein in the extract could be consistently detected. Additionally, the occurrence of streaks in the stained gel reduced the overall clarity and complicated the clear-cut interpretation of results. Such streaks have been variously attributed to the presence of membrane lipids, contaminants and non-specific oxidation of proteins (Luche *et al*., 2004.); however, in the present work, the inclusion of DTT in the equilibration and re-swelling buffers was not wholly effective in preventing streaks. Substitution of re-swelling buffer with DeStreak Rehydration Solution (pH 3-10), a product available

from GE Life Sciences (UK), was found to eliminate such artefacts (Fig 3.1, b). Information regarding the components of this buffer was not available from the company. However, it was successful in removing streaks caused by protein oxidation and presence of lipids in the gel.

Further minor modifications to the protocol were also found to have a beneficial effect on the quality of the gel end product. While the molecular mass standards could be detected on the final 2-D gel without much difficulty after using the 'standard' IPG strip equilibration protocol (20 – 30 minutes), it was determined empirically that efficient diffusion of analyte samples into the second dimension required a longer pre-equilibration duration of 45 minutes.

Variations in gel quality could also arise from the handling of the IPG strips. Experience through trial-and-error indicated that the latter were best handled when they were still nearly frozen and used immediately after removing from -20^{o}C storage. It was observed that an increase in temperature caused the gels to stick to the plastic strip and tear while the strip was being removed.

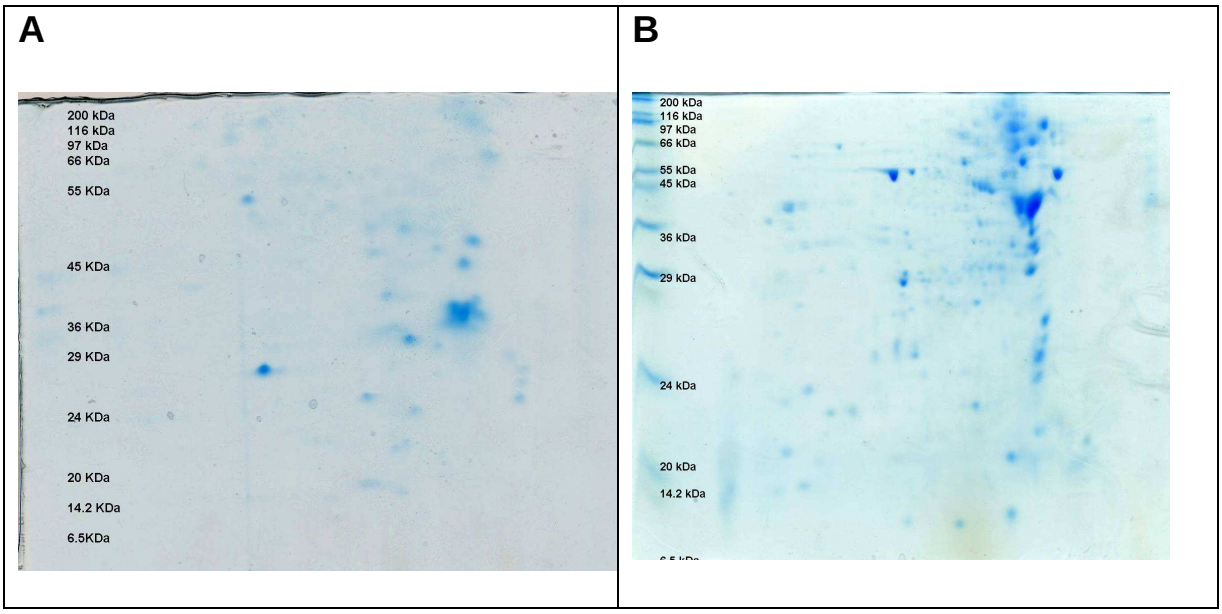

Fig 3.1: Establishment of optimized separation and detection parameters for the untreated RPE proteome sample.

a. 200 µg protein, standard extraction protocol, standard re-swelling buffer containing DTT;

b. 500 µg protein, organic solvent precipitation of protein, DeStreak Rehydration buffer. The organic solvent precipitation step was performed by taking 200µg of RPE extract and addition of a 4x volume of chilled acetone. Precipitates were air dried and resolubilized in 250µl of rehydration stock by gentle mixing. The standard strip re-swelling protocol consisted of rehydration in 7M urea, 2M thiourea, 15mM DTT and 4% Triton X-100. Gels were stained using Coomassie Brilliant Blue. Electrophoresis parameters were as outlined in section 2.2.10

Note: Gels shown in picture are not of the same sample

Attempts to further optimize the detection of protein spots on gels focused on replacing-supplementing Coomassie Brilliant Blue with more sensitive staining methods. The advantage of higher resolution detection of protein spots for a smaller amount of protein sample (150 µg) using a silver staining protocol were offset by increased background staining (Fig 3.2), with the latter limitation exacerbated by the practical difficulty of processing multiple gels simultaneously.

Fig 3.2: Detection of protein complement of untreated RPE extract by 2-gel gel electrophoresis and silver staining.

Protein present in initial sample - 150µg. Electrophoresis parameters were as outlined in section 2.2.10. Arrows indicate protein spots visible in final gel. Heavy background staining was obtained in the initial gels after destaining silver stained gel. Double staining partially rectified this problem and the gel obtained was much clearer.

The use of silver stain on gels, with subsequent staining in Coomassie Brilliant Blue, was also examined; such protocols have been reported to increase protein detection sensitivity on electrophoretic gels by up to eight-fold (Fernandez-Patron *et al* 1995; de Moreno *et al*, 1986; Irie *et al* 1982). Preliminary experiments indicated that the use of this technique may provide higher contrast preparations than the use of silver staining alone (Fig 3.3); indeed, removal of non-specific background staining was experienced, resulting in improved gel clarity. However, the relative convenience of the Coomassie blue method, in conjunction with the other assay improvements outlined above, dictated that it was the primary staining method used in this study. The final optimized 2-D gel electrophoresis protocol used in all subsequent experiments is described in Table 2.3, Section 2.2.10.6 of Materials & Methods.

Analysis of changes in RPE proteome treated with VEGF using 2-D electrophoresis was attempted in the initial period of study. It is nearly impossible to study tight junction protein changes by the 2-D electrophoresis method, owing to a very low percentage of membrane proteins in the RPE proteome extract prepared for this analysis. The 2-D electrophoretic analysis may prove to be an excellent tool for studying pathological changes in the total RPE proteome and would be handy in identifying key protein biomarkers in diseased RPE. The focus of this project was to look at the modulation of RPE barrier function, involving changes in expression of key membrane proteins involved in formation of tight junctions. Hence this method was found inadequate. Also owing to time constraints in the project, this experiment was not continued.

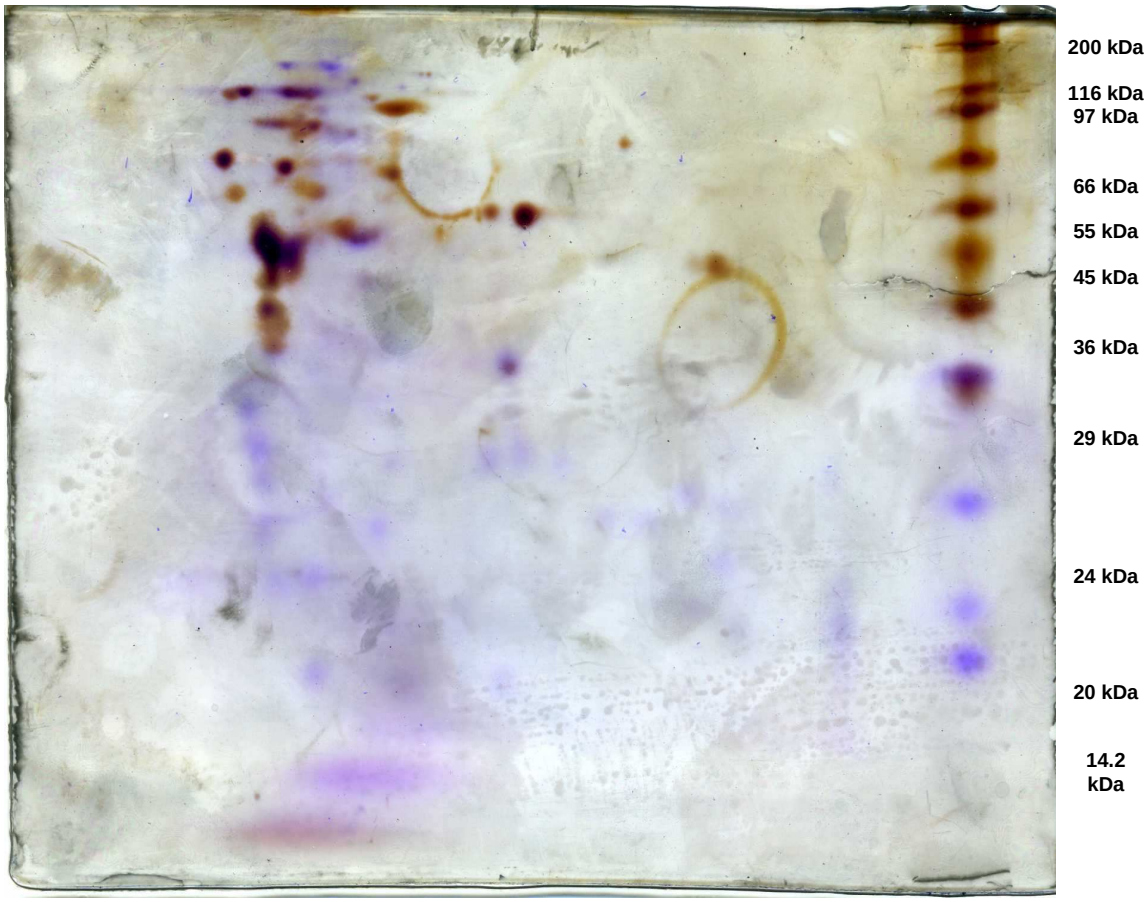

Fig 3.3: Detection of protein complement of untreated RPE extract by 2-dimensional gel electrophoresis. Gel was double stained using silver and Coomassie Brilliant Blue.

Protein loading: 200µg. Electrophoresis parameters were as outlined in section 2.2.10

3.2 Western Blotting

The modulation of expression of specific RPE proteins in response to growth factors was assessed by western blotting. This approach involved the separation of proteins by SDS-PAGE, followed by transfer to a nitrocellulose membrane and probing with specific antibodies. Antibody-antigen reactions were then detected by enzyme-linked conjugates (alkaline phosphatase or horse radish peroxidase).

Initial investigation of protein loading and staining performance on SDS-PAGE gels identified the required amount of protein per gel lane (gel not shown). The full complement of proteins capable of being visualized by this technique was apparent at a gel loading of 20µg of protein, without incurring serious lane distortion, and this was selected for subsequent use in western blotting experiments (Section 2.2.5). However, problems were encountered in transferring proteins from the gel to nitrocellulose using the dry cell blotter available in the laboratory. Attempts to effect consistent transfer of proteins using the standard current setting and recommended blotting times necessitated further optimization, and Beta actin was used as a loading control for this purpose.

Problems with non-specific binding were also encountered. The Invitrogen Novex® Western Breeze™ Chromogenic kit (anti-mouse) kit was used as the standard immuno-staining tool for colourimetric analysis of protein of interest. However, the Hammerstein casein blocking solution provided with the kit was not found to be suitable in all situations. The use of Bovine Serum Albumin [BSA; 3.0% (w/v) in TBS] was necessitated when certain custom dilutions of antibodies were to be used.

The proteins were initially visualized using BCIP/NBT (5-bromo 4-chloro 3'-indoyl phosphate/nitro-blue tetrazolium). Early experiments performed according to the manufacturer's instructions produced blots which suffered from high background staining, hampering the clear-cut interpretation of the protein bands (Fig 3.4 a). Further investigation of the problem indicated that the washing protocol was of key importance. Manufacturer's instructions specified that blots be subjected to a washing regime involving 3 x 5 minutes. rinses (in 1:15 diluted wash buffer). However, when the duration of wash steps was increased to 10 minutes per wash, background staining was greatly reduced (Fig 3.4 b).

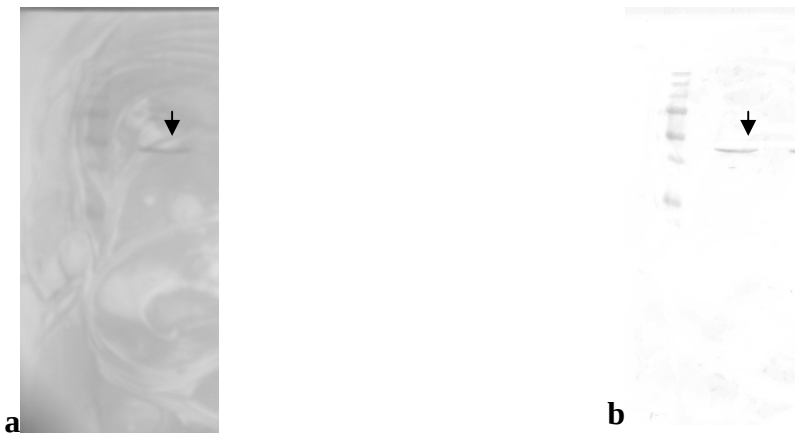

Fig 3.4: Influence of blot washing protocol on background staining.

Beta actin was used as a loading-transfer control. The blot was developed for enzymatic staining using either the manufacturer's washing protocol (5 minutes (**a)**) or the laboratory-derived method (**b**). The molecular markers were Precision Plus Protein™ WesternC™ standards (BioRad). Minigels were routinely used for western blot. Ponceau S was used to confirm protein transfer in advance of blot processing for antibody-enzyme staining. Arrows indicate beta actin band visible on the blot after development.

The next phase of the work involved further standardization of the system using representative RPE proteins (derived from treated/untreated cell preparations). Two tight junction proteins, of different molecular mass, were selected for this purpose: occludin, a 65kDa protein and Zo-1 with a molecular mass of 220kDa. A representative blot showing the staining of occludin is shown in Fig. 3.6. Optimal transfer times were found to be in the region of 2hours (occludin) to 3.5hours (Zo-1).

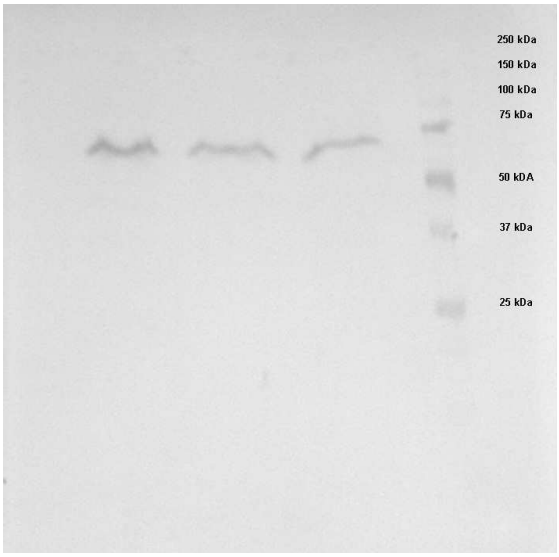

a **b** **c** **M**

Fig 3.5: Representative standardization blot for occludin.

ARPE-19 cells were treated with VEGF and RPE proteins extracted as described in section 2.2.2. VEGF (ng/ml): **A**, 100; **B**, 10; **C**, 0; **M**, molecular weight markers.

Amplification of the antibody-binding reaction by chemiluminescence (Fig. 3.6) was also investigated as a detection tool as this method is more sensitive (Conrad *et al*, 2001). The system used employed HRP-labelled secondary antibody and beta actin was initially used as a transfer control.

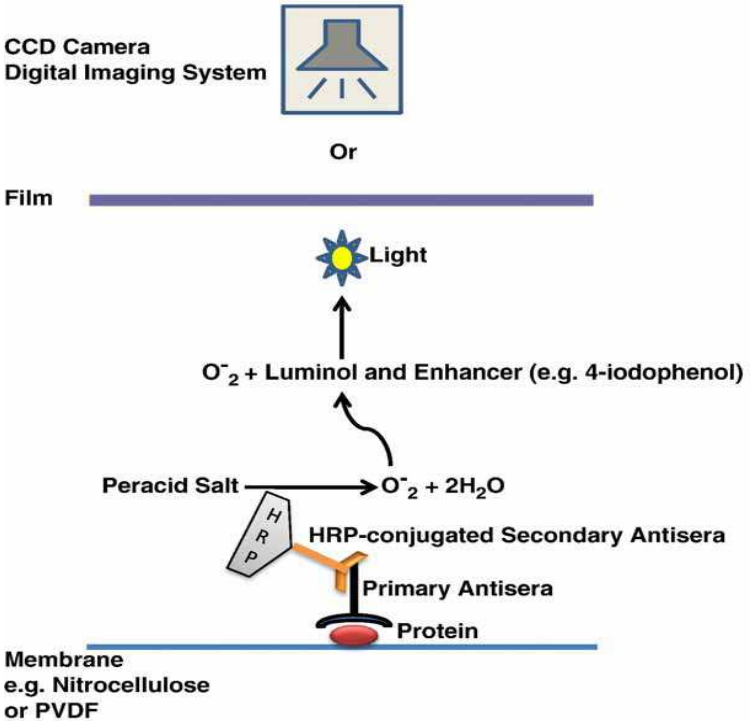

Fig 3.6: Principle of chemiluminescent visualization of proteins on western blot. (from MacPhee, 2010)

For optimal detection of tight junction proteins, overnight incubation with primary antibody at 4^{o}C on a shaker was followed as a rule, followed by incubation in secondary antibody at room temperature for 3 hours. Issues regarding the purity of commercially-sourced antibodies were identified as a vital factor in contributing to background staining. Tight junction antibodies bought from Invitrogen were the final choice after trying the product of a variety of other suppliers.

3.3 Immunoflourescence

Growth factors which showed a significant effect on RPE protein expression (as detected by western blotting) were selected for further study to examine their expression within cells. In the technique of immunofluorescence, antibodies are used directly on cultured, fixed cells, to probe for the expression of the tight junction protein of interest, thereby allowing direct visualization of its location in the cell.

For imaging convenience, it was essential to grow the cells on a surface which could be used with a microscope. While chamber slides (Labtek) were available, they suffered from the disadvantage of being prone to contamination due to the loose top cover (and were also relatively expensive). The use of 0.1% (w/v) gelatine coated sterile coverslips proved to be a viable alternative, although slight background staining was evident during image capture (Fig 3.7a) as compared with a non-gelatine coated control slide (Fig 3.7b). RPE cells did not exhibit auto-fluorescence (data not shown) when tested for the same.

Three different cells fixatives were investigated for optimal performance: acetone – formalin (1:1), formalin (3% v/v) and ice cold methanol. Of these, methanol was found to give superior results. Formalin fixation required an additional permeabilization step using Triton-X 100. Fixation using 100% methanol has been previously shown to preserve cell morphology (Nogouchi *et al*, 1997) and does not require additional permeabilization treatments. Hence this was the method of choice in the current study. The antibody staining protocol was initially tested using a vimentin antibody, which was found to work well using a 1:150 dilution (Fig 3.8).

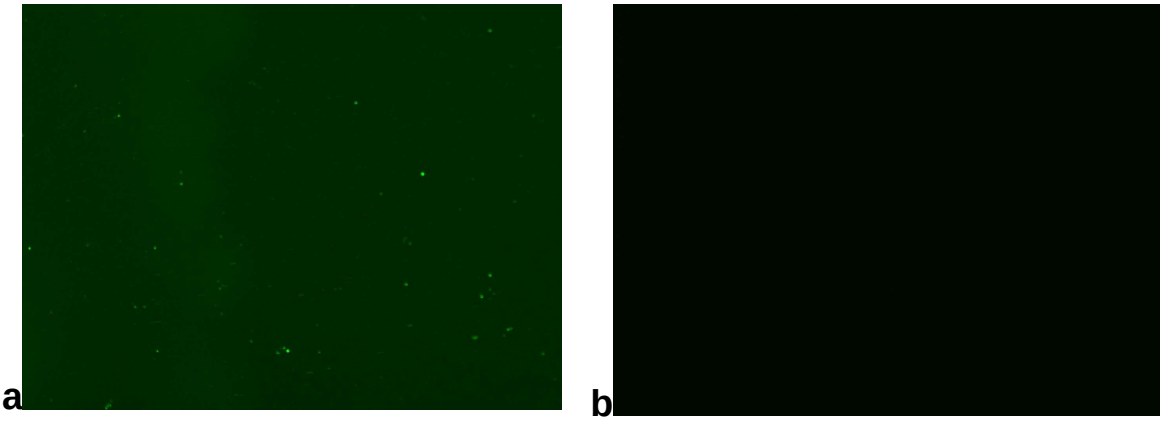

Fig 3.7: Gelatine coated slide: non-specific background staining using FITC label.

A 0.1% Gelatin coated blank cover slip (**a**) and uncoated cover slip (**b**) were tested for background fluorescence. No cells were cultured on these slides. Experimental conditions were the same as that for cultured cover slips. Gelatin coating contributed to background fluorescence.

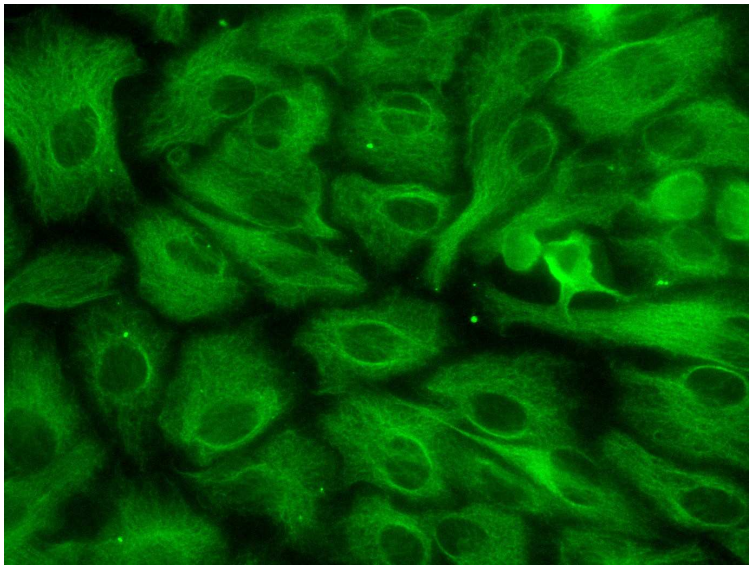

Fig 3.8: FITC-stained RPE cells probed for vimentin.

Untreated RPE cells cultured on coverslip was probed using 1:500 dilution of vimentin antibody. The cells were stained with FITC. Images captured at magnification: x40

Slightly more difficulty was encountered when using antibodies directed against tight junction proteins. Although Zo-1 presented little challenge, background staining was encountered with occludin antibody, compounded by the fact that it needed a longer incubation time to obtain satisfactory results. Indeed, achieving a balance between the antibody incubation duration required to effect detection of the target bio-molecule, and the avoidance of unacceptable background staining, was a recurring theme. For example, no staining was apparent if anti-claudin–1 was incubated at 4^{o}C for up to 16 hours. Extending the incubation duration to 24 hours at 4^{o}C for the primary antibody produced a target-specific signal, but contributed to non-specific binding (result not shown). Such a situation was also encountered in the case of RPE cells probed for claudins 2, 3, 4 and 5: heavy background signal was accompanied by a granular staining pattern in the cytoplasm (Fig 3.9). Fortuitously, certain claudin antibodies were being used simultaneously by other workers in the laboratory, and the dilutions optimised by immuno-histochemistry using breast and cervical carcinoma tissues, were also found to be suitable for the present studies; remaining claudin antibodies (claudins 2, 3 and 4) were used at dilutions recommended by the manufacturer, and provided adequate results. A representative set of images of RPE cells stained for Occludin and Zo-1 are shown in Fig 3.10.

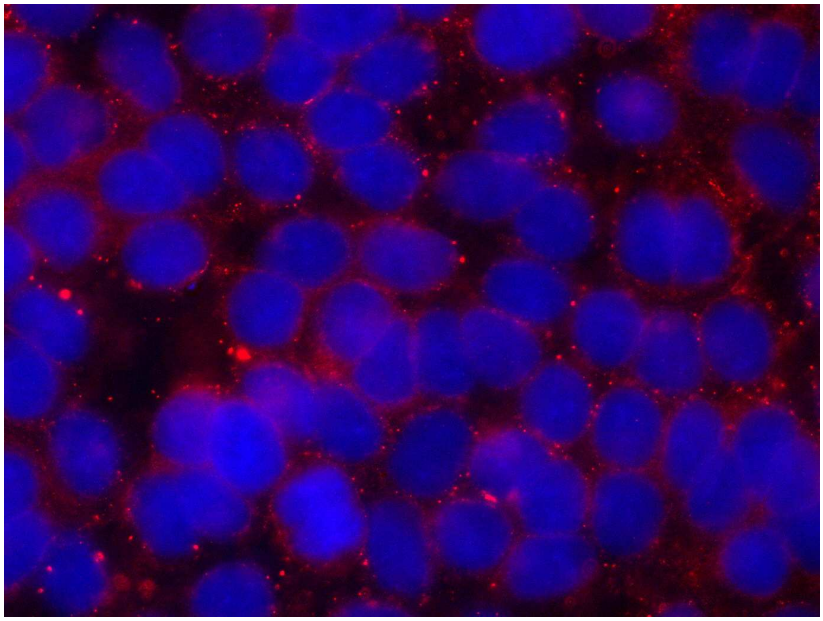

Fig 3.9: RPE cells stained for expression of Claudin-1

Untreated RPE cells cultured on coverslip probed using for claudin-1. Incubation time –16 hours. Texas Red staining shows granular cytoplasmic staining pattern; nuclei stained using DAPI. Magnification x40.

a)

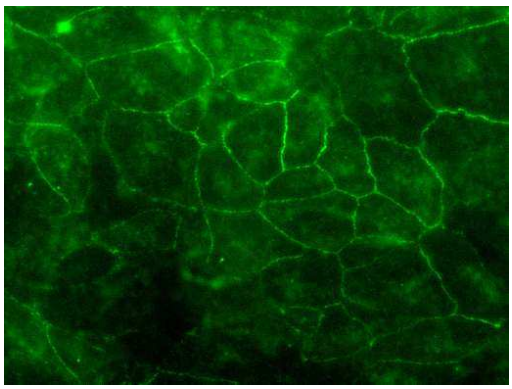

b)

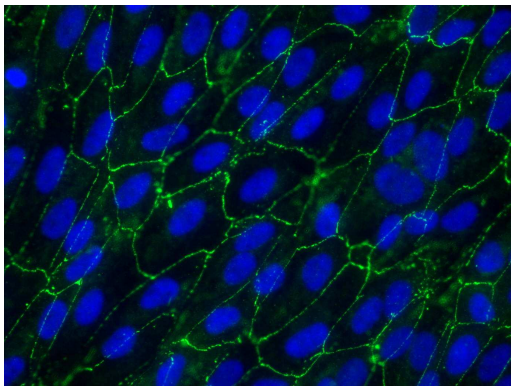

c)

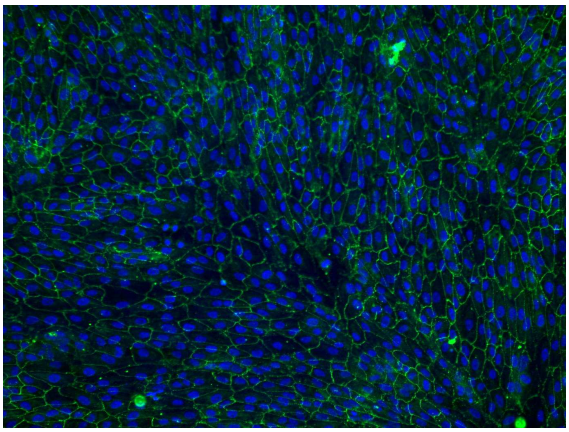

Fig 3.10: Untreated RPE cells probed for (a) occludin, (b, c) Zo-1. (Optimized) Incubation time used – 12 hours. The cells were stained using FITC. Nuclei stained using DAPI in **b** and **c**. Magnification x40, except **c** (x10).

Chapter 4

Effect of Growth Factors on the outer Blood Retinal Barrier

4.1. Introduction

Vascular endothelial growth factor is the collective name for a family of pro-angiogenic growth factors. VEGFs are primarily involved in development and differentiation of vascular endothelium and promote neovascularisation. VEGF has been identified as a key protein involved in the breakdown of the BRB. However, the molecular mechanism of this has to be further elucidated.

4.1.1 VEGF structure and functions

Vascular endothelial growth factors belong to the VEGF / PDGF (Platelet Derived Growth Factor) group of the cysteine knot super-family of hormones and growth factors (Holmes and Zachary, 2005). The VEGF family consists of a group of structurally and functionally related pro-angiogenic growth factors named VEGF-A, VEGF-B, VEGF-C, VEGF-D, VEGF-E, VEGF-F and Placental growth factor (PlGF). Of these, VEGF-A, B, C, D and PlGF are expressed in humans (Holmes and Zachary, 2005). VEGF-A is the most thoroughly studied among the VEGF family and has nine isoforms produced by alternative splicing of a single VEGF gene consisting of eight exons (Bhishitkul, 2006). These isoforms are named on the basis of the number of amino acids present in their sequence as indicated by the subscript number. Currently identified isoforms of VEGF-A are $VEGF_{121}$, $VEGF_{145}$, $VEGF_{148}$, $VEGF_{162}$, $VEGF_{165}$, $VEGF_{165b}$, $VEGF_{183}$, $VEGF_{189}$ and $VEGF_{206}$ (Shams and Ianchulev, 2006).

Studies conducted by Hartnett *et al*., 2003 showed that co-culture of RPE cells with endothelial cells reduced the barrier properties of the RPE and the reduction was in part mediated by soluble VEGF. The same study reported greater release of soluble VEGF into the medium compared to solo culture of RPE. VEGF and cytokines

including TNF-α have been shown to disrupt RPE barrier function (Ablonczy and Crosson 2007, Hartnett *et al* 2003) and to cause a reduction in regulated removal of subretinal fluid, leading to macular oedema (Funatsu *et al* 2009, Ablonczy and Crosson 2007). Patients suffering from Proliferative Diabetic Retinopathy (PDR) were reported to have a very high level of VEGF (5.42ng/ml) as compared to a non-diabetic subject (9pg/ml) (Funatsu *et al*, 2005, Mitamura *et al*, 2002). However, the exact molecular mechanism that leads to growth-factor-mediated disruption of oBRB has not been elucidated.

The biological effects of VEGF are mediated through a family of tyrosine kinase receptors known as VEGF Receptors (VEGFRs) (Holmes and Zachary, 2005). The VEGFRs differ considerably in their signalling properties and are assisted by non-signalling co-receptors in the signalling cascade. VEGFR-1 and VEGFR-2 play a key role in angiogenesis of blood vessels while VEGFR-3 is associated with lymphangiogenesis. Fig 4.1 shows the association of various isoforms with VEGFRs.

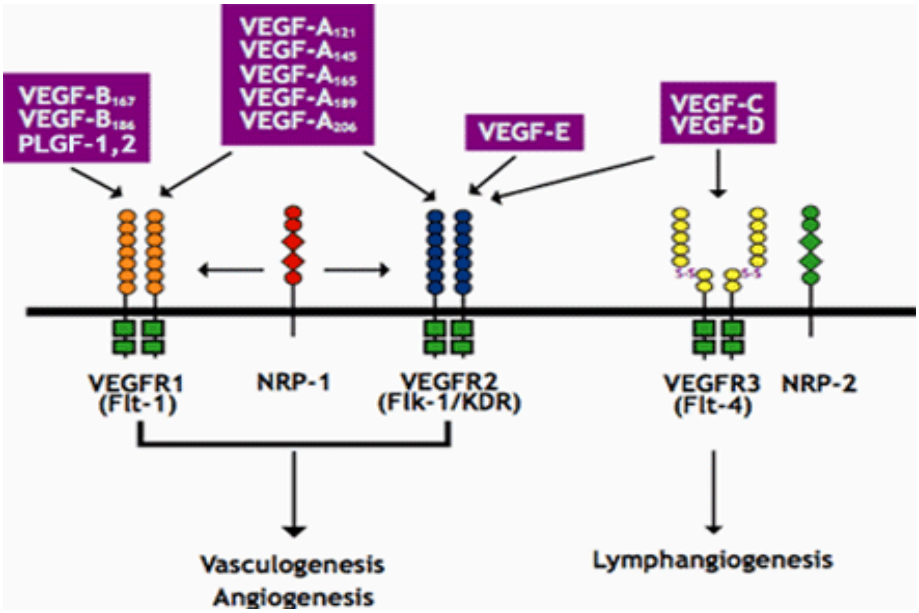

Fig: 4.1 – VEGF - VEGFR interaction (Source: Hicklin and Ellis, 2005)

4.1.2 Placental Growth Factor

PlGF is a 38kDa, pro-angiogenic member of the VEGF family and shares several functional traits of other VEGF isoforms. As the name indicates, PlGF is expressed in placental cells and is primarily involved in embryonic vasculogenesis. However, PlGF is also produced by non-placental cells including RPE (Miyamoto *et al* 2008).

PlGF occurs as a homodimer and shares substantial structural similarity with VEGF-A (Miyamoto *et al*, 2008). Four PlGF isoforms are produced by alternative splicing of the PlGF gene (Yang *et al* 2003). PlGF isoforms do not interact with VEGFR2, but selectively bind to the VEGFR-1 receptor. PlGF is produced by RPE under hypoxic conditions (Hollborn *et al* 2006). Patients suffering from PDR were reported to have very high levels of PlGF of up to 1.039ng/ml (Mitamura *et al*, 2002). PlGF is found in very low levels of between 7pg/ml to 12pg/ml in the vitreous fluid of control non-diabetic patients (Mitamura Y *et al* 2002).

4.2. Aims

VEGF and PlGF are key proteins that cause breakdown of iBRB. The RPE has been found to produce VEGF and PlGF directly (Kaur *et al*. 2008, Kannan *et* al. 2006, Strauss 2005). Hollborn *et al*, (2006) reported that unstimulated RPE secretes between 100 to 250pg/ml VEGF into the medium (Hollborn *et al*, 2006). However, the effect of PlGF and VEGF on the Retinal Pigment Epithelial barrier has not been extensively investigated. In this study, it was therefore of interest to examine the latter aspect. The expression and localization of occludin and Zo-1 on RPE membrane was studied using western blotting and immunoflourescence staining. The toxicity of growth factors used was investigated using a standard Trypan blue assay.

4.3. Cell Culture and Growth Factor Treatment

ARPE-19 cells were cultured as described in section 2.2.1 until desired confluence was achieved. The cells were then washed thrice to remove all traces of serum and incubated in serum-free medium for 6 hours. Afterwards, the monolayer was rinsed with sterile PBS and treated with 10-100ng/ml VEGF or 1-10ng/ml PlGF for 24 hours. Following treatment, the cell monolayer was rinsed with sterile PBS to remove any traces of medium. The cells were then extracted as described in section 2.2.2. Protein analysis of the cell extract was performed using the Bradford assay as described in section 2.2.3.

Equal amounts of protein per sample were loaded to minigels. Electrophoresis was performed as described in section 2.2.4. The separated proteins were then blotted to a nitrocellulose membrane using the optimized method described in 2.2.5. Transfer time used was 2 hours for Occludin and 3.5 hours for Zo-1.

Cell viability assay was performed using trypan blue (Sigma Aldrich) as described in section 2.2.6

4.4 Results and Discussion

4.4.1 Occludin expression in VEGF treated RPE

In this study, changes in tight junction expression were observed in cultured RPE cells exposed to different concentrations of VEGF or PlGF for a 24 hour period.

Analysis of VEGF-mediated protein expression by western blot (Fig 4.2) yielded inconclusive results; an apparent down-regulation in expression of occludin in RPE treated with VEGF was evident (Fig 4.3), but this was not statistically significant ($P > 0.05$) when subjected to densitometric analysis using Imaxia Gelfox (Table 4.1). Parametric analysis was done using ANOVA

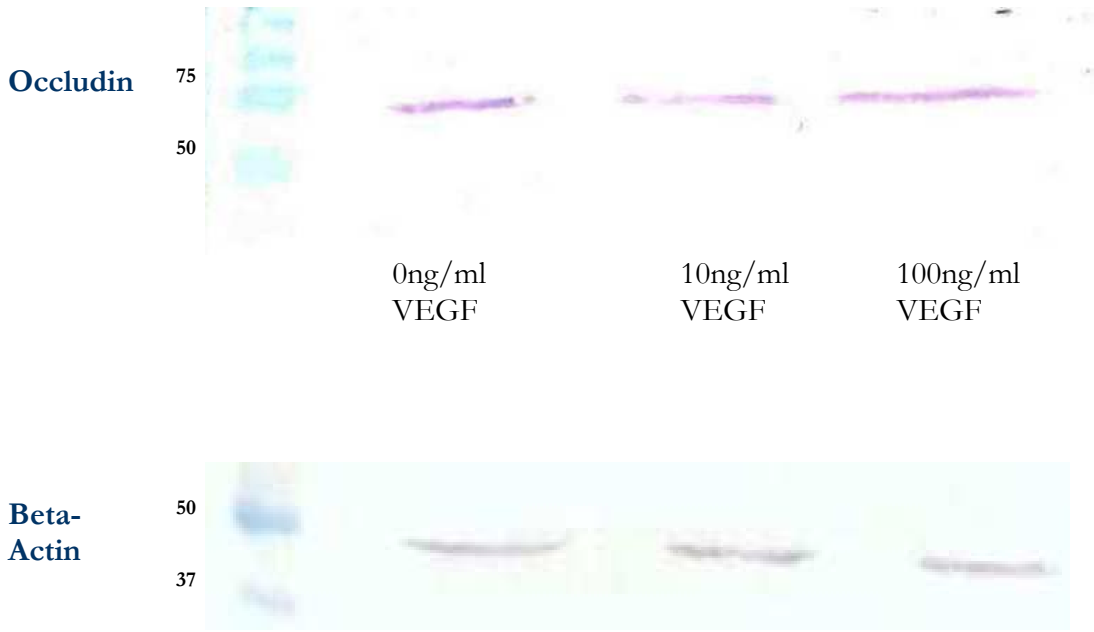

Fig: 4.2 – Western blot analysis of effect of VEGF on occludin in RPE.

The blot was developed using chromogenic substrate BCIP/NBT. Normalisation of blots was achieved using beta actin. Blot was done in duplicate.

VEGF concentration	Mean	P Value
0ng/ml	7557	0.366
10ng/ml	6443.5	
100ng/ml	5597.5	

Table 4.1 Mean pixel intensities for two sets of samples shows a decrease in occludin band intensity with exposure to VEGF. P-value calculated using single factor ANOVA shows that the change is not statistically significant.

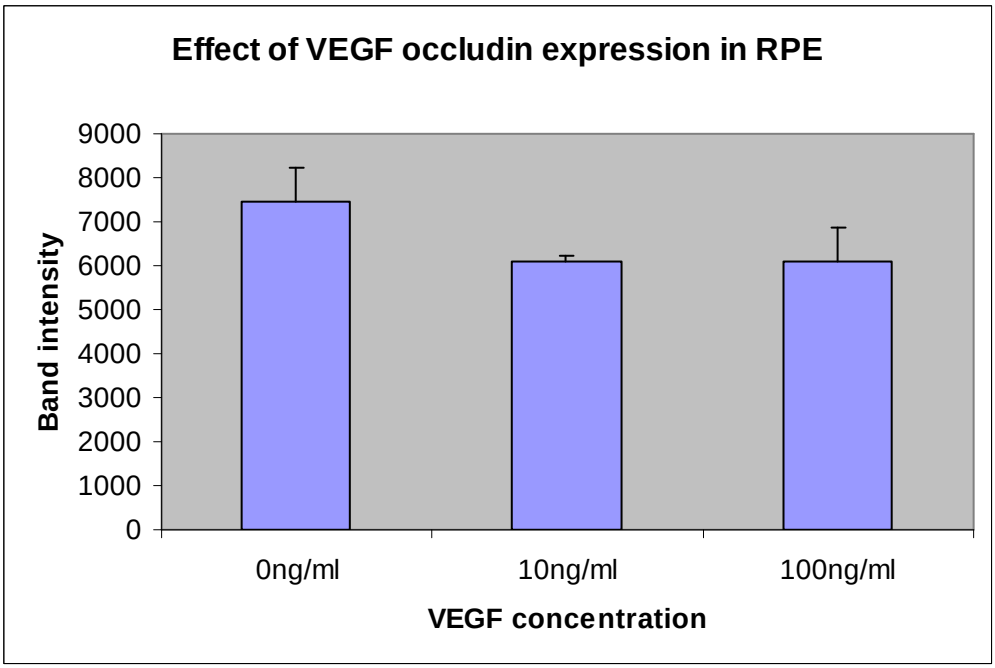

Fig: 4.3 Effect of occludin expression in RPE cells treated with VEGF.

Occludin in RPE is down-regulated with exposure to VEGF. The graph represents the mean value for two western blot analyses and the standard error of the mean is represented by Y-error bars.

However, investigation of cellular occludin expression by immunoflourescence imaging confirmed a reduction in occludin production, evident by a loss of junctional staining in RPE cells, after exposure to 1.0 and 10ng/ml VEGF (Fig 4.4). Such concentrations of VEGF are representative of in vivo levels associated with the disease state. For example, vitreous VEGF in a diabetic patient was found to be elevated as high as 5.424ng/ml, while in a healthy individual, it is 9.0pg/ml (Mitamura *et al* 2002).

Increased paracellular permeability of RPE cells following exposure to high concentrations of VEGF has been reported previously (Ablonczy and Crosson 2007; Geisen *et al* 2006), and is recognised as an early sign of macular oedema and oBRB breakdown (Ablonczy and Crosson 2007; Caldwell *et al* 2005). However, Ghassemifar and colleagues (2006) reported that VEGF increased the TEER of ARPE-19 cells, and tightened the RPE junction. Such contradictory results reflect the complexity of the cellular control mechanism RPE function and point to the need for further studies in this area.

a)

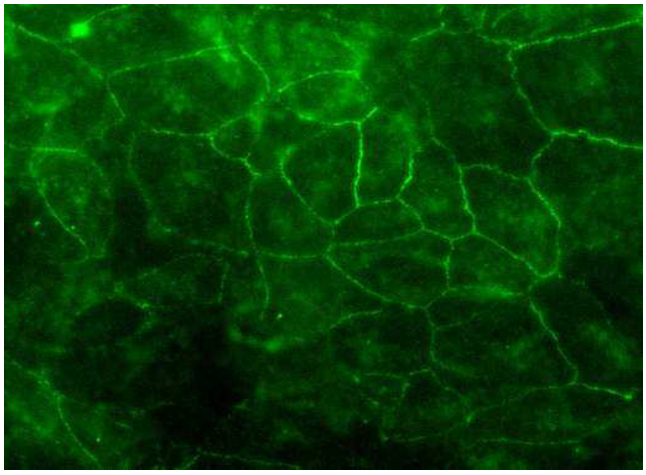

b)

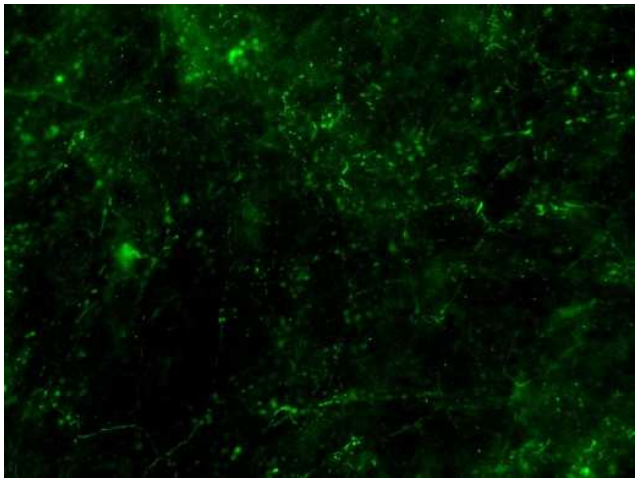

c)

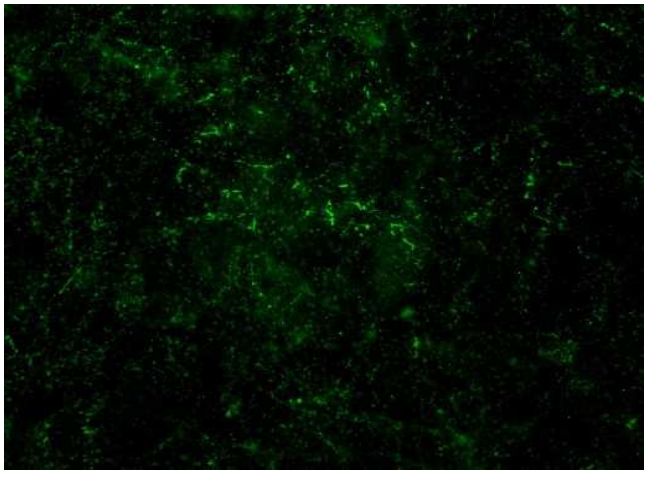

Fig: 4.4 Immunoflourescence staining showing junctional loss of occludin in cultured RPE cells treated with VEGF Untreated (**a**), treated with 10ng/ml (**b**) and 100ng/ml VEGF(**c**). RPE cells were stained using FITC and images captured at 40x magnification.

4.4.2. Zo-1 expression in RPE treated with VEGF

Expression of ZO-1 in RPE was not found to vary significantly following treatment with VEGF, as determined by western blotting (Fig 4.5). Densitometric analysis of band intensities indicated a progressive increase in expression of Zo-1 in VEGF treated RPE, although this was not statistically significant as evident from Table 4.2

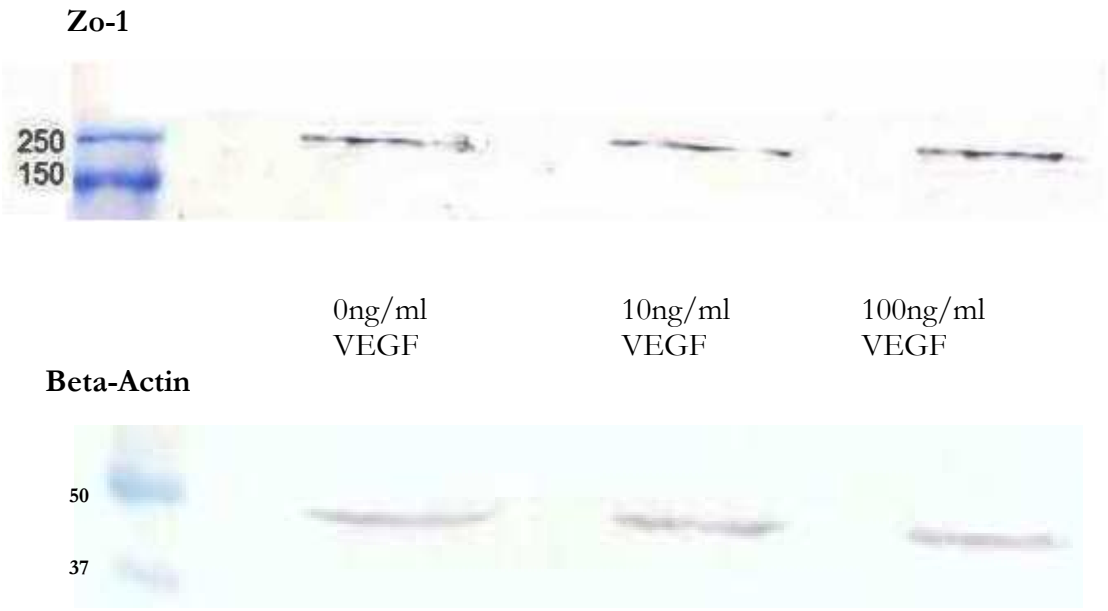

Fig: 4.5 - Western blot analysis of effect of VEGF on Zo-1 in RPE.

The blot was developed using chromogenic substrate BCIP/NBT. Normalisation of blots was achieved using beta actin. Blot was done in triplicate.

VEGF concentration	Band intensity (Mean ±SEM)	P Value
0ng/ml	4422.33 ± 907.4	0.273
10ng/ml	6205.67 ± 1323.6	
100ng/ml	7219 ± 1060.3	

Table 4.2 Mean band intensities (± standard error of mean) for three sets of samples treated with VEGF shows an increase in Zo-1 band intensity with exposure to VEGF. P-value calculated using ANOVA shows that this change is not statistically significant.

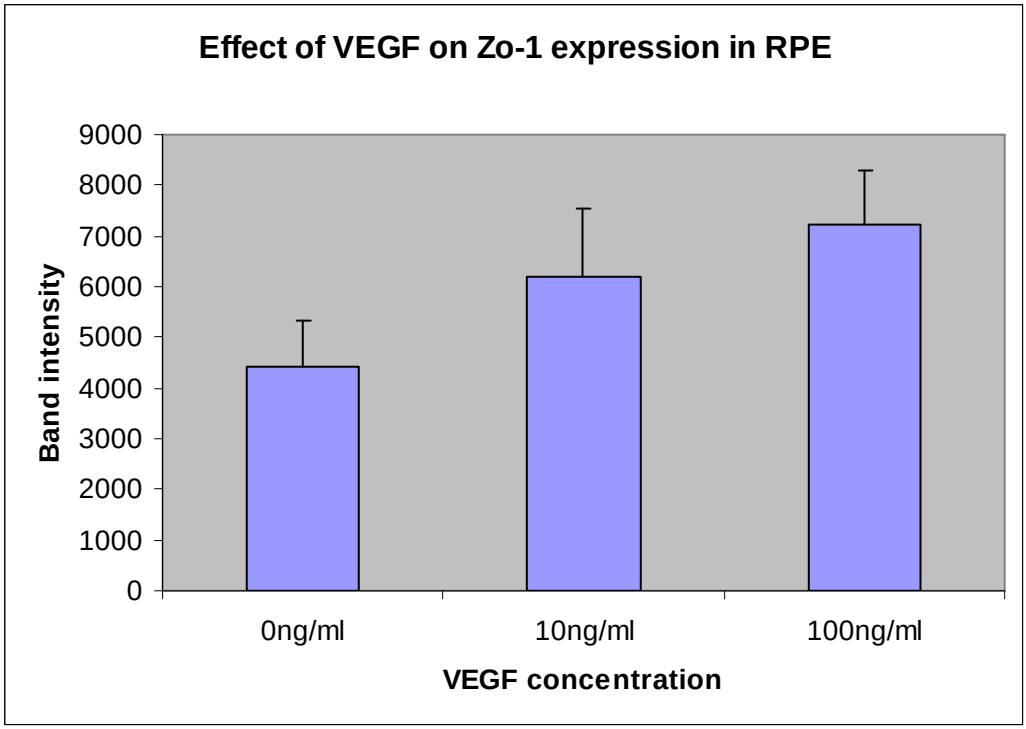

Fig: 4.6 Effect of Zo-1 expression in RPE cells treated with VEGF.

Zo-1 in RPE is up-regulated with exposure to VEGF. The graph represents the mean value for three sets of data and the standard error is represented by Y-error bars.

Investigation of Zo-1 expression in RPE using immunoflourescence staining showed de-localization of Zo-1 from membrane after treatment with 1.0ng/ml and 10.0ng/ml VEGF (Fig 4.7).

Zo-1 is a member of the MAGUK family of proteins and interacts with occludin and claudins to maintain integrity of the barrier (Balda *et al*, 2003). Thus VEGF may affect barrier function by modulating Zo-1 levels, which may affect Zo-1 interaction with occludin and the claudin tight junction proteins. Additional factors to consider in future experiments would be to compare apical versus basolateral administration of VEGF, expression of VEGFR1 and VEGFR2 and effects on TEER. This additional data would allow us to predict more fully the effects of VEGF on RPE barrier properties, and on the outer BRB in vivo.

Cultured ARPE cells have been reported to express very high levels of VEGF of upto 777.2pg/ml in media, constitutively (Geisen *et al*, 2006). Basal administration of upto 500ng/ml VEGF did not produce significant change in permeability in the RPE while apical administration of upto 1ng/ml produced a significant increase in permeability. Our data shows about 20% decrease in occludin expression in the RPE treated with 100ng/ml VEGF as compared to the untreated sample. Although this value is not statistically significant ($P>0.05$), this is in agreement with studies mentioned earlier (Ablonczy and Crosson 2007, Geisen *et al* 2006).

a)

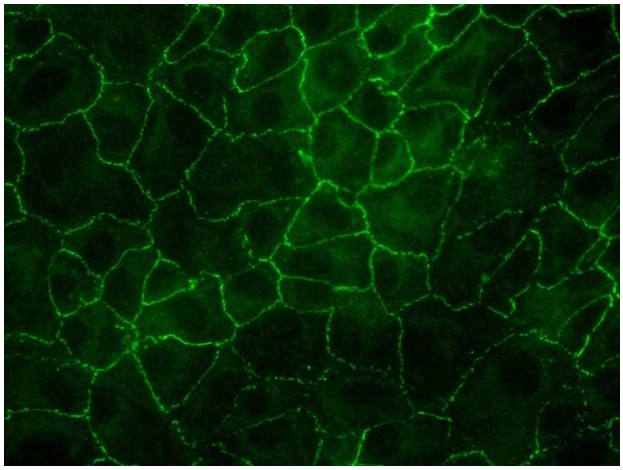

b)

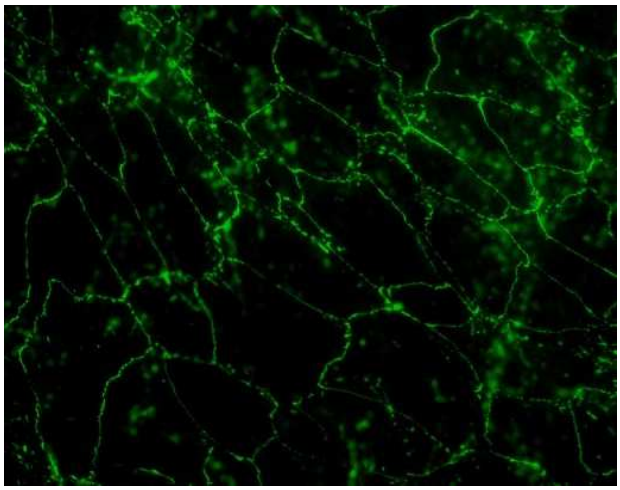

c)

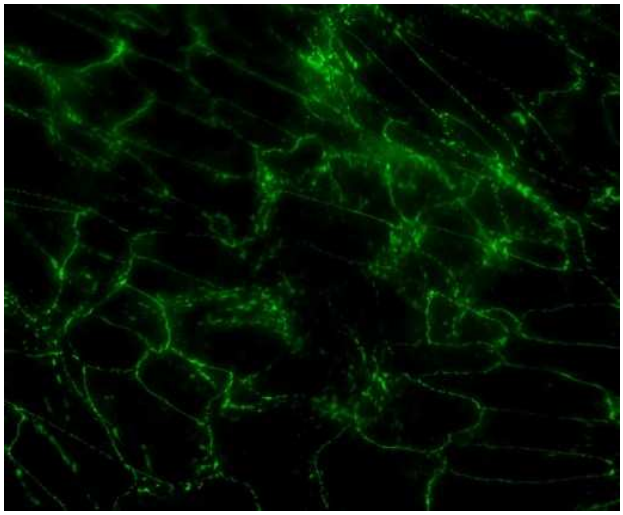

Fig: 4.7 Immunoflourescence staining showing junctional loss of Zo-1 in cultured RPE cells treated with VEGF: Untreated (a), treated with 10ng/ml (b) and 100ng/ml VEGF(c). RPE cells were stained using FITC and images captured at 40x magnification.

4.4.3. Occludin expression in RPE treated with PlGF

VEGF and PlGF belong to the same family of pro-angiogenic growth factors and shares significant similarity in their amino acid sequence (Holmes and Zachary, 2005). Unstimulated ARPE cells secrete ~5ng/ml PlGF *in vitro* (Hollborn *et al* 2006). This is close to the level found in a normal vitreous fluid reported by Mitamura *et al* (2002).

Western blot analysis of PlGF induced occludin expression (Fig 4.8) showed an increase in protein expression. Statistical analysis of mean occludin band intensities showed a progressive increase in protein expression (Fig 4.9). However, the two tailed P-values indicated that this change was not statistically significant (Table 4.3)

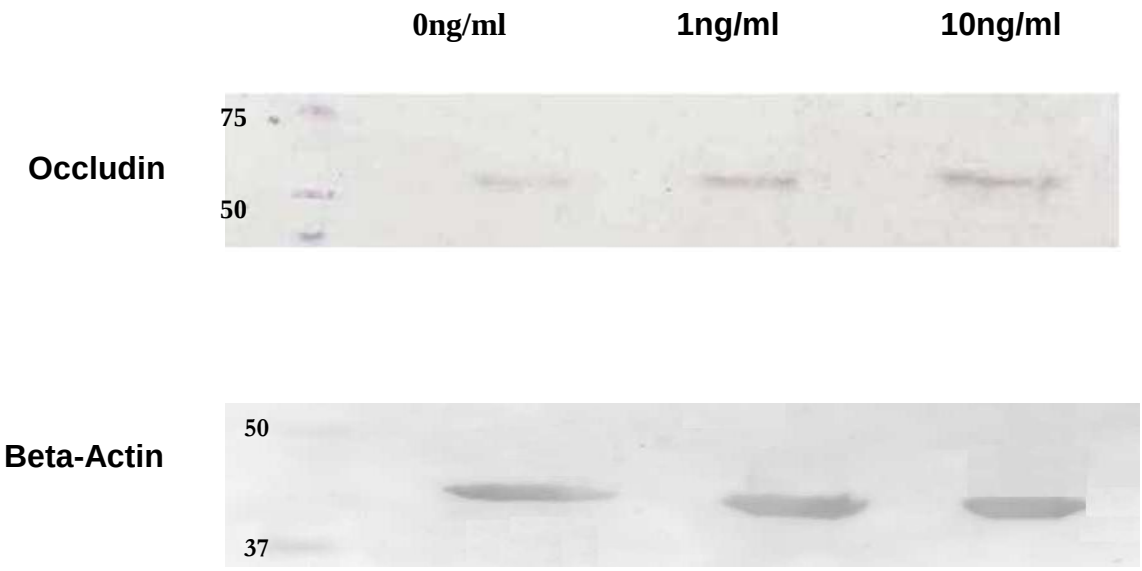

Fig: 4.8 - Western blot analysis of effect of PlGF on occludin in RPE.

The blot was developed using chromogenic substrate BCIP/NBT. Normalisation of blots was achieved using beta actin. Blot was done in triplicate.

PlGF concentration	Band intensity (Mean ±SEM)	P Value
0ng/ml	2059.67 ± 247.1	0.0259
10ng/ml	2606 ± 224.5	
100ng/ml	3996.67 ± 554.8	

Table 4.3 The table shows mean occludin band intensities (± standard error of mean) for three sets of samples treated with VEGF. The data was compared and a P value ≤0.05 in a single parametric ANOVA was considered statistically significant.

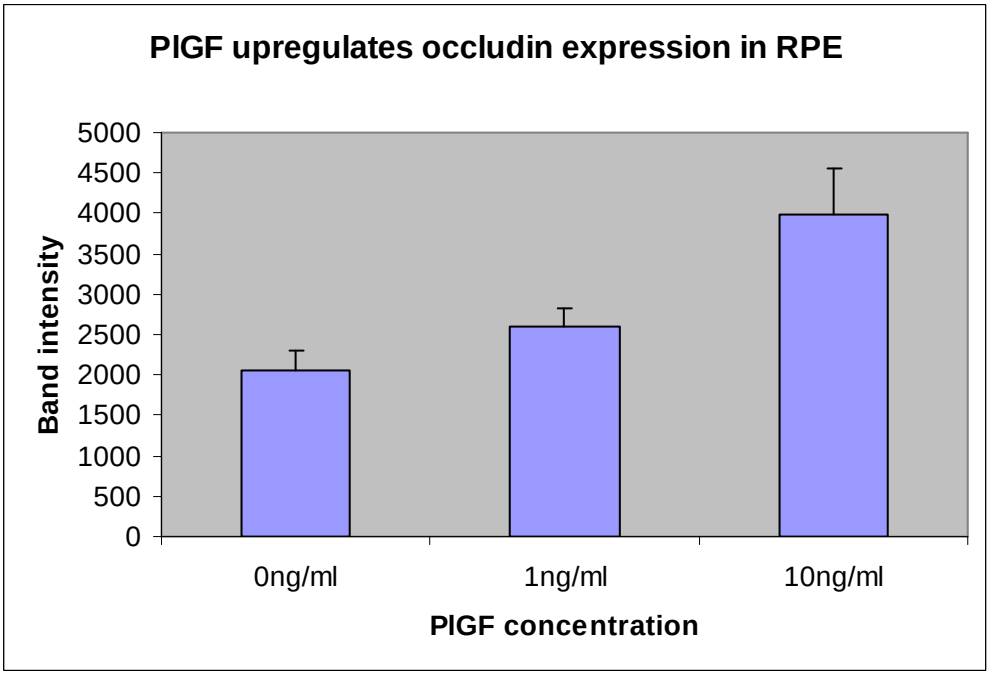

Fig: 4.9 Effect of occludin expression in RPE cells treated with PlGF.

Occludin in RPE is up-regulated with exposure to PlGF. The graph represents the mean value for three sets of data and the standard error is represented by Y-error bars.

Immunoflourescent staining showed a loss of junctional staining for occludin when cells were treated with PlGF (Fig 4.10). A study using FACS analysis could be performed in the future, whereby occludin expression on PLGF-treated and control RPE are quantitated

a)

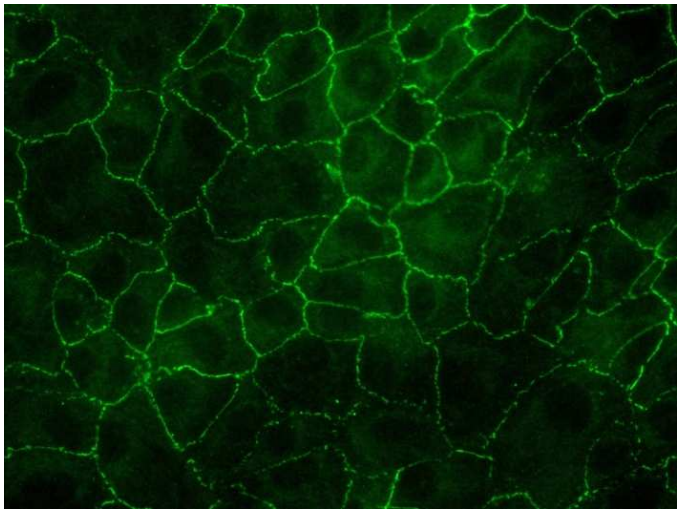

b)

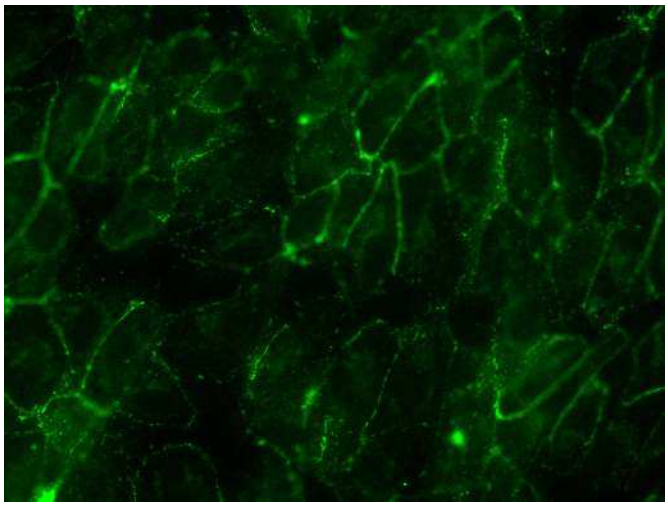

Fig: 4.10 Immunoflourescence staining showing junctional loss of occludin in cultured RPE cells treated with PlGF: Untreated (a) and treated with 10ng/ml (b) PlGF. RPE cells were stained using FITC and images captured at 40x magnification.

PlGF levels as high as 1.034ng/ml was reported in the vitreous fluid of patients suffering from PDR (Mitamura *et al*, 2002). Elevated vitreous PlGF of up to 806.5pg/ml was reported in patients suffering from PDR with macular oedema and may contribute to retinal oedema and accumulation of sub-retinal fluid in diabetic retinopathy (Miyamoto *et al* 2007). Intra-vitreous PlGF level in a healthy individual is reported to be between 7 – 12 pg/ml. In diabetic patients, the vitreous levels were found to be elevated to 100-1000pg/ml (Mitamura *et al* 2002).

Although PlGF was expected to increase the paracellular permeability in RPE, it was seen to upregulate the occludin content in RPE, indicating possible strengthening of tight junctions. PlGF acts purely through VEGFR-1. VEGFR-1 activation stimulates expression of Pigment Epithelium derived factor (PEDF) which is a potent antagonist to VEGF and PlGF (Ohno-Matsui *et al* 2003). PEDF reverses redistribution of occludin from tight junctions caused by VEGF and PlGF (Ho *et al* 2006, Ablonczy *et al* 2009). Immunofluorescence images showed occludin localization at the RPE membranes (Fig 4.10). PEDF was also found to upregulate occludin in retina of diabetic rats (Yu *et al* 2010). This antagonistic effect of PEDF may be the reason for up-regulation of occludin in PlGF-treated RPE cells as observed from western blotting.

PlGF has been reported to produce no significant changes in permeability of the RPE (Ablonczy and Crosson 2007) although it has been found in elevated levels along with VEGF in patients suffering from diabetes (Miyamoto *et al* 2008, Mitamura *et al* 2002). A recent study reports that prolonged exposure to PlGF leads to BRB breakdown (Kowalczuk *et al*, 2011). Immunoflourescence staining of occludin in

PlGF treated RPE showed change in membrane localization of occludin (Fig 4.10). This study involved a standard growth factor exposure time of 24 hours. By far, results reported regarding behaviour of PlGF in the retina are contradictory and further studies are warranted. A time dependant study of changes in barrier function may be useful in studying this further.

Viability data obtained from trypan blue assay (Fig 4.11) showed that RPE cells retained 100% viability after exposure to 100ng/ml VEGF or PlGF.

4.5 Viability Assay

RPE cells were treated with 1ng/ml and 10ng/ml PlGF and 10ng/ml and 100ng/ml VEGF as described in section 2.2.2. Cell viability assay was performed as per protocol outlined in 2.2.6.

a) VEGF

A total of 98 cells were counted in 4 chambers of haemocytometer under microscope. All cells were unstained after exposure to trypan blue for 5 minutes.

b) PlGF

A total of 103 cells were counted in 4 chambers of the haemocytometer under microscope. All cells were unstained after exposure to trypan blue for 5 minutes.

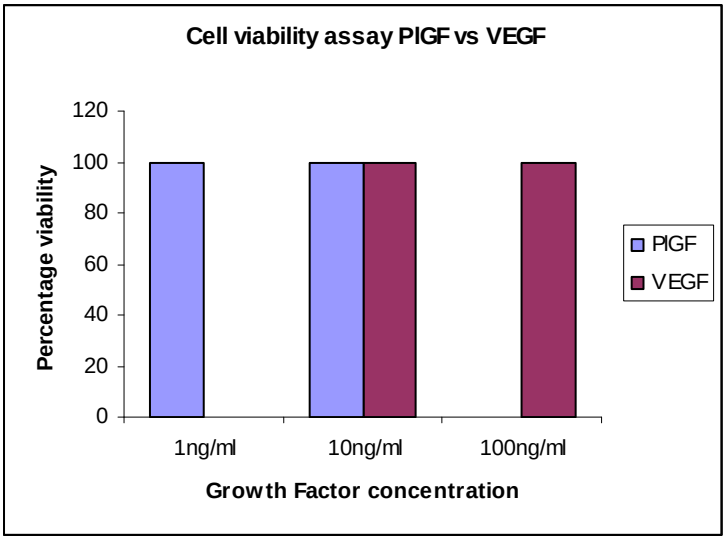

Fig 4.11 - Percentage viability of cells treated with PlGF / VEGF for 24 hours.

Cell viability assay performed on RPE cells showed that RPE cells retained viability after stepping down medium to serum free media for 6 hours followed by growth factor treatment for 24 hours (Fig 4.11).

Chapter 5

Effect of Cytokines on the outer Blood Retinal Barrier

5.1 Introduction

An intact tight junction barrier is crucial for maintenance of retinal homeostasis. Pathogenesis and progression of several disorders involving breakdown of tight junctions are mediated by cytokines (Capaldo and Nusrat, 2009, Harada *et al.* 2006). RPE cells play an important role in the immune response. For instance, they express Major Histocompatibility complex (MHC) molecules, adhesion molecules, FasL and cytokines (Holtkamp *et al*, 2001). Cytokines such as Tumor necrosis factor alpha (TNF–α), Interleukin-1 beta (IL-1β) and Interferon-gamma (IFN-γ) regulate cells and also express immune and inflammatory properties (Demircan *et al*, 2006). RPE cells express chemokine receptors basally (Yamada *et al*., 2006, Blaauwgeers HG *et al*., 1999). It has been recognised that low grade inflammation plays a role in AMD. Thus the inflammatory response in AMD lesions is characterised by an infiltration of the BRB, including the RPE layer, by both macrophages and lymphocytes (Penfold *et al*., 2002, Reddy *et al*., 1995).

Studies involving AMD eyes were pursued, where the composition of drusen, extracellular deposits and plaques that accumulate in close association with the RPE, were investigated (Grossniklaus *et al*., 2005, Anderson DH *et al*., 2002, Hageman GS *et al*., 2001). The presence of few small drusen in the macula of patients aged over 40 is not considered harmful; however the increase in size and number of drusen deposits contributes to progressive AMD (An E *et al*, 2008). Drusen has been shown to attract macrophages to the sub-RPE space (Lopez PF *et al*, 1991) and results showed the major cellular components in CNV membranes included macrophages and fibroblasts (Grossniklaus *et al*., 2005). It is known that the major inflammatory cytokines produced by macrophages, neutrophils and lymphocytes are IFN-gamma, TNF–α and

IL1-β (An E *et al*, 2008), and these cytokines may be produced locally at the RPE. Furthermore, TNF-α and IL1-β are linked with pro-inflammatory RPE cell functions (Hollborn *et al*., 2001, Elner VM *et al*., 1997). TNF–α and IL-1 has been found in ocular specimens of autoimmune anterior uveitis (Patel and Chan, 2008) and the neovascular membranes of wet AMD (Wan L *et al* 2010, An E *et al*, 2008). In this work we have studied two pro-inflammatory cytokines, IL1-β, which is produced by activated macrophages, and TNF–α, which is produced primarily by macrophages, as well as other cell types.

5.2 Tumor necrosis factor alpha (TNF-α)

Tumor necrosis factors (TNFs) are a family of immuno-modulatory cytokines which are produced in response to inflammatory stimuli. TNFs are usually produced by activated macrophages and monocytes in the human body. Tumor necrosis factor alpha (TNF-α) is a potent pro-inflammatory cytokine with a number of biological effects (Holtkamp 2001). It is produced in the body, primarily by monocytes and macrophages, and plays a key role in initiation of immune responses in the body.

RPE cells express TNF-α receptors on their apical side (An E *et al* 2008). However, it is unclear whether RPE cells are a source of TNF-α. TNF-α has been implicated in pathogenesis of AMD (Dias JR *et al* 2011, Wan L *et al* 2010) and Diabetic Retinopathy (Joussen AM *et al*, 2002). TNF-α has been reported to stimulate production of VEGF by RPE cells, in pathogenesis of neovascular AMD. Kociok N *et al*., 1998 found no evidence for expression of TNF-α in non-stimulated RPE cells, in agreement with Tanihara H *et al*., (1992). However, it was reported that stimulation of RPE cells with IL-1B induce expression of TNF-α mRNA, although the protein was

not secreted (Tanihara H *et al*., 1992). De Kozak *et al* (1994) described production of TNF-α by three different strains of rat RPE cells in a constitutive manner, and this secretion of TNF-α correlated to their susceptibility to uveitis. Gustavsson C *et al* (2008) and Limb GA *et* al (1996) reported elevated levels of serum TNF-α may serve as an independent serum marker for development of PDR in type-1 diabetic patients.

5.3 Interleukin -1 beta (IL-1β)

The Interleukins are a large family of immuno-modulatory cytokines. Some of these are produced by RPE cells (Holtkamp *et al*, 2001). Interleukin-1 (IL-1) is one of the most potent mediators of immune response. These responses are either pro-inflammatory or lead to activation of immune system (Holtkamp *et al*, 2001). Two forms of IL-1 identified are Interleukin – 1 alpha (IL-1α) and Interleukin -1 beta (IL-1β). IL-1β is a potent pro-inflammatory cytokine which is found in elevated levels in patients suffering from proliferative vitreo retinopathy (PVR) and ocular inflammation (Demircan *et al*. 2006, Patel *et al*. 2006, Liou *et al*., 2002, Franks *et al*. 1992). Unstimulated RPE cells do not express genes for IL-1β or IL-1α, but the gene expression is readily induced by external stimuli such as endotoxin or lipopolysaccharide (Holtkamp *et al*, 2001). IL-1 produced by RPE cells play a role in inflammatory processes involving the retina (Holtkamp *et al*, 2001).

RPE cells express multiple receptors for cytokines including the Interleukin-1 receptor IL-1R (Leung *et al* 2009). RPE cells when stimulated with TNF – α and IL-1β, secretes IL-6 and IL-8 which are pro-inflammatory cytokines (Jaffe *et al*. 1995, Elner *et al*, 1992). IL-6 was found to activate macrophages and T-cells in vitro. Elevated levels of IL-6 were found in vitreous of patients suffering from PDR and

PVR as compared to a healthy eye (Canataroglu *et al*. 2005, Kojima *et al*, 2001). IL-8 is a pro-angiogenic cytokine and has the ability to activate neutrophils after they arrive at the site of infection (Holtkamp *et al*, 2001). RPE cells secrete IL-6 and IL-8 basally, towards the choroidal side, in a polarized manner (Holtkamp *et al*, 1998).

5.4 Aims

TNF- α and IL-1β have been associated with inflammatory conditions involving RPE and has been implicated in the pathogenesis of AMD and DR (Wan L *et al*, 2010, Demircan *et al* 2006). TNF-α is produced locally at oBRB by macrophages in low grade inflammatory conditions related to AMD. TNF-α may modulate expression of RPE tight junctions and disrupt oBRB. Elevated level of IL-1β is found in the vitreous of patients suffering from proliferative vitreo retinopathy (PVR) and ocular inflammation (Demircan *et al*. 2006, Patel *et al*. 2006, Liou *et al*., 2002, Franks *et al*. 1992). IL-1β may affect localization and expression of TJ proteins. Change in expression and localization of occludin, Zo-1, β-catenin and claudins were studied using western blotting and immunoflourescence staining. Toxicity of cytokines to the RPE was investigated using a standard Trypan blue assay.

5.5 Cell culture and cytokine treatment

ARPE-19 cells were cultured as described in section 2.2.1 until desired confluence was achieved. They cell monolayer was then rinsed with sterile PBS and incubated with serum free medium for 6 hours followed by treatment with 1ng/ml to 10ng/ml of TNF-α or IL-1β for 24 hours in serum free medium. After treatment, the cell monolayer was rinsed with sterile PBS to remove any traces of medium. The cells were then extracted as described in section 2.2.2. Protein analysis of the cell extract

was performed using the Bradford assay. Equal amounts of protein per sample were loaded on to minigels. Electrophoresis was performed as described in section 2.2.4. The separated proteins were then blotted to a nitrocellulose membrane as described in 2.2.5. Transfer time used was 2 hours for Occludin, β-catenin and claudins and 3.5 hours for Zo-1.

5.6 Results and Discussion

5.6.1 Occludin expression in RPE treated with TNF-α

RPE cells exposed to various concentrations of TNF-α or IL-1β showed significant alterations in expression of specific tight junction proteins investigated in this study. Western blot analysis of occludin expression in RPE exposed to TNF-α for 24 hours showed a strong down-regulation of the protein (Fig 5.1). Mean occludin band intensities showed a statistically significant ($P \leq 0.05$) decrease in occludin expression when treated with TNF-α (Table 5.1)

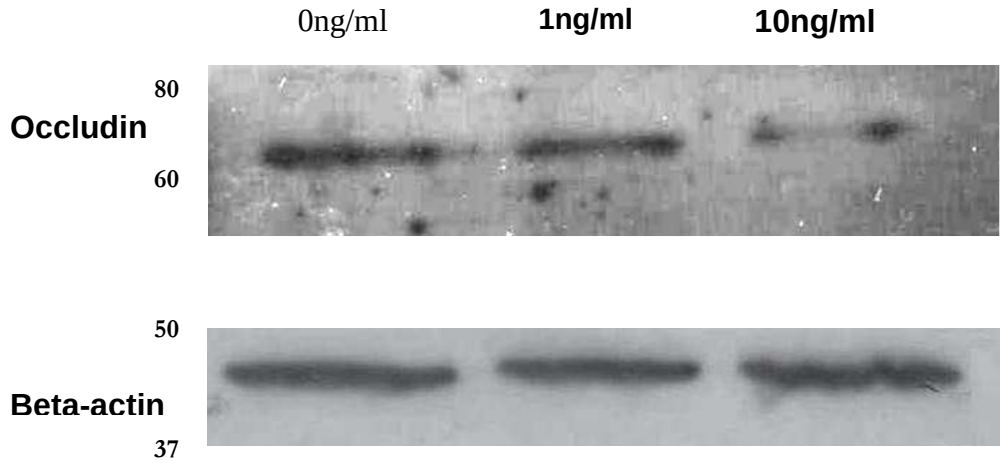

Fig.5.1 Western blot analysis of RPE cells treated with 0ng/ml, 1ng/ml and 10ng/ml TNF-α showing down-regulation of occludin.

The blot was developed using chemiluminescence. Normalisation of blots was achieved using beta actin. Blot was performed twice.

TNF-α concentration	Mean	P Value
0ng/ml	8603.5	0.0144
1ng/ml	7061	
10ng/ml	1516.5	

Table 5.1 Mean band intensities for two sets of samples shows a decrease in occludin band intensity with exposure to TNF-α. P-value calculated by single factor ANOVA shows that this change is statistically significant ($P \leq 0.05$) for 10ng/ml TNF-α treated RPE

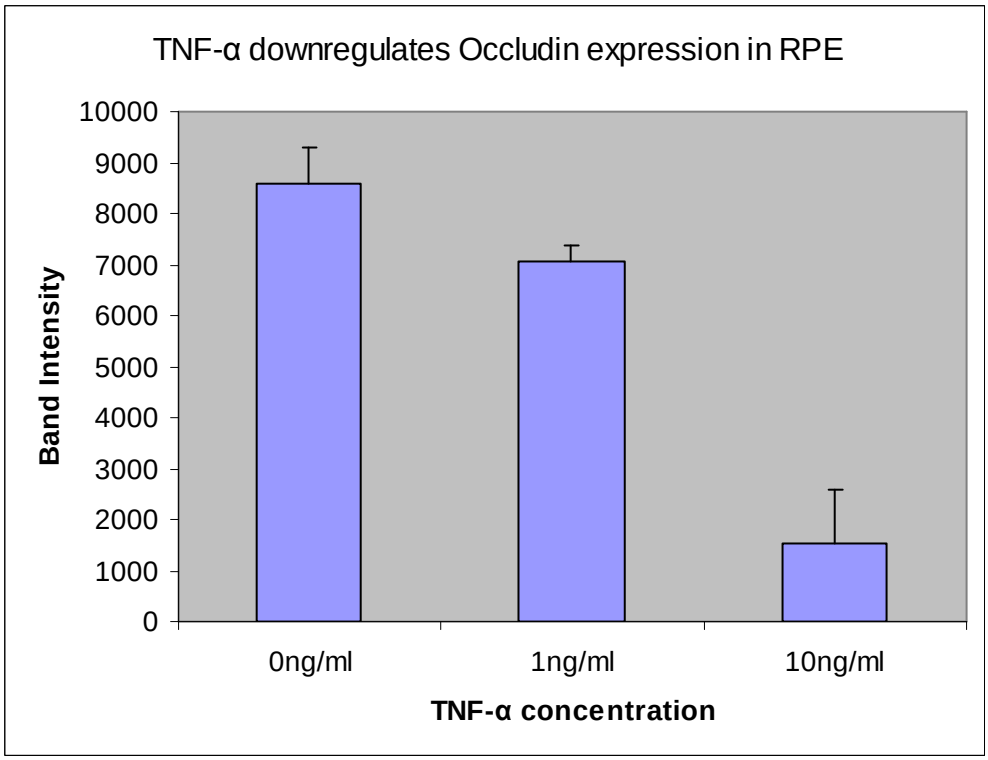

Fig 5.2. Effect of TNF-α treatment on occludin expression in RPE cells.

Occludin in RPE is down-regulated with exposure to TNF-α. The graph represents the mean value for two western blot analyses and the standard error of the mean is represented by Y-error bars.

5.6.2 Zo-1 expression in RPE cells treated with TNF-α

Zo-1 is associated with the cytoplasmic domain of occludin and assists in localization of occludin on the membrane, in order to form tight junctions (Umeda *et al*, 2006). Change in Zo-1 distribution affects stability of the occludin molecule and may cause disruption of the occludin dimer. Zo-1 in RPE is significantly down-regulated by TNF-α treatment, as evident from western blot analysis (Fig 5.3).

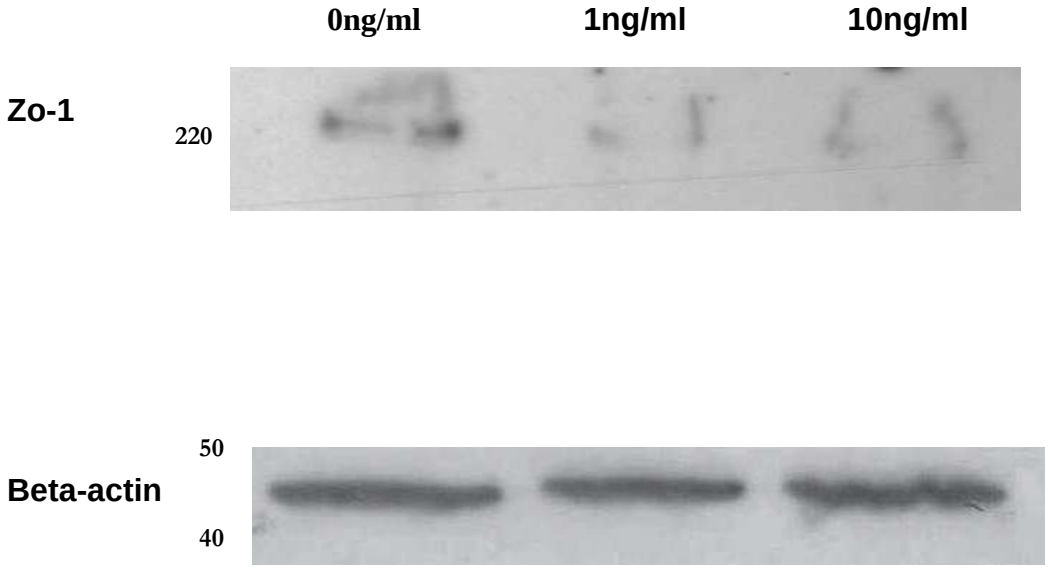

Fig.5.3. Western blot analysis of RPE cells treated with 0ng/ml, 1ng/ml and 10ng/ml TNF-α showing down-regulation of Zo-1.

The blot was developed using chemiluminescence. Normalisation of blots was achieved using beta actin. Blot was performed twice.

TNF-α concentration	Band intensity (Mean ±SEM)	P Value
0ng/ml	8434.3 ± 3564	0.129
1ng/ml	2294.3± 821	
10ng/ml	1997.3 ± 336	

Table 5.2 - Mean band intensities (± standard error of mean) for three sets of samples treated with TNF-α shows a progressive decrease in Zo-1 band intensity with exposure to TNF-α. P-value calculated using single factor ANOVA shows that this change is not statistically significant (P>0.05)

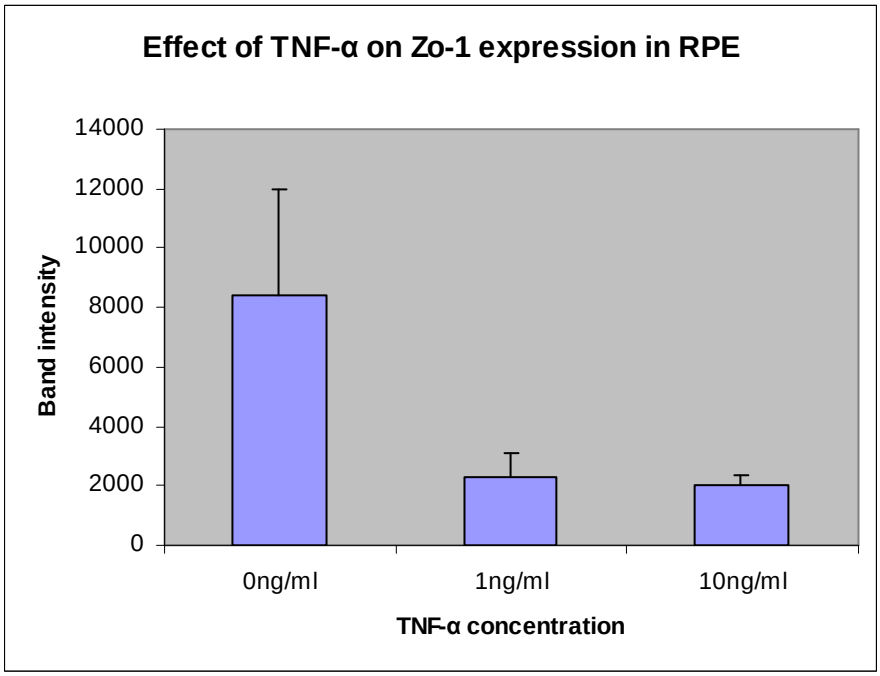

Fig 5.4. Effect of TNF-α treatment on Zo-1 expression in RPE cells.

Zo-1 in RPE is down-regulated with exposure to TNF-α. The graph represents the mean value for three western blot analyses and the standard error of the mean is represented by Y-error bars.

Cultured RPE cells treated with TNF-α were fixed and then stained for Zo-1 using FITC. The staining showed disruption of membrane junctions and loss of Zo-1 when treated with 1ng/ml TNF-α (Fig 5.5).

a)

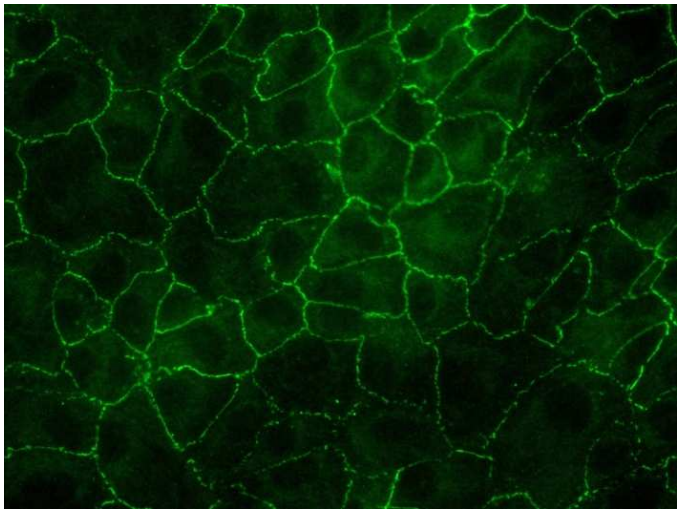

b)

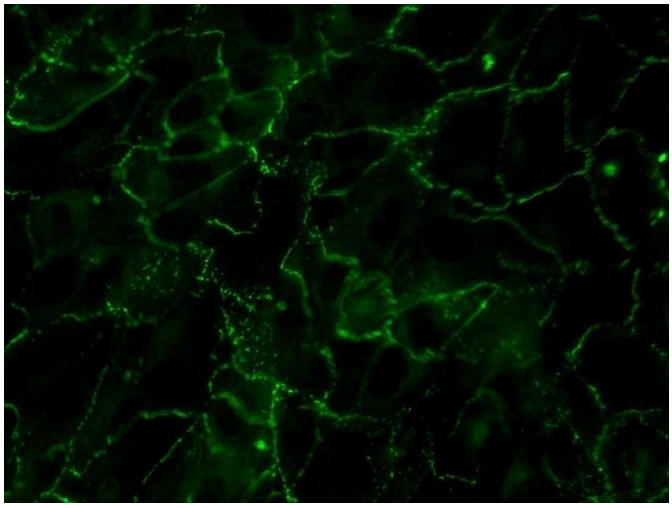

Fig: 5.5 Immunoflourescence staining showing change in localization of Zo-1 in cultured RPE cells treated with TNF-α: Untreated (a) and Treated with 1ng/ml TNF-α (b). RPE cells were stained using FITC and images captured at 40x magnification.

There are very few studies on TNF-α mediated regulation of tight junction proteins in oBRB (Gan *et al* 2011, Narayan *et al* 2003). A study of salivary gland epithelia exposed to TNF-α and IFNγ *in vivo* showed down-regulated occludin and Zo-1 expression and disrupted barrier function in salivary glands (Ewert *et al*., 2010).

5.6.3 Claudin -2 expression in RPE cells treated with TNF-α

To investigate whether, TNF-α mediates expression of claudins in RPE, changes in selected claudins were studied. Data from western blot showed an increase in claudin-2 band density in RPE treated with 1ng/ml TNF-α (Fig 5.6). Densitometric analysis of claudin-2 bands (Table 5.3) showed that this increase was statistically significant ($P \leq 0.05$).

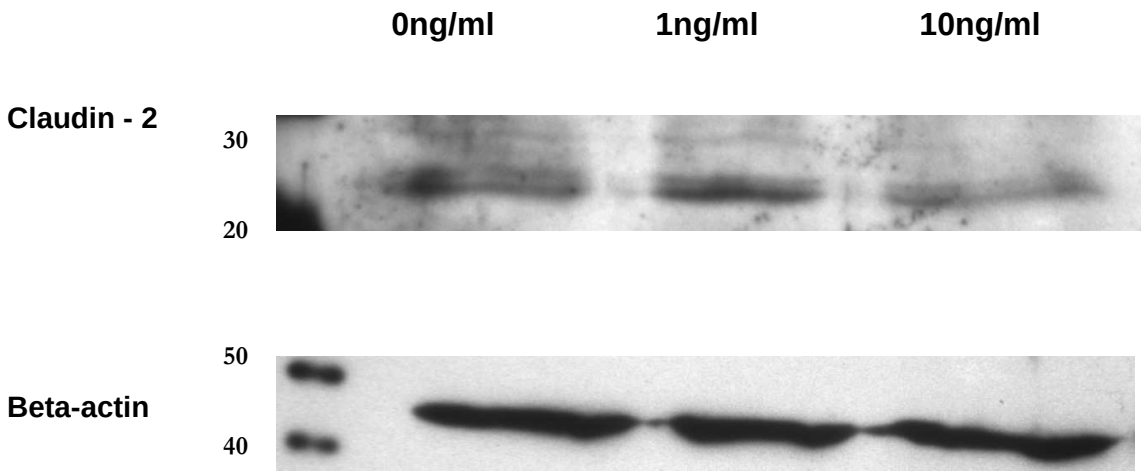

Fig.5.6 Western blot analysis of RPE cells treated with 0ng/ml, 1ng/ml and 10ng/ml TNF-α showing up-regulation of claudin-2.

The blot was developed using chemiluminescence. Normalisation of blots was achieved using beta actin. Blot was performed twice.

10ng/ml TNF-α treated RPE show a slight drop in claudin-2 expression (Fig 5.7) which could be explained by reduced viability of cells treated with 10ng/ml TNF-α.

TNF-α concentration	Mean	P Value
0ng/ml	14997	0.0376
1ng/ml	28685	
10ng/ml	20066	

Table 5.3: Mean band intensities for two sets of samples shows increase in claudin-2 band intensity with exposure to 1ng/ml TNF-α. P-value calculated using single factor ANOVA shows that this change is statistically significant ($P \leq 0.05$) for TNF-α treated RPE.

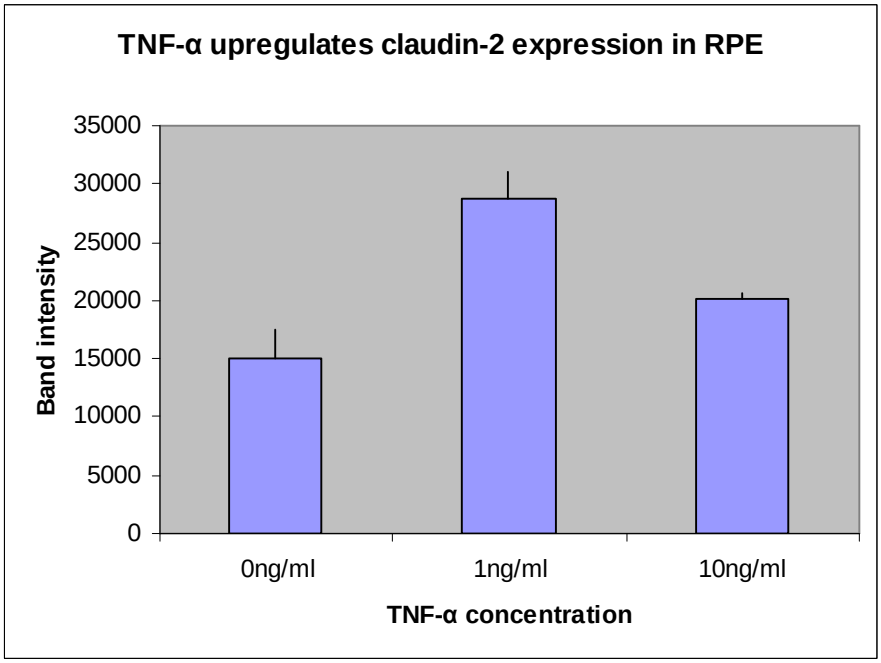

Fig 5.7 Effect of TNF-α treatment on claudin-2 expression in RPE cells.

Claudin-2 in RPE is up-regulated with exposure to TNF-α. The graph represents the mean value for two western blot analyses and the standard error of the mean is represented by Y-error bars.

5.6.4 Claudin – 3 expression in RPE cells treated with TNF-α.

An increase in expression of claudin-3 in RPE when stimulated with 1ng/ml TNF-α, was observed from western blot analysis (Fig 5.8). Mean band density calculated showed an increase in claudin-3 expression in 1ng/ml TNF-α treated RPE (Fig 5.9). However, statistical analysis of claudin-3 band densities (Table 5.4) showed that this change is not significant (P>0.05). The reduction in claudin-3 expression when treated with higher concentration of TNF-α may be attributed to the reduced viability of RPE cells as observed from trypan blue assay (Fig 5.24)

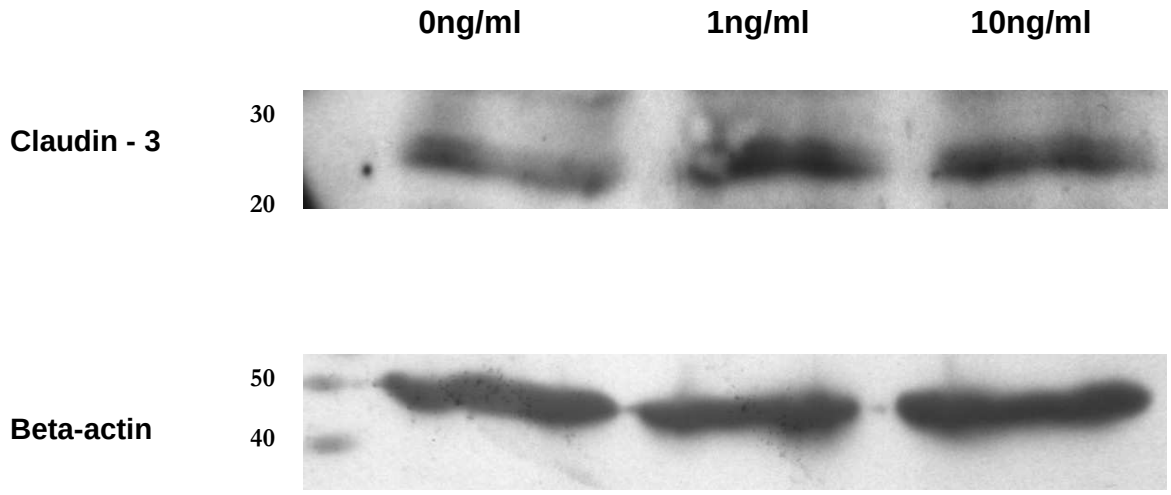

Fig 5.8 Western blot analysis of RPE cells treated with 0ng/ml, 1ng/ml and 10ng/ml TNF-α showing change in claudin-3 expression.

The blot was developed using chemiluminescence. Normalisation of blots was achieved using beta actin. Blot was performed twice.

TNF-α concentration	Mean	P Value
0ng/ml	16741.5	0.621
1ng/ml	21422	
10ng/ml	16675	

Table 5.4: Mean band intensities for two sets of samples shows an increase in claudin-3 band intensity with exposure to 1ng/ml TNF-α. P-value calculated using single factor ANOVA shows that this change is not statistically significant for TNF-α treated RPE

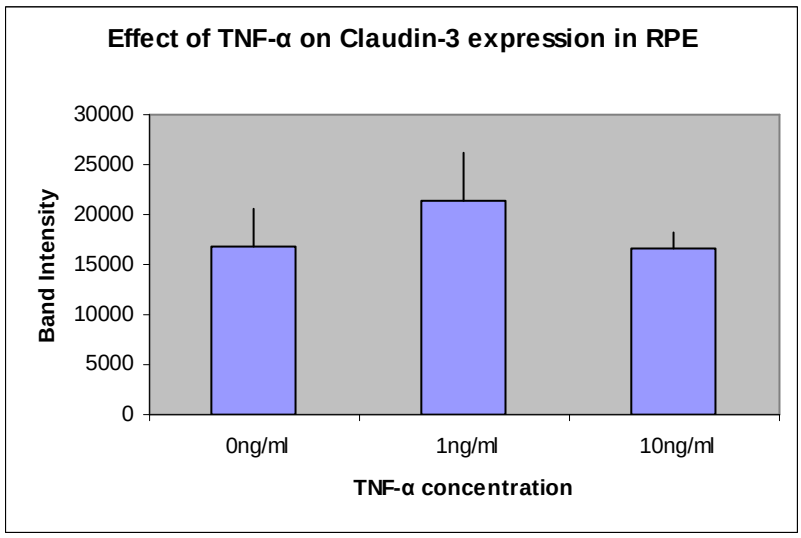

Fig 5.9 Effect of TNF-α treatment on claudin-3 expression in RPE cells.

Claudin-3 expression in RPE is higher with exposure to 1ng/ml TNF-α. The graph represents the mean value for two western blot analyses and the standard error of the mean is represented by Y-error bars

5.6.5 Claudin – 4 expression in RPE cells treated with TNF-α.

TNF-α treated RPE cells showed up-regulation of claudin-4, as indicated by western blotting data (Fig 5.10). Densitometric analysis showed that this effect was not statistically significant (P>0.05) for TNF-α treated RPE. The reduction in claudin-4 expression when treated with higher concentration of TNF-α may be attributed to the reduced viability of RPE cells as observed from trypan blue assay (Fig 5.24)

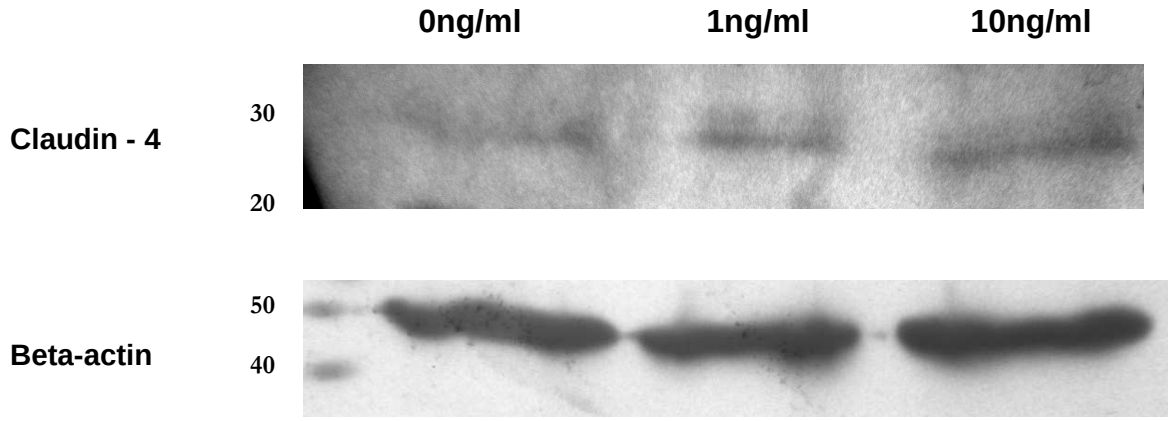

Fig 5.10 Western blot analysis of RPE cells treated with 0ng/ml, 1ng/ml and 10ng/ml TNF-α showing up-regulation of claudin-4.

The blot was developed using chemiluminescence. Normalisation of blots was achieved using beta actin. Blot was performed thrice.

Density analysis shows a slight up-regulation of claudin-4 in RPE treated with 1ng/ml TNF-α (Table 5.5), although not statistically significant. A similar study on salivary epithelium (Ewert *et al*, 2010) shows a strong increase in expression of claudin-4 in epithelial cells exposed to pro-inflammatory cytokines TNF-α and IFNγ while down-regulating occludin and Zo-1 expression.

TNF-α concentration	Band intensity (Mean ±SEM)	P Value
0ng/ml	3467.67 ± 595	0.0673
1ng/ml	6232.67 ± 222	
10ng/ml	6047 ± 1111	

Table 5.5: Mean band intensities (± standard error of mean) for three sets of samples treated with TNF-α shows an increase in claudin-4 band intensity with exposure to TNF-α. P-value calculated using single factor ANOVA shows that this change is not statistically significant for TNF-α treated samples.

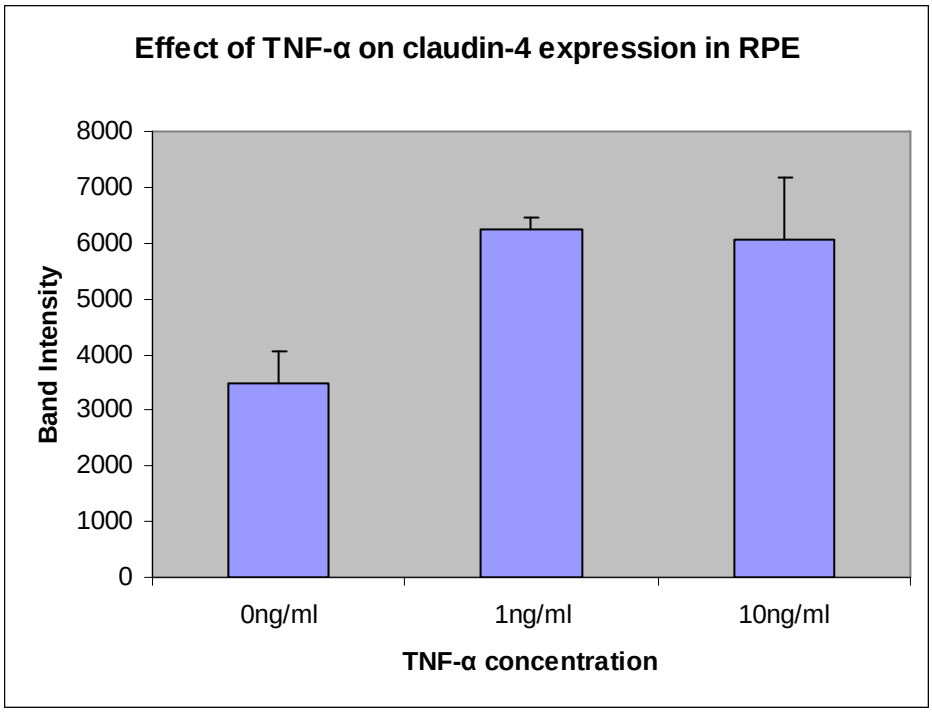

Fig 5.11 Effect of TNF-α treatment on claudin-4 expression in RPE cells.

Claudin-4 in RPE is up-regulated with exposure to TNF-α. The graph represents the mean value for three western blot analyses and the standard error of the mean is represented by Y-error bars.

5.6.6 Beta-catenin expression in RPE cells treated with TNF-α.

Beta catenin expression change indicates change in adherens junctions located basally in the RPE layer. Protein blot analysis indicated a decrease in beta catenin expression in RPE treated with TNF-α, against untreated RPE (Fig 5.12, Fig 5.13). Statistical analysis of band intensities, however, showed that this is not statistically significant (Table 5.6).

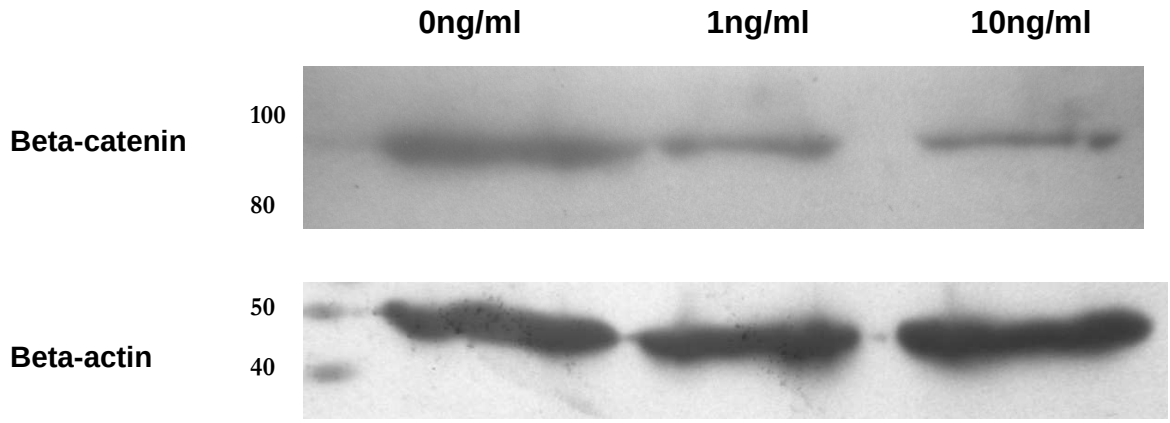

Fig 5.12 Western blot analysis of RPE cells treated with 0ng/ml, 1ng/ml and 10ng/ml TNF-α showing down-regulation of beta-catenin

The blot was developed using chemiluminescence. Normalisation of blots was achieved using beta actin. Blot was performed thrice.

Investigation of change in beta-catenin localization using immunoflourescence did not show a noticeable change (Fig 5.14). Overall, the data obtained from these results is as yet inconclusive and further studies are warranted.

TNF-α concentration	Band intensity (Mean ±SEM)	P Value
0ng/ml	19131.67 ± 5516	0.331
1ng/ml	16432.33 ± 3106	
10ng/ml	9842.68 ± 3348	

Table 5.6: Mean band intensities (± standard error of mean) for three sets of samples treated with TNF-α shows decrease in beta-catenin band intensity with exposure to TNF-α. P-value calculated using single factor ANOVA shows that this change is not statistically significant (P>0.05).

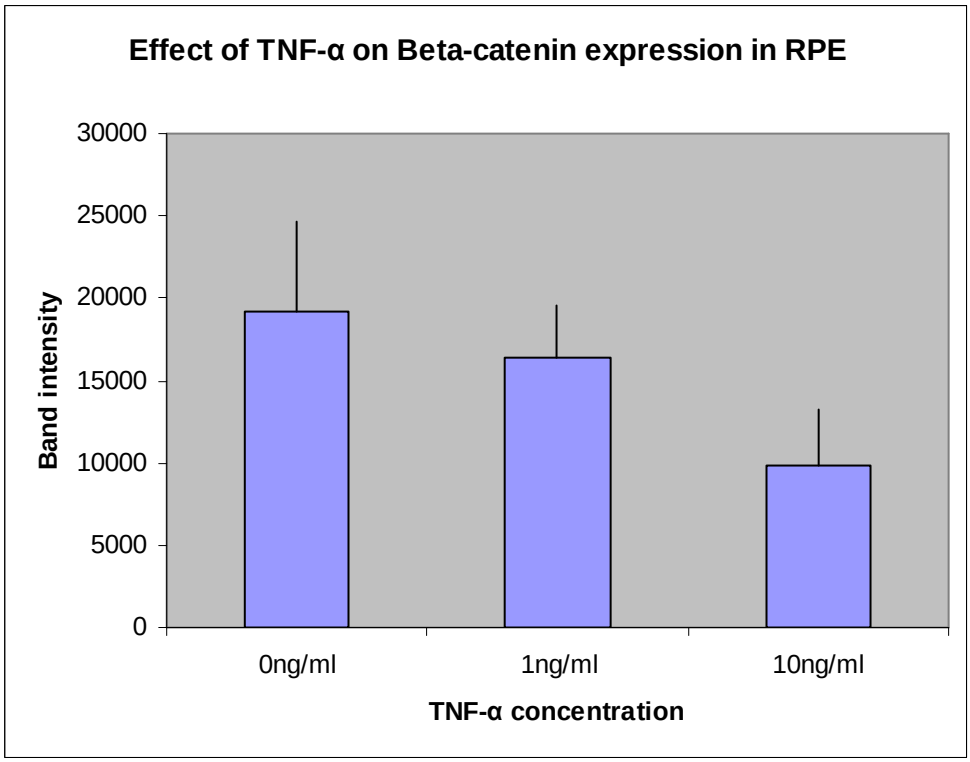

Fig 5.13 Effect of TNF-α treatment on beta-catenin expression in RPE cells.

Beta-catenin expression in RPE is down-regulated with exposure to TNF-α. The graph represents the mean value for three western blot analyses and the standard error of the mean is represented by Y-error bars

a)

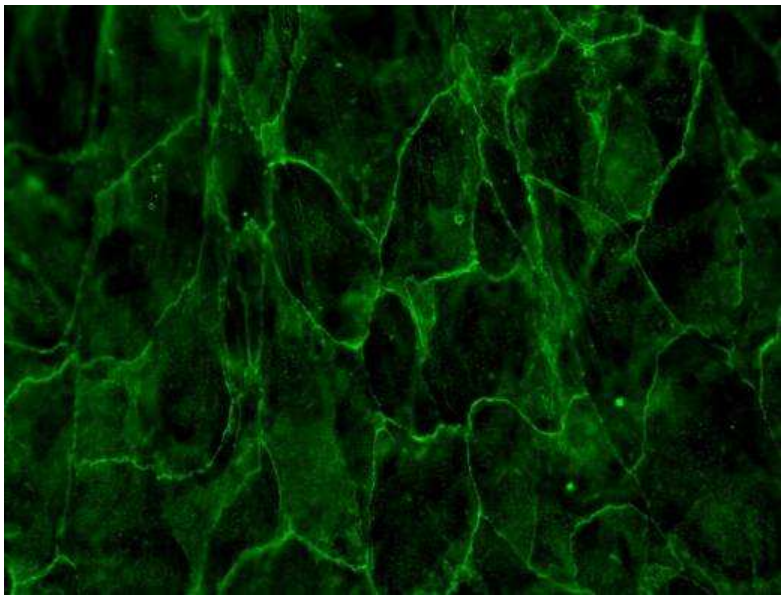

b)

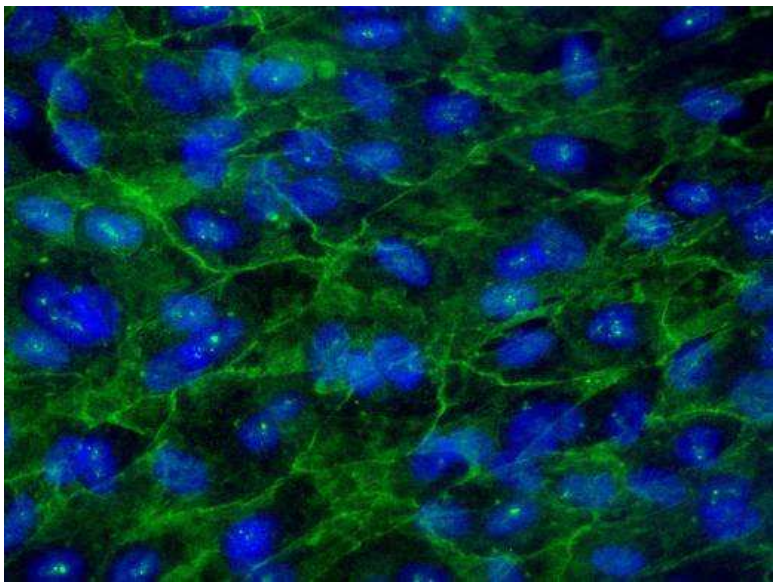

Fig: 5.14 Immunoflourescence staining showing change in localization of β-catenin in cultured RPE cells exposed to 0ng/ml (a) and 1ng/ml (b) TNF-α. RPE cells were stained using FITC and nuclei stained using DAPI. Magnification used: 40x.

5.6.7 Occludin expression in RPE cells treated with IL-1β

Western blot analysis of RPE cells treated with IL-1β showed a positive increase in expression of occludin (Fig 5.14). Mean values (± standard error of mean) were calculated from band density analysis of three sets of data (Table 5.7). The mean band intensities show a progressive increase in occludin expression with increasing concentrations of IL-1β (Fig 5.15). Statistical analysis of data obtained showed that this change is significant for 10ng/ml IL-1β treated sample.

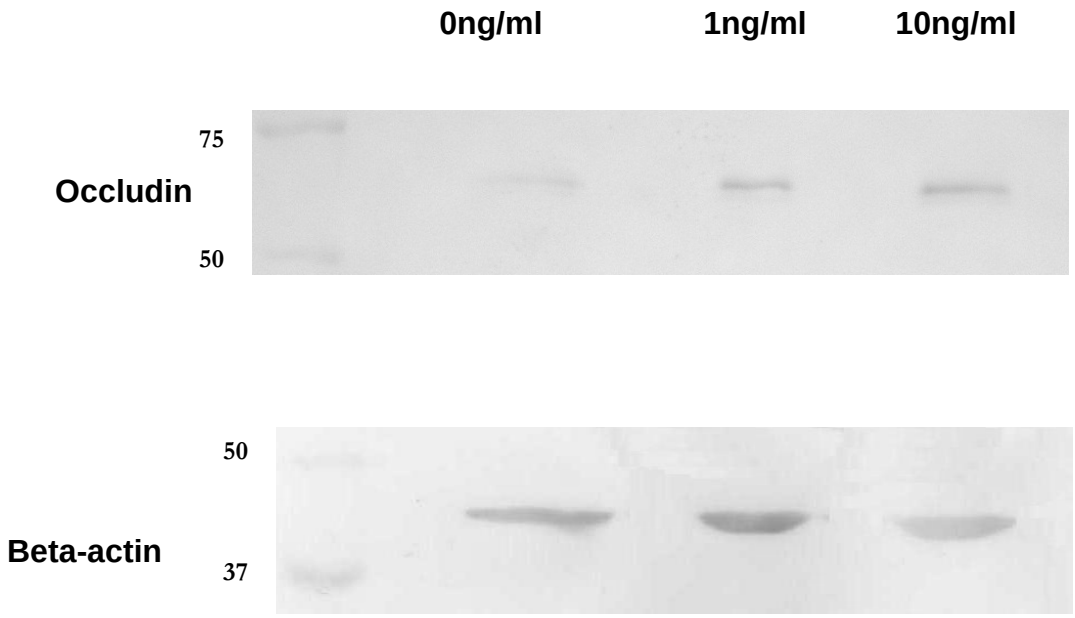

Fig.5.14. Western blot result analysis of RPE cells treated with 0, 1 and 10ng/ml of IL-1β.

Blot was developed using chromogenic substrate – BCIP / NBT. Normalisation of blots was achieved using beta actin. Blot was performed thrice.

IL-1β concentration	Band intensity (Mean ±SEM)	P Value
0ng/ml	1698 ± 454	0.019
1ng/ml	3519.3 ± 680	
10ng/ml	5006.3 ± 575	

Table 5.7 Mean band intensities (± standard error of mean) for three sets of samples treated with IL-1β shows increase in occludin band intensity with exposure to IL-1β. P-value calculated using single factor ANOVA shows that this change is statistically significant ($P \leq 0.05$).

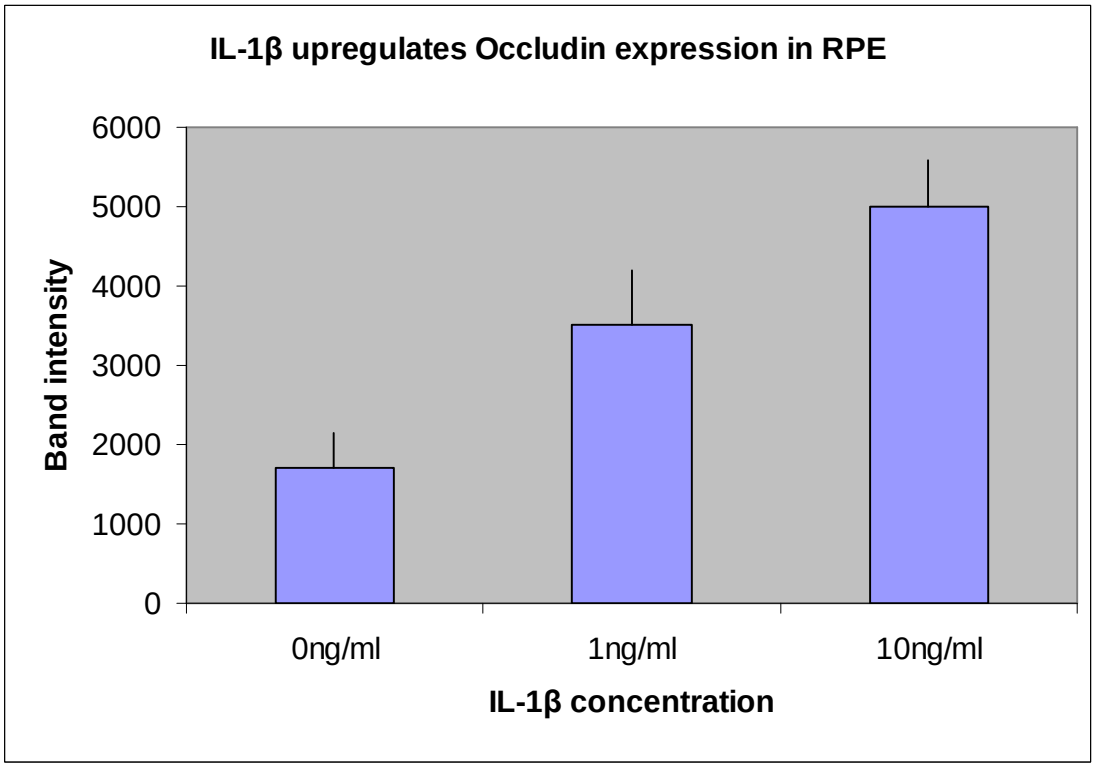

Fig 5.15 Effect of IL-1β treatment on occludin expression in RPE cells.

Occludin expression in RPE is up-regulated with exposure to IL-1β. The graph represents the mean value for three western blot analyses and the standard error of the mean is represented by Y-error bars

Immunoflourescence data showed change in occludin localization in RPE cells treated with IL-1β (Fig 5.16) although IL-1β treated RPE shows occludin upregulation (Table 5.7). Further studies are recommended to understand whether the folding pattern of occludin is affected by IL-1β affecting it's localisation at tight junctions.

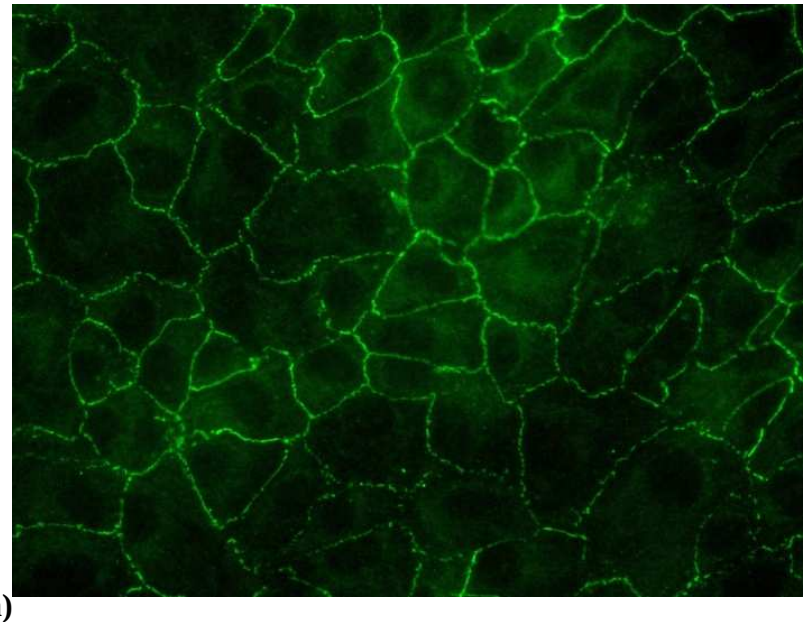

a)

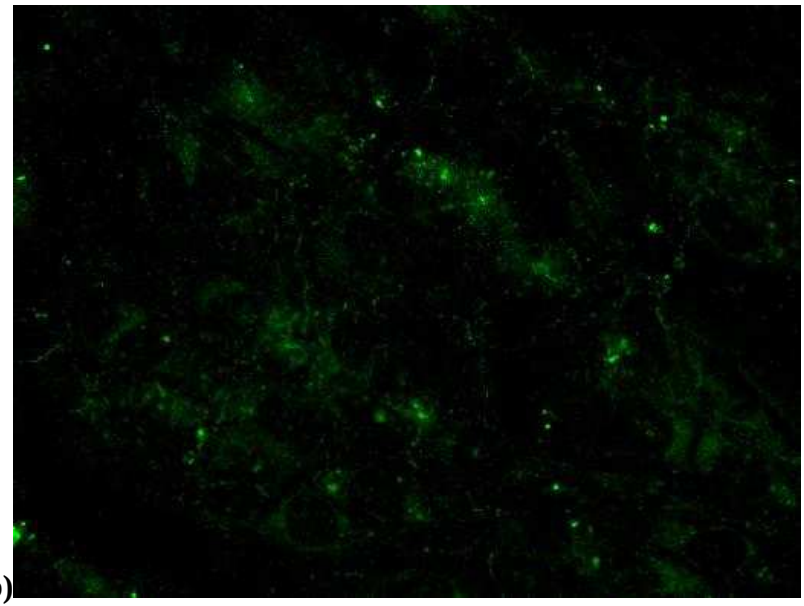

b)

Fig 5.16 Immunoflourescence staining showing change in localization of occludin in cultured RPE cells treated with IL-1β: Untreated (a) and Treated with 10ng/ml IL-1β (b). RPE cells were stained using FITC and images captured at 40x magnification.

5.6.8 Zo-1 expression in RPE cells treated with IL-1β

RPE exposed to IL-1β showed clear loss of Zo-1, as indicated by western blot analysis (Fig 5.17). Mean values calculated from band density analysis of two sets of data (Table 5.8) showed that this change was statistically significant for 10ng/ml IL-1β treated RPE. Analysis of mean band density values of two blots showed progressive down-regulation of Zo-1 with increase in concentration of IL-1β (Fig 5.18)

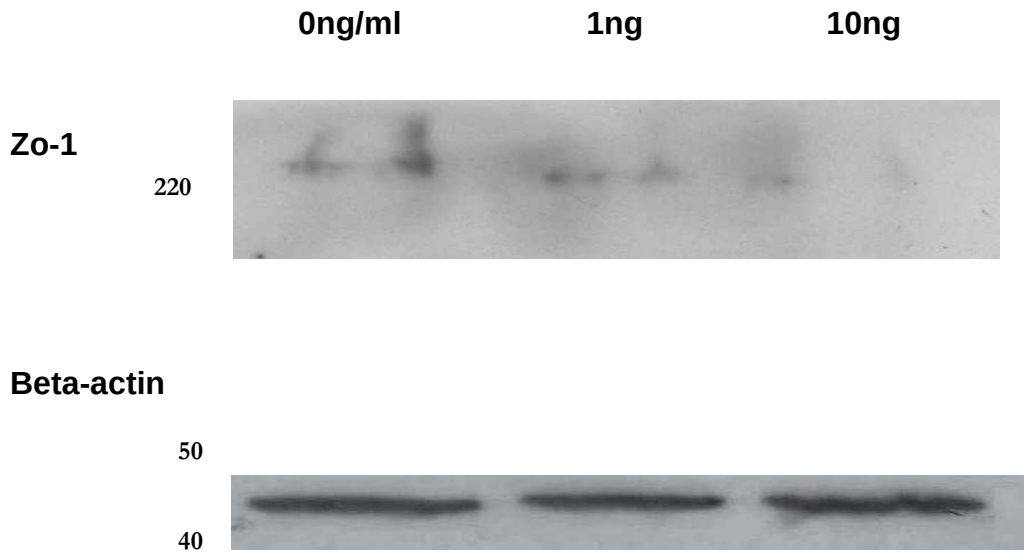

Fig 5.17 Western blot analysis of RPE cells treated with 0ng/ml, 1ng/ml and 10ng/ml IL-1β showing down-regulation of Zo-1.

The blot was developed using BCIP/NBT substrate. Normalisation of blots was achieved using beta actin. Experiment was performed twice.

IL-1β concentration	Mean	P Value
0ng/ml	7457	0.037
1ng/ml	4992.5	
10ng/ml	1794	

Table 5.8: Mean band intensities for two sets of samples treated with IL-1β shows a decrease in Zo-1 band intensity with exposure to IL-1β. P-value calculated using single factor ANOVA shows that this change is statistically significant (P≤0.05) for IL-1β treated RPE.

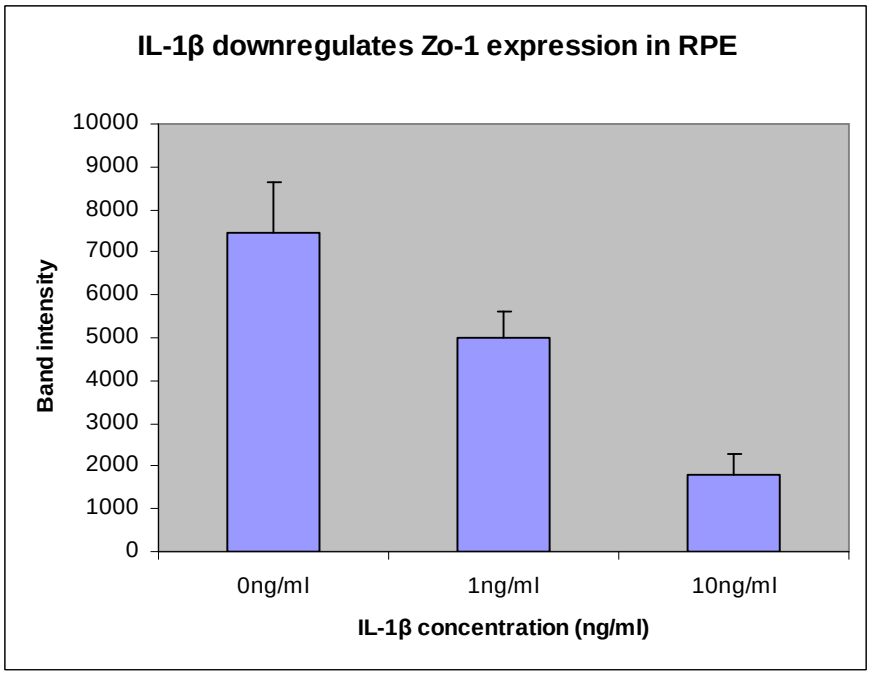

Fig 5.18 Effect of IL-1β treatment on Zo-1 expression in RPE cells.

Zo-1 is significantly down-regulated with exposure to IL-1β. The graph represents the mean value for two sets of data. The standard error of the mean is represented by Y-error bars.

A decrease in Zo-1 as observed from western blotting suggested that membrane localization of Zo proteins may be affected. Immunoflourescence staining of 10ng/ml IL-1β treated RPE showed loss of Zo-1 from membrane junctions (Fig 5.19).

a)

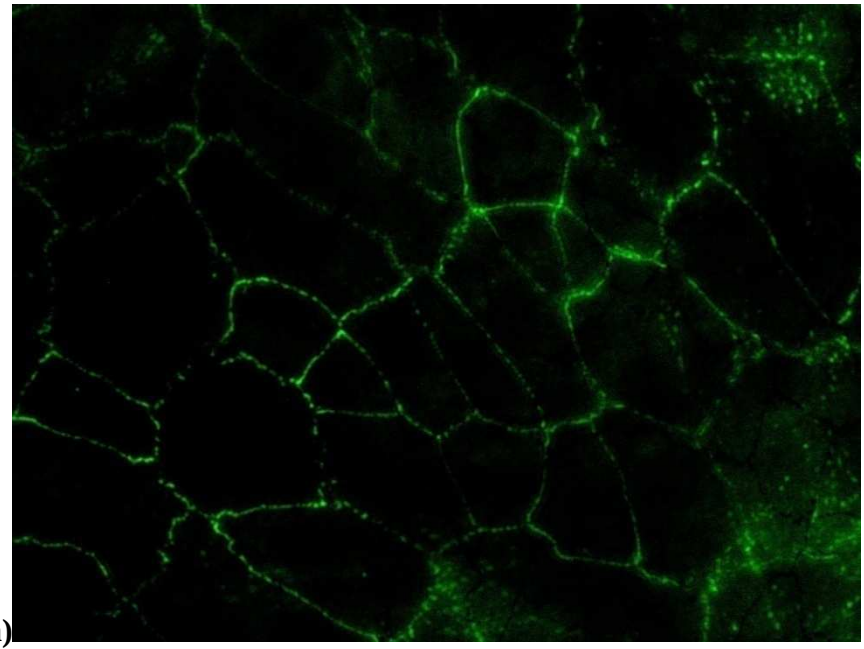

b)

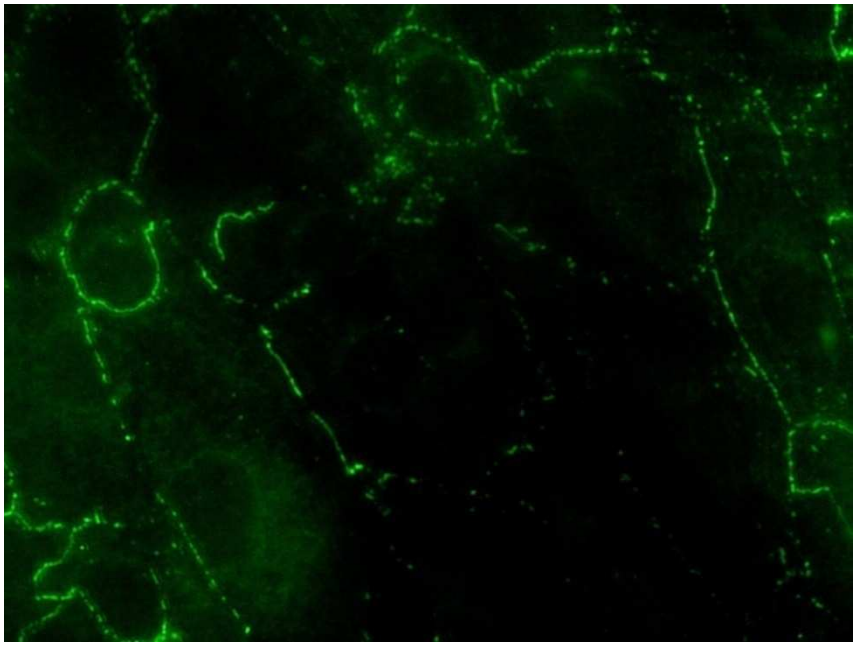

Fig: 5.19 Immunoflourescence staining showing junctional loss of Zo-1 in cultured RPE cells exposed to different concentrations of IL-1β: Untreated (a) and Treated with 10ng/ml IL-1β (b). RPE cells were stained using FITC and images captured at 40x magnification.

5.6.9 Claudin – 1 expression in RPE cells treated with IL-1β

Claudins associate in a heteromeric manner to form tight junctions (Furuse, 2010). An increase in claudin-1 expression was shown by western blotting data (Fig 5.20). Mean band density values showed that this change was statistically significant for 10ng/ml IL-1β treated RPE (Table 5.9). Claudin-1 was progressively up-regulated with exposure to increased concentrations of IL-1β (Fig 5.21).

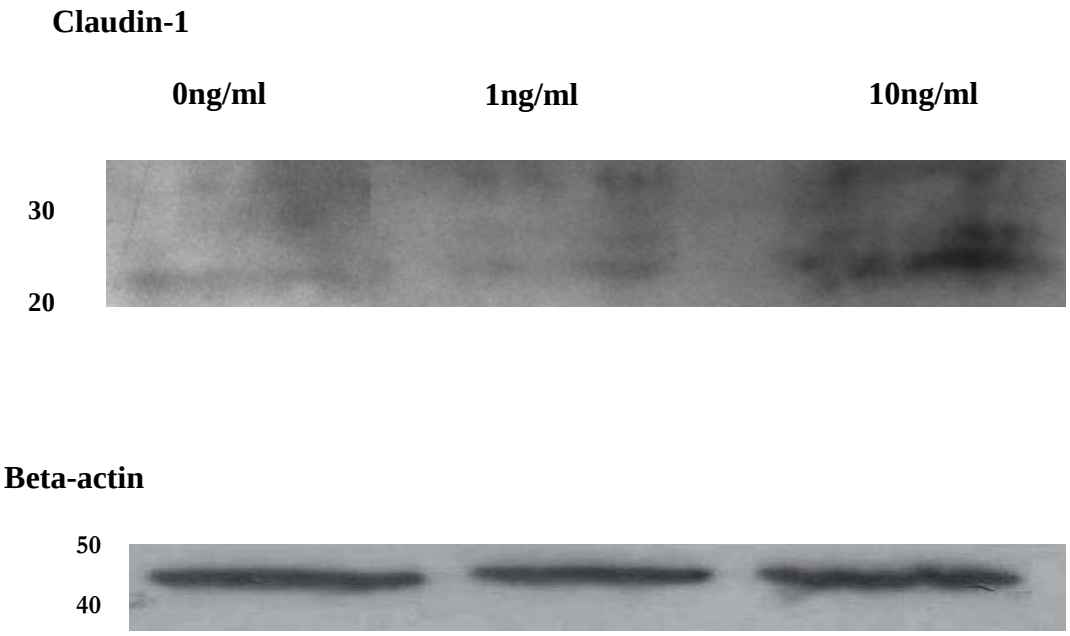

Fig 5.20: Western blot analysis of RPE cells treated with 0ng/ml, 1ng/ml and 10ng/ml IL-1β showing up-regulation of claudin-1.

The blot was developed using chemiluminescence substrate. Normalisation of blots was achieved using beta actin. Experiment was performed twice.

TNF-α concentration	Mean	P Value
0ng/ml	1016.5	0.033
1ng/ml	2219	
10ng/ml	5489.5	

Table 5.9 Mean band intensities for two sets of samples shows an increase in claudin-1 band intensity with exposure to IL-1β. P-value calculated using single factor ANOVA shows that this change is statistically significant ($P \leq 0.05$) for IL-1β treated RPE

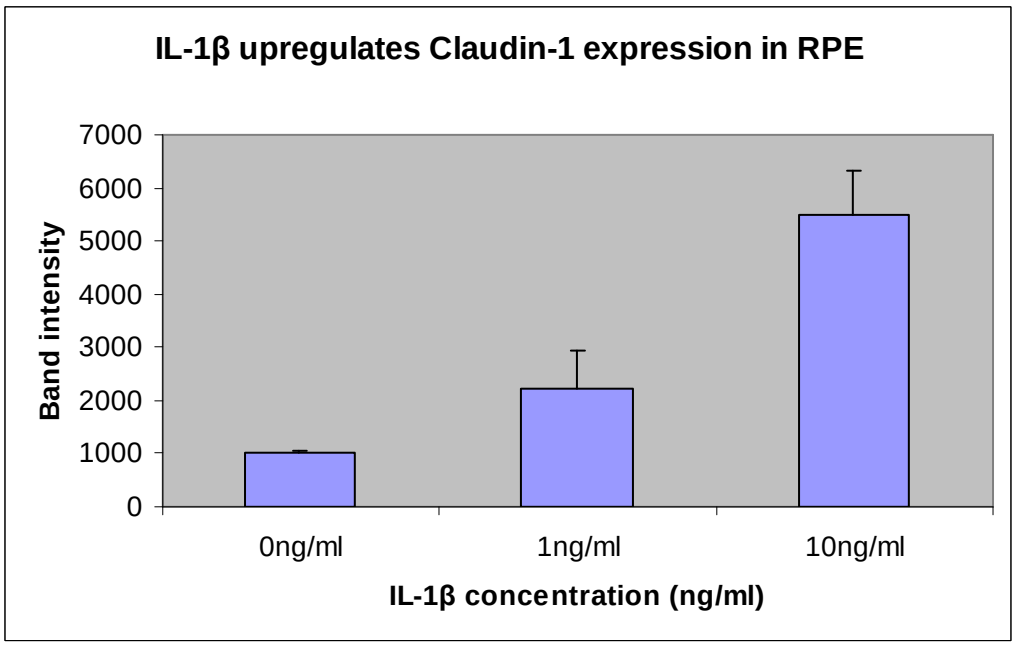

Fig 5.21 Effect of IL-1β treatment on claudin-1 expression in RPE.

Claudin-1 expression shows progressive increase in RPE cells treated with increasing concentrations of IL-1β. The graph represents the mean value for two sets of data. The standard error of the mean is represented by Y-error bars.

5.6.10 Claudin – 3 expression in RPE cells treated with IL-1β

Data obtained from western blotting showed an increase in claudin-3 with IL-1β treatment (Fig 5.22). Statistical analysis of three sets of data (Table 5.10) showed that this change was not statistically significant.

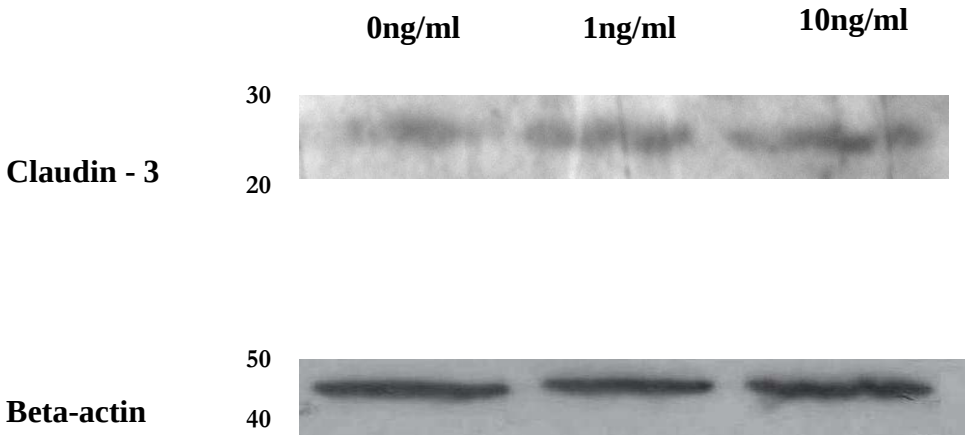

Fig 5.22 **Western blot analysis of RPE cells treated with 0ng/ml, 1ng/ml and 10ng/ml IL-1β showing up-regulation of claudin-3.**

The blot was developed using chemiluminescence substrate. Normalisation of blots was achieved using beta actin. Experiment was performed thrice.

IL-1β concentration	Band intensity (Mean ±SEM)	P Value
0ng/ml	2382.3 ± 803.87	0.070
1ng/ml	3798.3 ± 328.75	
10ng/ml	1435.7 ± 1490.5	

Table 5.10 Mean band intensities (± standard error of mean) for three sets of samples treated with IL-1β shows increase in claudin-3 band intensity with exposure to 1ng/ml IL-1β. P-value calculated using single factor ANOVA shows that this change is not statistically significant (P>0.05).

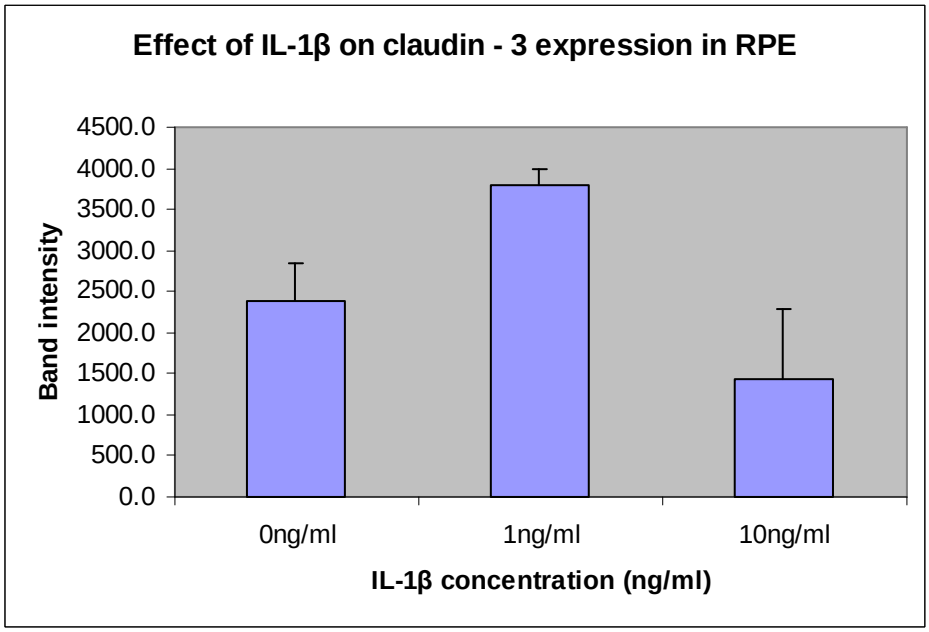

Fig 5.23 Effect of IL-1β treated RPE cells on claudin-3 expression.

Claudin-3 expression in RPE is increased with exposure to 1ng/ml IL-1β. The graph represents mean values for triplicate determinations. The standard error of the mean is represented by Y-error bars.

5.7 Viability assay

RPE cells were treated with 1ng/ml and 10ng/ml TNFα and 1ng/ml and 10ng/ml IL-1β as described in section 2.2.2. Cell viability assay was performed as per protocol outlined in section 2.2.6.

a) TNFα

Cell viability for samples treated with 1ng/ml and 10ng/ml TNF-α were found to be about 95% (57 viable out of 60cells) and 92% (40 viable out of 45cells) respectively, after exposure to trypan blue for 5 minutes.

b) IL-1β

Cells exposed to 1ng/ml and 10ng/ml IL-1β for 24 hours showed 99% (99 viable out of 100 cells) and 97% (68 viable out of 70 cells) viability respectively, after exposure to trypan blue for 5 minutes.

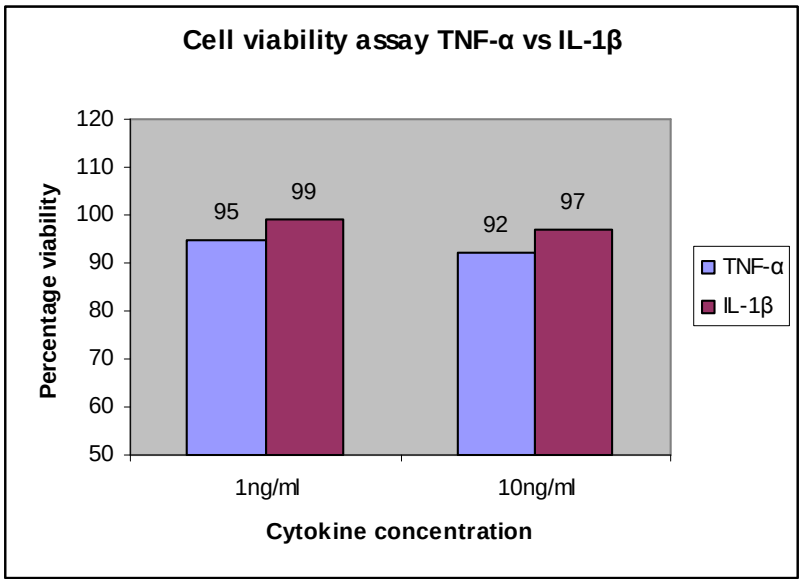

	1ng/ml	10ng/ml
TNF-α	95	92
IL-1β	99	97

Fig: 5.24 - Graph showing percentage viability of cells treated with 1ng/ml and 10ng/ml of TNFα / IL-1β for 24 hours.

Both cytokines are released as a part of inflammatory response produced during later stages of non-neovascular ARMD (Nagineni *et al*, 2011). TNF-α and IL-1β are not secreted by unstimulated RPE cells (Holtkamp *et al*. 2001). Differential levels of TNF-α and IL-1β were found in vitreous in various studies. However, it was generally demonstrated that vitreous levels of TNF-α and IL-1β are elevated in PVR and PDR (Kojima *et al*, 2001) and the difference in result may be attributed to leakage of cytokines through a disrupted oBRB into systemic circulation through a disrupted BRB as suggested by Demircan *et al*, (2006)

A decrease in Zo-1 expression suggests that membrane localization of Zo proteins may be affected. This suggests possible disruption of the membrane barrier in response to increased exposure to IL-1β and TNF-α. Immunoflourescence images of RPE cells exposed to 10ng/ml IL-1β (Fig 5.17) shows nearly complete loss of Zo-1. Also, RPE cells exposed to 1ng/ml and 10ng/ml TNF-α shows 5% and 8% loss in viability respectively (Fig 5.24). The data obtained suggests that IL-1β and TNF-a may play a role in breakdown of outer BRB in ARMD, leading to photoreceptor damage and vision loss.

We found a considerable down-regulation of β-catenin in RPE exposed to TNF-α (Fig 5.13). This may indicate a disruption of adherens junctions in RPE with exposure to TNF-α in pathological conditions. β-catenin associates with cadherins cytoplasmically and plays a role in connecting them to F-actin. However, E-cadherin expression was not detected in cultured ARPE-19 cells using western blot (data not shown).

Data obtained from western blotting shows that IL-1β up-regulates occludin expression in RPE (Fig 5.15) over 24 hours. This contradicts results obtained by Abe T *et al* (2003) where occludin expression was down-regulated with exposure to 10ng/ml IL-1β. This could be explained by the difference in experimental conditions provided in both studies. Abe T *et al*. (2003) do not state whether RPE was exposed to IL-1β in a serum free environment. Serum contains other cytokines which may interfere with or mask the effects of IL-1β. RPE cells treated with 1ng/ml IL-1β shows up-regulated claudin – 1 expression (Fig 5.21). This is in agreement with the study conducted by Abe T *et al* (2003). Moreover, in their study, claudin-1 and occludin expression was measured over a much longer period of time as opposed to the 24 hour period used in this study. Our immunoflourescence results show abnormal occludin distribution, with discontinuous, diffuse staining for occludin, for IL-1β treated RPE (Fig 5.16). IL-1β is shown to differentially regulate occludin expression in other tissues. IL-1β down-regulates occludin expression in human foetal astrocytes (Duffy HS *et al*, 2000), but does not influence the occludin expression in HaCaT keratinocyte cells (Rozlomiy and Markov, 2010).

Claudin-3 was up-regulated in RPE treated with 1ng/ml IL-1β (Fig 5.22). Claudin-3 forms heterotypic tight junctions in epithelia by binding to claudin-1 or claudin-2 (Furuse 2010, Milatz *et al*, 2010, Turksen and Troy 2004). Increase in claudin-3 and claudin-4 expression may be in parallel with that of claudin-2 (Fig 5.7) or claudin-1 (Fig 5.19) expression in cytokine stimulated RPE. Transfection of MDCK-II kidney tubule cells with claudin-3 caused in increase in TEER (Milatz S *et al*, 2010) but brings no change in MDCK-I cells (Turksen and Troy, 2004). The functions of

claudin-3 are not fully elucidated. Hence further studies are required to understand this behaviour of claudin-3

Viability data obtained using Trypan blue assay (Fig 5.24) shows progressive decrease in viability of RPE cells with increased concentration of cytokines added. This may explain the slight drop in expression of claudins which were over-expressed when exposed to 1ng/ml TNF-α or IL-1β.

Overall, our data indicates that pro-inflammatory cytokines TNF-α and IL-1β may have a regulatory effect on RPE barrier in pathological conditions.

Chapter 6

Discussion

The most recent WHO factsheet on blindness reports that about 285 million people worldwide are visually impaired. Of these, 65% are aged 50years and up. AMD has been listed as one of the major causes of vision loss in the west. Breakdown of the blood retinal barrier is the hallmark of AMD, which leads to severe retinal damage and vision loss. The exact molecular mechanism which leads to disruption of this BRB tissue has not been fully elucidated. The pathology and progression of AMD is also not fully understood.

Studies on the RPE tissue which lines the outer layer of retina showed that it plays a significant role in maintenance of the retinal integrity. The RPE was also shown to secrete several cytokines and growth factors to the surrounding medium under pathological conditions such as hypoxia. VEGF, PlGF, TNF-α and IL-1β are found at elevated levels in vitreous of patients suffering from AMD.

Experimental conditions employed in this study involved stimulation of cultured ARPE-19 cells with various concentrations of growth factors or cytokines for 24 hours. Protein expression analysis of E-cadherin in RPE cells showed no signal for E-cadherin in cultured ARPE-19 cells (data not shown). Cultured brain endothelial cells (Endo BalbC) were used as a positive control. Earlier studies show that though human RPE cells express E-cadherin in vivo, this decrease in vitro with progressive cell culture passages (Burke and Hong, 2006).

6.1 Effect of VEGF on oBRB

Studies conducted by Brankin *et al* (2005) showed that VEGF165 had a synergistic effect on inner BRB permeability both *in vivo* and *in vitro*. VEGF significantly

increased BRMEC paracellular permeability and induced iBRB breakdown. Increased vitreal VEGF levels were found in AMD patients. Progressive stages of AMD are known to cause choroidal neovascularisation as a result of hypoxia induced VEGF secretion. VEGF treatment of RPE layer *in vitro* did not indicate any significant change in the overall occludin content at first glance, when probed using western blotting. Fluorescence microscopy showed change in localization of occludin from membrane in VEGF treated RPE cells. Zo-1 associates with the cytoplasmic terminal of occludin and is responsible for stabilization of occludin and claudins in tight junctions (Fanning *et al*. 1998). Earlier studies on retinal endothelial cells have shown a significant increase in Zo-1 expression with *in vitro* VEGF treatment (Ghassemifar *et al*. 2006, Brankin and Stitt 2003). Other researchers in the lab have found that VEGF also caused an increase in expression of Zo-1 protein and mRNA levels for RPE (by personal communication with Dr. Brenda Brankin).

There is evidence that VEGF induces phosphorylation of Zo-1 *in vitro* (Bates, 2010) and indirectly contributes to phosphorylation of occludin (Harhaj *et al* 2006). However, relatively little published data is available regarding how this may be significant in VEGF induced breakdown of the RPE barrier. Further studies are required to investigate whether VEGF induced phosphorylation of Zo-1 attenuates interaction with occludin, leading to membrane de-localization of occludin. A FITC dextran permeability assay and changes in trans-epithelial electrical resistance (TEER) would provide conclusive evidence on whether RPE barrier permeability is altered by VEGF treatment.

6.2 Effect of PlGF on oBRB

PlGF is actively secreted by RPE cells subjected to hypoxic conditions (Hollborn *et al*, 2006). PlGF is a member of VEGF family and has been reported to potentiate the activity of VEGF (Hollborn *et al* 2006). PlGF reportedly induced phosphorylation of occludin at serine and threonine residues, which may modify its capacity to associate with Zo-1 cytoplasmically (Brankin and Stitt, 2003). Investigation of change in polarity of RPE cells would provide more conclusive evidence on this. Little information is available on the effect of PlGF on permeability of the RPE barrier (Carmeliet P *et al*, 2001).

Elevated PlGF of upto 1ng/ml was found in vitreous of diabetic patients (Mitamura *et al* 2002). The effect of PlGF on occludin expression in RPE is not yet fully confirmed (Kowalczuk *et al*., 2011, Ablonczy and Crosson 2007, Mitamura *et al*. 2002). Our data did not show any significant change in RPE occludin content with PlGF treatment. Hollborn *et al* (2006) suggested that PlGF may have an autocrine or paracrine effect on RPE cells. Further investigation into change in permeability and polarity of RPE is required to obtain better insight in this matter. A synergistic increase in VEGF along with PlGF was observed by Hollborn M *et al* (2006). It was suggested that PlGF may stimulate secretion of VEGF by RPE cells in pathological conditions (Dull *et al*. 2001, Park *et al*, 1994).

6.3 Effect of TNF-α and IL-1β on oBRB

RPE cells are continuously exposed to oxidative stress and pro-inflammatory stimuli (Strauss, 2005). The pro-inflammatory cytokines, IL-1β and TNF-α, are released by macrophages during inflammation associated with several ocular dystrophies.

Differential levels of TNF-α and IL-1β were found in vitreous in various studies. However, it was generally demonstrated that vitreous and serum levels of TNF-α and IL-1β are elevated in PVR and PDR (Demircan *et al*, 2006, Kojima *et al*, 2001) and the presence of vitreous haemorrhage and oBRB breakdown may lead to leakage of cytokines into the systemic circulation (Demircan *et al*, 2006)

Cytokine gene expression is readily induced in RPE cells by inflammatory stimuli (Holtkamp *et al*, 2001) and hence RPE cells may act as a source of IL-1β and TNF-α in AMD pathogenesis. Vitreous levels of IL-1β were found to be elevated in progressive DR (Patel *et al*, 2008(a), Demircan *et al* 2006). Differential concentrations of IL-1β and TNF-α were obtained in different studies involving retinal inflammation (Gustavsson *et al*., 2008, Demircan *et al*., 2006, Kauffmann *et al*., 1994). It was hence suggested that both serum and vitreous concentrations of cytokines IL-1β and TNF-α must be taken into account, as vitreous haemorrhage and oBRB breakdown leads to leakage of IL-1β and TNF-α into the systemic circulation. Results suggested simultaneous production of IL-1β and TNF-α from the RPE and macrophages (Demircan *et al*, 2006).

TNF-α is secreted locally by macrophages infiltrating into the outer retina under pathologic conditions. Stimulated RPE cells secrete IL-1β basally in a polarized manner (Holtkamp *et al*., 2001). RPE shows immunoreactivity to both cytokines (Oh *et al*, 1999, Jaffe *et al*, 1992). Increased concentration of TNF-α in surrounding medium is toxic to RPE cells and caused occludin loss from RPE. Loss of both tight junction and adherens junctions indicate possible change in polarity of RPE cells.

RPE exposed to TNF-α showed an increase in claudin-2 expression. Claudin–2 was up-regulated significantly when treated with 1ng/ml TNF-α. This result was in agreement with studies involving TNF-α-induced change in Claudin-2 in intestine and RPE (Gan *et al*. 2011, Yu 2009, Mazzon and Cuzzorea, 2008). A cationic pore function of Claudin-2 has been suggested (Gupta and Ryan 2010, Lal-Nag and Morin 2009, Zeissig *et al* 2007). An increase in Claudin-2 expression possibly indicates an increase in ion channel permeability of RPE cells. A similar increase in expression of claudin-2 has been reported in colon stimulated with TNF-α (Weber *et al*. 2010, Hering and Schulzke 2009). An over-expression of claudin-2 has been reported to reduce TEER and increase paracellular water flux (Rosenthal *et al*., 2010).

Increase in occludin expression has been shown to enhance baseline barrier properties of epithelia (Van Itallie *et al*, 2010). It is possible that cytokines increase the permeability of the RPE barrier to both charged and non-charged solutes by up-regulating the pore proteins, while down-regulating proteins that restrict paracellular permeability. This has to be further confirmed using a permeability assay.

Claudin-4 expression in non-retinal tissues is stimulated by exposure to TNF-α (Ewert *et al*, 2010, Gupta and Ryan 2010). Claudin-3 and 4 are reportedly up-regulated in several carcinomas in conjunction with increased TNF-α expression (Gupta and Ryan, 2010, Yuan *et al* 2009). However, their role in the retinal barrier modulation is poorly investigated.

There was a clear loss of Zo-1 and the band intensity of 10ng/ml IL-1β-treated samples was significantly lower than that of control. Zo proteins have a pivotal role in

binding occludin and claudins to the actin cytoskeleton and stabilizing the tight junctions. Even though occludin expression in RPE was upregulated by IL-1β treatment, loss of Zo-1 may cause destabilization of occludin molecules in RPE, resulting in the granular staining of occludin observed in IL-1β treated cells. Further studies are warranted to understand whether IL-1β causes direct loss of occludin from RPE; and to identify whether the loss of Zo-1 affects the polarity of the RPE cells. Overall, study indicates that TNF- α and IL-1β may play a regulatory role in blood ocular barrier function and in development of ocular inflammation.

In a study similar to the one presented in this thesis, Abe *et al* (2003) found that claudin-1 expression was reduced in RPE cells treated with 10ng/ml IL-1β. Our data, on the contrary, shows a significant upregulation of claudin-1 in IL-1β treated RPE. Even though this seems to contradict to the data discussed in this thesis; the experimental conditions employed by Abe *et al.,* were different, and the claudin-1 expression was measured after a much longer period, rather than 24 hours employed in our experiment. Rozlomiy and Markov (2010) demonstrated that treatment of human keratinocyte (HaCaT) cells with IL-1β up-regulated claudin-1 as part of the wound healing process. Our data shows that TNF- α and IL-1β may play a regulatory role in blood ocular barrier function and in development of ocular inflammation.

Immunoflourescence was not carried out for claudins, as the claudins could not be detected in initial staining. Claudin family of proteins have been observed to have a host of other functions other than being a structural component of tight junctions. In order to get better insight to the significance of the results presented, further roles of claudins in RPE need to be identified. Downregulation of claudin using siRNA

interference is recommended as a future approach to elucidate the role of specific claudin in RPE. Further studies of the effects of cytokines on claudins 2, 3 and 4 in RPE are also indicated.

Inflammation plays an important role in pathogenesis and progression of ARMD. There is evidence of increased TNF-α secretion in exudative ARMD (Nagineni *et al*, 2011). Activation of the RPE with TNF- α or IL-1β results in secretion of RANTES, MCP-1 and interleukin 6 and interleukin 8, which affect oBRB function (Crane *et al*, 2000).

TNF antagonists have become recognized over the past decade as a key controller of inflammatory conditions. Anti-TNF-α therapy has been found to be helpful in controlling ARMD-related inflammation and stabilizing vascular angiogenesis (Missotten *et al*., 2007). The role of IL-1β in ocular inflammation is not completely elucidated. IL-1β does not directly modulate barrier properties in the tissue. It stimulates secretion of other pro-inflammatory chemokines such as IL-6, IL-8 and RANTES (Crane *et al*. 2000). It has been suggested that expression of endogenous interleukin-1 receptor antagonist (Jaffe *et al* 1992) may help in maintaining interleukin homeostasis in ocular inflammatory disease.

6.4 Conclusion

VEGF, PlGF, TNF-α and IL-1β play an important role in modulation of barrier properties of oBRB. Differential regulation of oBRB by the selected cytokines and growth factors may be helpful in further research on control of inflammation and pathological breakdown of oBRB in AMD and PDR.

6.5 Future Work

- VEGF and PlGF treatment of RPE did not yield conclusive results on change in permeability of RPE layer. Analysis of permeability change of RPE to determine opening of tight junctions, using Flourescein Dextran assay and changes in TEER measurement.

- Determination of effects of apical versus basolateral administration of PlGF and VEGF on RPE monolayer.

- Change in Zo-1 expression and loss of occludin may affect polarity of RPE cells in the oBRB. Analysis of change in polarity of RPE cells with growth factor and cytokine treatment using Na+ K+ ATPase assay

- The functions of claudins in RPE are not merely structural. Downregulation of claudins in RPE using siRNA interference to study the role of individual claudins in RPE.

References

Abe T, Sugano E, Saigo Y, Tamai M. Interleukin-1beta and barrier function of retinal pigment epithelial cells (ARPE-19): aberrant expression of junctional complex molecules. Invest Ophthalmol Vis Sci. 2003 Sep; 44 (9):4097-104.

Adamis AP, Shima DT, Yeo KT, Yeo TK, Brown LF, Berse B, D'Amore PA, Folkman J. Synthesis and secretion of vascular permeability factor/vascular endothelial growth factor by human retinal pigment epithelial cells. Biochem Biophys Res Commun. 1993 Jun 15; 193 (2):631-8.

Adson A, Raub TJ, Burton PS, Barsuhn CL, Hilgers AR, Audus KL, Ho NF. Quantitative approaches to delineate paracellular diffusion in cultured epithelial cell monolayers. J Pharm Sci. 1994 Nov; 83 (11):1529-36.

Alegria-Schaffer A, Lodge A, Vattem K. Performing and optimizing Western blots with an emphasis on chemiluminescent detection. Methods Enzymol. 2009; 463:573-99.

Allen IV and Brankin B. 1993. Pathogenesis of Multiple Sclerosis-the immune diathesis and the role of viruses. J Neuropathol Exp Neurol. 1993 Mar;52(2):95-105

Amasheh M, Fromm A, Krug SM, Amasheh S, Andres S, Zeitz M, Fromm M, Schulzke JD. TNFalpha-induced and berberine-antagonized tight junction barrier impairment via tyrosine kinase, Akt and NFkappaB signaling. J Cell Sci. 2010 Dec 1; 123 (Pt 23):4145-55.

Amasheh M, Grotjohann I, Amasheh S, Fromm A, Söderholm JD, Zeitz M, Fromm M, Schulzke JD. Regulation of mucosal structure and barrier function in rat colon exposed to tumor necrosis factor alpha and interferon gamma in vitro: a novel model for studying the pathomechanisms of inflammatory bowel disease cytokines. Scand J Gastroenterol. 2009; 44 (10):1226-35.

Amasheh S, Dullat S, Fromm M, Schulzke JD, Buhr HJ, Kroesen AJ. Inflamed pouch mucosa possesses altered tight junctions indicating recurrence of inflammatory bowel disease. Int J Colorectal Dis. 2009 Oct; 24 (10):1149-56.

An E, Gordish-Dressman H, Hathout Y. Effect of TNF-alpha on human ARPE-19-secreted proteins. Mol Vis. 2008; 14:2292-303.

Anderson DH, Mullins RF, Hageman GS, Johnson LV. A role for local inflammation in the formation of drusen in the aging eye. Am J Ophthalmol. 2002 Sep; 134 (3):411-31.

Anderson JM, Van Itallie CM, Fanning AS. Setting up a selective barrier at the apical junction complex. Curr Opin Cell Biol. 2004 Apr; 16 (2):140-5.

Anderson JM, Van Itallie CM. Tight junctions: closing in on the seal. Curr Biol. 1999 Dec 16-30; 9 (24):R922-4.

Anderson JM, Van Itallie CM. Tight junctions. Curr Biol. 2008 Oct 28; 18 (20):R941-3.

Anderson JM. Molecular structure of tight junctions and their role in epithelial transport. News Physiol Sci. 2001 Jun; 16:126-30.

Anderson JM, Van Itallie CM. Physiology and function of the tight junction. Cold Spring Harb Perspect Biol. 2009 Aug; 1 (2):a002584.

Anderson JM, Fanning AS, Lapierre L, Van Itallie CM. Zonula occludens (ZO)-1 and ZO-2: membrane-associated guanylate kinase homologues (MAGuKs) of the tight junction. Biochem Soc Trans. 1995 Aug; 23 (3):470-5.

Anderson JM, Van Itallie CM. Tight junctions and the molecular basis for regulation of paracellular permeability. Am J Physiol. 1995 Oct; 269 (4 Pt 1):G467-75.

Angelow S, Yu AS. Structure-function studies of claudin extracellular domains by cysteine-scanning mutagenesis. J Biol Chem. 2009 Oct 16; 284 (42):29205-17.

Angelow S, Ahlstrom R, Yu AS. Biology of claudins. Am J Physiol Renal Physiol. 2008 Oct; 295 (4):F867-76.

Antonetti DA, Barber AJ, Bronson SK, Freeman WM, Gardner TW, Jefferson LS, Kester M, Kimball SR, Krady JK, LaNoue KF, Norbury CC, Quinn PG, Sandirasegarane L, Simpson IA, JDRF Diabetic Retinopathy Center Group. Diabetic retinopathy: seeing beyond glucose-induced microvascular disease. Diabetes. 2006 Sep; 55 (9):2401-11.

Antonetti DA, Barber AJ, Khin S, Lieth E, Tarbell JM, Gardner TW. Vascular permeability in experimental diabetes is associated with reduced endothelial occludin content: vascular endothelial growth factor decreases occludin in retinal endothelial cells Penn State Retina Research Group. Diabetes. 1998 Dec; 47 (12):1953-9.

Antonetti DA, Lieth E, Barber AJ, Gardner TW. Molecular mechanisms of vascular permeability in diabetic retinopathy. Semin Ophthalmol. 1999 Dec; 14 (4):240-8.

Antonetti DA, Barber AJ, Hollinger LA, Wolpert EB, Gardner TW. Vascular endothelial growth factor induces rapid phosphorylation of tight junction proteins occludin and zonula occluden 1 A potential mechanism for vascular permeability in diabetic retinopathy and tumors. J Biol Chem. 1999 Aug 13; 274 (33):23463-7.

Aschenbrenner S, Walz B. Pleated septate junctions in leech photoreceptors: ultrastructure, arrangement of septa, gate and fence functions. Cell Tissue Res. 1998 Aug; 293 (2):253-69.

Aw S, Koster JC, Pearson W, Nichols CG, Shi NQ, Carneiro K, Levin M. The ATP-sensitive K(+)-channel (K(ATP)) controls early left-right patterning in Xenopus and chick embryos. Dev Biol. 2010 Oct 1; 346 (1):39-53.

Balda MS, Matter K. Transmembrane proteins of tight junctions. Semin Cell Dev Biol. 2000 Aug; 11 (4):281-9.

Balda MS, Flores-Maldonado C, Cereijido M, Matter K. Multiple domains of occludin are involved in the regulation of paracellular permeability. J Cell Biochem. 2000 Apr; 78 (1):85-96.

Balda MS, Matter K. Tight junctions. J Cell Sci. 1998 Mar; 111 (Pt 5):541-7.

Balda MS, Whitney JA, Flores C, González S, Cereijido M, Matter K. Functional dissociation of paracellular permeability and transepithelial electrical resistance and disruption of the apical-basolateral intramembrane diffusion barrier by expression of a mutant tight junction membrane protein. J Cell Biol. 1996 Aug; 134 (4):1031-49.

Bates DO. Vascular endothelial growth factors and vascular permeability. Cardiovasc Res. 2010 Jul 15; 87 (2):262-71.

B. Brankin, and A.W. Stitt. Effects of Endostatin, Placental Growth Factor and Vascular Endothelial Growth Factor on Blood Retinal Barrier Function. Invest. Ophthalmol. Vis. Sci. 44: E-Abstract 3913.

Bentzel CJ, Reczek PR. Permeability changes in Necturus proximal tubule during volume expansion. Am J Physiol. 1978 Mar; 234 (3):F225-34.

Berl T. How do kidney cells adapt to survive in hypertonic inner medulla?. Trans Am Clin Climatol Assoc. 2009; 120:389-401.

Bhisitkul RB. Vascular endothelial growth factor biology: clinical implications for ocular treatments. Br J Ophthalmol. 2006 Dec; 90 (12):1542-7.

Bird AC. Therapeutic targets in age-related macular disease. J Clin Invest. 2010 Sep 1; 120 (9):3033-41.

Blaauwgeers HG, Holtkamp GM, Rutten H, Witmer AN, Koolwijk P, Partanen TA, Alitalo K, Kroon ME, Kijlstra A, van Hinsbergh VW, Schlingemann RO. Polarized vascular endothelial growth factor secretion by human retinal pigment epithelium and localization of vascular endothelial growth factor receptors on the inner choriocapillaris Evidence for a trophic paracrine relation. Am J Pathol. 1999 Aug; 155 (2):421-8.

Blasig IE, Bellmann C, Cording J, Vecchio GD, Zwanziger D, Huber O, Haseloff RF. Occludin Protein Family: Oxidative Stress and Reducing Conditions. Antioxid Redox Signal. 2011 May 5;

Blume LF, Denker M, Gieseler F, Kunze T. Temperature corrected transepithelial electrical resistance (TEER) measurement to quantify rapid changes in paracellular permeability. Pharmazie. 2010 Jan; 65 (1):19-24.

Boucher RC. Chemical modulation of airway epithelial permeability. Environ Health Perspect. 1980 Apr; 35:3-11.

Bourdeau RW, Malito E, Chenal A, Bishop BL, Musch MW, Villereal ML, Chang EB, Mosser EM, Rest RF, Tang WJ. Cellular functions and X-ray structure of

anthrolysin O, a cholesterol-dependent cytolysin secreted by Bacillus anthracis. J Biol Chem. 2009 May 22; 284 (21):14645-56.

Brankin B, Campbell M, Canning P, Gardiner TA, Stitt AW. Endostatin modulates VEGF-mediated barrier dysfunction in the retinal microvascular endothelium. Exp Eye Res. 2005 Jul; 81 (1):22-31.

Brankin B, Hart MN, Cosby SL, Fabry Z, Allen IV. 1995. Adhesion molecule expression and lymphocyte adhesion to cerebral endothelium. J Neuroimmunol 56(1):1-8.

Bösl MR, Stein V, Hübner C, Zdebik AA, Jordt SE, Mukhopadhyay AK, Davidoff MS, Holstein AF, Jentsch TJ. Male germ cells and photoreceptors, both dependent on close cell-cell interactions, degenerate upon ClC-2 Cl(-) channel disruption. EMBO J. 2001 Mar 15; 20 (6):1289-99.

Burke JM, Hong J. Fate of E-cadherin in early RPE cultures: transient accumulation of truncated peptides at nonjunctional sites. Invest Ophthalmol Vis Sci. 2006 Aug; 47(8):3635-43

Caldwell RB, Bartoli M, Behzadian MA, El-Remessy AE, Al-Shabrawey M, Platt DH, Liou GI, Caldwell RW. Vascular endothelial growth factor and diabetic retinopathy: role of oxidative stress. Curr Drug Targets. 2005 Jun; 6 (4):511-24.

Campbell M, Humphries M, Kenna P, Humphries P, Brankin B. Altered expression and interaction of adherens junction proteins in the developing OLM of the Rho(-/-) mouse. Exp Eye Res. 2007 Nov; 85 (5):714-20.

Campbell M, Collery R, McEvoy A, Gardiner TA, Stitt AW, Brankin B. Involvement of MAPKs in endostatin-mediated regulation of blood-retinal barrier function. Curr Eye Res. 2006 Dec; 31 (12):1033-45.

Campbell M, Humphries M, Kennan A, Kenna P, Humphries P, Brankin B. Aberrant retinal tight junction and adherens junction protein expression in an animal model of autosomal dominant Retinitis pigmentosa: the Rho(-/-) mouse. Exp Eye Res. 2006 Sep; 83 (3):484-92.

Canataroglu H, Varinli I, Ozcan AA, Canataroglu A, Doran F, Varinli S. Interleukin (IL)-6, interleukin (IL)-8 levels and cellular composition of the vitreous humor in proliferative diabetic retinopathy, proliferative vitreoretinopathy, and traumatic proliferative vitreoretinopathy. Ocul Immunol Inflamm. 2005 Sep-Oct; 13 (5):375-81.

Capaldo CT, Nusrat A. Cytokine regulation of tight junctions. Biochim Biophys Acta. 2009 Apr; 1788 (4):864-71.

Carmeliet P, Moons L, Luttun A, Vincenti V, Compernolle V, De Mol M, Wu Y, Bono F, Devy L, Beck H, Scholz D, Acker T, DiPalma T, Dewerchin M, Noel A, Stalmans I, Barra A, Blacher S, Vandendriessche T, Ponten A, Eriksson U, Plate KH, Foidart JM, Schaper W, Charnock-Jones DS, Hicklin DJ, Herbert JM, Collen D, Persico MG. Synergism between vascular endothelial growth factor and placental

growth factor contributes to angiogenesis and plasma extravasation in pathological conditions. Nat Med. 2001 May; 7 (5):575-83.

Caserta JA, Hale ML, Popoff MR, Stiles BG, McClane BA. Evidence that membrane rafts are not required for the action of Clostridium perfringens enterotoxin. Infect Immun. 2008 Dec; 76 (12):5677-85.

Chappelow AV, Kaiser PK. Neovascular age-related macular degeneration: potential therapies. Drugs. 2008; 68 (8):1029-36.

Chittchang M, Mitra AK, Johnston TP. Interplay of secondary structure and charge on the diffusion of a polypeptide through negatively charged aqueous pores. Pharm Res. 2007 Mar; 24 (3):502-11.

Citi S. The molecular organization of tight junctions. J Cell Biol. 1993 May; 121 (3):485-9.

Coers W, Vos JT, Huitema S, Dijk F, Weening JJ. Biological alterations of rat podocytes cultured under basolateral hydrostatic pressure. Pathobiology. 1996; 64 (4):222-32.

Colegio OR, Van Itallie CM, McCrea HJ, Rahner C, Anderson JM. Claudins create charge-selective channels in the paracellular pathway between epithelial cells. Am J Physiol Cell Physiol. 2002 Jul; 283 (1):C142-7.

Coleman HR, Chan CC, Ferris FL 3rd, Chew EY. Age-related macular degeneration. Lancet. 2008 Nov 22; 372 (9652):1835-45.

Conhaim RL, Eaton A, Staub NC, Heath TD. Equivalent pore estimate for the alveolar-airway barrier in isolated dog lung. J Appl Physiol. 1988 Mar; 64 (3):1134-42.

Conrad CC, Malakowsky CA, Talent J, Rong D, Lakdawala S, Gracy RW. Chemiluminescent standards for quantitative comparison of two-dimensional electrophoresis western blots. Proteomics. 2001 Mar; 1 (3):365-9.

Cotton CU, Weinstein AM, Reuss L. Osmotic water permeability of Necturus gallbladder epithelium. J Gen Physiol. 1989 Apr; 93 (4):649-79.

Coyne CB, Vanhook MK, Gambling TM, Carson JL, Boucher RC, Johnson LG. Regulation of airway tight junctions by proinflammatory cytokines. Mol Biol Cell. 2002 Sep; 13 (9):3218-34.

Crane IJ, Wallace CA, McKillop-Smith S, Forrester JV. Control of chemokine production at the blood-retina barrier. Immunology. 2000 Nov; 101 (3):426-33.

Cunha-Vaz J, Bernardes R, Lobo C. Blood-retinal barrier. Eur J Ophthalmol. 2010 Nov 11; 21 (S6):3-9.

Cunha-Vaz JG, Shakib M, Ashton N. Studies on the permeability of the blood-retinal barrier. I. On the existence, development, and site of a blood-retinal barrier. Br J Ophthalmol. 1966 Aug; 50 (8) 441-53

Curry FR. Microvascular solute and water transport. Microcirculation. 2005 Jan-Feb; 12 (1):17-31.

Dalkara D, Kolstad KD, Guerin KI, Hoffmann NV, Visel M, Klimczak RR, Schaffer DV, Flannery JG. AAV Mediated GDNF Secretion From Retinal Glia Slows Down Retinal Degeneration in a Rat Model of Retinitis Pigmentosa. Mol Ther. 2011 Apr 26

de Kozak Y, Naud MC, Bellot J, Faure JP, Hicks D. Differential tumor necrosis factor expression by resident retinal cells from experimental uveitis-susceptible and -resistant rat strains. J Neuroimmunol. 1994 Nov; 55 (1):1-9.

De Moreno MR, Smith JF, Smith RV. Silver staining of proteins in polyacrylamide gels: increased sensitivity through a combined Coomassie blue-silver stain procedure. Anal Biochem. 1985 Dec; 151 (2):466-70.

DeMaio L, Tarbell JM, Scaduto RC Jr, Gardner TW, Antonetti DA. A transmural pressure gradient induces mechanical and biological adaptive responses in endothelial cells. Am J Physiol Heart Circ Physiol. 2004 Feb; 286 (2):H731-41.

Dias JR, Rodrigues EB, Maia M, Magalhães O Jr, Penha FM, Farah ME. Cytokines in neovascular age-related macular degeneration: fundamentals of targeted combination therapy. Br J Ophthalmol. 2011 May 5;

Docchio F, Boulton M, Cubeddu R, Ramponi R, Barker PD. Age-related changes in the fluorescence of melanin and lipofuscin granules of the retinal pigment epithelium: a time-resolved fluorescence spectroscopy study. Photochem Photobiol. 1991 Aug; 54 (2):247-53.

Dörfel MJ, Huber O. Modulation of tight junction structure and function by kinases and phosphatases targeting occludin. J Biomed Biotechnol. 2012; 2012 : 807356

Duffy HS, John GR, Lee SC, Brosnan CF, Spray DC. Reciprocal regulation of the junctional proteins claudin-1 and connexin43 by interleukin-1beta in primary human fetal astrocytes. J Neurosci. 2000 Dec 1; 20 (23):RC114.

Dull RO, Yuan J, Chang YS, Tarbell J, Jain RK, Munn LL. Kinetics of placenta growth factor/vascular endothelial growth factor synergy in endothelial hydraulic conductivity and proliferation. Microvasc Res. 2001 Mar; 61 (2):203-10.

Dvoryanchikov G, Sinclair MS, Perea-Martinez I, Wang T, Chaudhari N. Inward rectifier channel, ROMK, is localized to the apical tips of glial-like cells in mouse taste buds. J Comp Neurol. 2009 Nov 10; 517 (2):spc1.

Dvoryanchikov G, Sinclair MS, Perea-Martinez I, Wang T, Chaudhari N. Inward rectifier channel, ROMK, is localized to the apical tips of glial-like cells in mouse taste buds. J Comp Neurol. 2009 Nov 1; 517 (1):1-14.

Eckert R. Gap-junctional single-channel permeability for fluorescent tracers in mammalian cell cultures. Biophys J. 2006 Jul 15; 91 (2):565-79.

Elner SG, Elner VM, Bian ZM, Lukacs NW, Kurtz RM, Strieter RM, Kunkel SL. Human retinal pigment epithelial cell interleukin-8 and monocyte chemotactic protein-1 modulation by T-lymphocyte products. Invest Ophthalmol Vis Sci. 1997 Feb; 38 (2):446-55.

Elner SG, Strieter RM, Elner VM, Rollins BJ, Del Monte MA, Kunkel SL. Monocyte chemotactic protein gene expression by cytokine-treated human retinal pigment epithelial cells. Lab Invest. 1991 Jun; 64 (6):819-25.

Elner VM, Scales W, Elner SG, Danforth J, Kunkel SL, Strieter RM. Interleukin-6 (IL-6) gene expression and secretion by cytokine-stimulated human retinal pigment epithelial cells. Exp Eye Res. 1992 Mar; 54 (3):361-8.

Enck AH, Berger UV, Yu AS. Claudin-2 is selectively expressed in proximal nephron in mouse kidney. Am J Physiol Renal Physiol. 2001 Nov; 281 (5):F966-74.

Epple HJ, Schneider T, Troeger H, Kunkel D, Allers K, Moos V, Amasheh M, Loddenkemper C, Fromm M, Zeitz M, Schulzke JD. Impairment of the intestinal barrier is evident in untreated but absent in suppressively treated HIV-infected patients. Gut. 2009 Feb; 58 (2):220-7.

Estienne V, Brisbarre N, Blanchin S, Durand-Gorde JM, Carayon P, Ruf J. An in vitro model based on cell monolayers grown on the underside of large- pore filters in bicameral chambers for studying thyrocyte-lymphocyte interactions. Am J Physiol Cell Physiol. 2004 Dec; 287 (6):C1763-8.

Ewert P, Aguilera S, Alliende C, Kwon YJ, Albornoz A, Molina C, Urzúa U, Quest AF, Olea N, Pérez P, Castro I, Barrera MJ, Romo R, Hermoso M, Leyton C, González MJ. Disruption of tight junction structure in salivary glands from Sjögren's syndrome patients is linked to proinflammatory cytokine exposure. Arthritis Rheum. 2010 May; 62 (5):1280-9.

Farrar GJ, Kenna PF, Humphries P. On the genetics of retinitis pigmentosa and on mutation-independent approaches to therapeutic intervention. EMBO J. 2002 Mar 1; 21 (5):857-64.

Feldman GJ, Mullin JM, Ryan MP. Occludin: structure, function and regulation. Adv Drug Deliv Rev. 2005 Apr 25; 57 (6):883-917.

Fernandez-Patron C, Hardy E, Sosa A, Seoane J, Castellanos L. Double staining of coomassie blue-stained polyacrylamide gels by imidazole-sodium dodecyl sulfate-zinc reverse staining: sensitive detection of coomassie blue-undetected proteins. Anal Biochem. 1995 Jan 1; 224 (1):263-9.

Findley MK, Koval M. Regulation and roles for claudin-family tight junction proteins. IUBMB Life. 2009 Apr; 61 (4):431-7.

Firth JA. Endothelial barriers: from hypothetical pores to membrane proteins. J Anat. 2002 Jun; 200 (6):541-8.

Fissell WH, Fleischman AJ, Humes HD, Roy S. Development of continuous implantable renal replacement: past and future. Transl Res. 2007 Dec; 150 (6):327-36.

Florian P, Amasheh S, Lessidrensky M, Todt I, Bloedow A, Ernst A, Fromm M, Gitter AH. Claudins in the tight junctions of stria vascularis marginal cells. Biochem Biophys Res Commun. 2003 Apr 25; 304 (1):5-10.

Frank RN. Growth factors in age-related macular degeneration: pathogenic and therapeutic implications. Ophthalmic Res. 1997; 29 (5):341-53.

Franke WW. Discovering the molecular components of intercellular junctions--a historical view. Cold Spring Harb Perspect Biol. 2009 Sep; 1 (3):a003061.

Franks WA, Limb GA, Stanford MR, Ogilvie J, Wolstencroft RA, Chignell AH, Dumonde DC. Cytokines in human intraocular inflammation. Curr Eye Res. 1992; 11 Suppl:187-91.

Fraser WD, Baines AD. Application of a fiber-matrix model to transport in renal tubules. J Gen Physiol. 1989 Nov; 94 (5):863-79.

Frey TA, Antonetti DA. Alterations to the Blood-Retinal Barrier in Diabetes: Cytokines and Reactive Oxygen Species. Antioxid Redox Signal. 2011 Feb 5.

Friedman DS, O'Colmain BJ, Muñoz B, Tomany SC, McCarty C, de Jong PT, Nemesure B, Mitchell P, Kempen J, Eye Diseases Prevalence Research Group. Prevalence of age-related macular degeneration in the United States. Arch Ophthalmol. 2004 Apr; 122 (4):564-72.

Frizzell RA, Schultz SG. Ionic conductances of extracellular shunt pathway in rabbit ileum Influence of shunt on transmural sodium transport and electrical potential differences. J Gen Physiol. 1972 Mar; 59 (3):318-46.

Fu BM, Adamson RH, Curry FE. Test of a two-pathway model for small-solute exchange across the capillary wall. Am J Physiol. 1998 Jun; 274 (6 Pt 2):H2062-73.

Fu BM, Chen B. A model for the modulation of microvessel permeability by junction strands. J Biomech Eng. 2003 Oct; 125 (5):620-7.

Funatsu H, Noma H, Mimura T, Eguchi S, Hori S. Association of vitreous inflammatory factors with diabetic macular edema. Ophthalmology. 2009 Jan; 116 (1):73-9.

Funatsu H, Yamashita H, Noma H, Mimura T, Nakamura S, Sakata K, Hori S. Aqueous humor levels of cytokines are related to vitreous levels and progression of diabetic retinopathy in diabetic patients. Graefes Arch Clin Exp Ophthalmol. 2005 Jan; 243 (1):3-8.

Furuse M. Molecular basis of the core structure of tight junctions. Cold Spring Harb Perspect Biol. 2010 Jan; 2 (1):a002907.

Furuse M. Knockout animals and natural mutations as experimental and diagnostic tool for studying tight junction functions in vivo. Biochim Biophys Acta. 2009 Apr; 1788 (4):813-9.

Furuse M, Tsukita S. Claudins in occluding junctions of humans and flies. Trends Cell Biol. 2006 Apr; 16 (4):181-8.

Furuse M, Sasaki H, Tsukita S. Manner of interaction of heterogeneous claudin species within and between tight junction strands. J Cell Biol. 1999 Nov 15; 147 (4):891-903.

Furuse M, Sasaki H, Fujimoto K, Tsukita S. A single gene product, claudin-1 or -2, reconstitutes tight junction strands and recruits occludin in fibroblasts. J Cell Biol. 1998 Oct 19; 143 (2):391-401.

Furuse M, Fujita K, Hiiragi T, Fujimoto K, Tsukita S. Claudin-1 and -2: novel integral membrane proteins localizing at tight junctions with no sequence similarity to occludin. J Cell Biol. 1998 Jun 29; 141 (7):1539-50.

Furuse M, Hirase T, Itoh M, Nagafuchi A, Yonemura S, Tsukita S, Tsukita S. Occludin: a novel integral membrane protein localizing at tight junctions. J Cell Biol. 1993 Dec; 123 (6 Pt 2):1777-88.

Gao N, Lu M, Echeverri F, Laita B, Kalabat D, Williams ME, Hevezi P, Zlotnik A, Moyer BD. Voltage-gated sodium channels in taste bud cells. BMC Neurosci. 2009 Mar 12; 10:20.

Gardner TW, Antonetti DA, Barber AJ, Lieth E, Tarbell JA. The molecular structure and function of the inner blood-retinal barrier Penn State Retina Research Group. Doc Ophthalmol. 1999; 97 (3-4):229-37.

Geisen P, McColm JR, King BM, Hartnett ME. Characterization of barrier properties and inducible VEGF expression of several types of retinal pigment epithelium in medium-term culture. Curr Eye Res. 2006 Sep; 31 (9):739-48.

Gelberg H, Healy L, Whiteley H, Miller LA, Vimr E. In vivo enzymatic removal of alpha 2-->6-linked sialic acid from the glomerular filtration barrier results in podocyte charge alteration and glomerular injury. Lab Invest. 1996 May; 74 (5):907-20.

Ghassemifar R, Lai CM, Rakoczy PE. Regulation of tight junction proteins in cultured retinal pigment epithelial cells and in VEGF overexpressing transgenic mouse retinas. Adv Exp Med Biol. 2006; 572:179-85.

González-Mariscal L, Betanzos A, Avila-Flores A. MAGUK proteins: structure and role in the tight junction. Semin Cell Dev Biol. 2000 Aug; 11 (4):315-24.

González-Mariscal L, Betanzos A, Nava P, Jaramillo BE. Tight junction proteins. Prog Biophys Mol Biol. 2003 Jan; 81 (1):1-44.

Grainger CI, Greenwell LL, Lockley DJ, Martin GP, Forbes B. Culture of Calu-3 cells at the air interface provides a representative model of the airway epithelial barrier. Pharm Res. 2006 Jul; 23 (7):1482-90.

Green KJ, Getsios S, Troyanovsky S, Godsel LM. Intercellular junction assembly, dynamics, and homeostasis. Cold Spring Harb Perspect Biol. 2010 Feb; 2 (2):a000125.

Grossniklaus HE, Miskala PH, Green WR, Bressler SB, Hawkins BS, Toth C, Wilson DJ, Bressler NM. Histopathologic and ultrastructural features of surgically excised subfoveal choroidal neovascular lesions: submacular surgery trials report no 7. Arch Ophthalmol. 2005 Jul; 123 (7):914-21.

Grossniklaus HE, Ling JX, Wallace TM, Dithmar S, Lawson DH, Cohen C, Elner VM, Elner SG, Sternberg P Jr. Macrophage and retinal pigment epithelium expression of angiogenic cytokines in choroidal neovascularization. Mol Vis. 2002 Apr 21; 8:119-26.

Guo P, Weinstein AM, Weinbaum S. A dual-pathway ultrastructural model for the tight junction of rat proximal tubule epithelium. Am J Physiol Renal Physiol. 2003 Aug; 285 (2):F241-57.

Gupta IR, Ryan AK. Claudins: unlocking the code to tight junction function during embryogenesis and in disease. Clin Genet. 2010 Apr; 77 (4):314-25.

Gustavsson C, Agardh E, Bengtsson B, Agardh CD. TNF-alpha is an independent serum marker for proliferative retinopathy in type 1 diabetic patients. J Diabetes Complications. 2008 Sep-Oct; 22 (5):309-16.

Hageman GS, Luthert PJ, Victor Chong NH, Johnson LV, Anderson DH, Mullins RF. An integrated hypothesis that considers drusen as biomarkers of immune-mediated processes at the RPE-Bruch's membrane interface in aging and age-related macular degeneration. Prog Retin Eye Res. 2001 Nov; 20 (6):705-32.

Hamel C. Retinitis pigmentosa. Orphanet J Rare Dis. 2006 Oct 11; 1:40.

Hamel CP. Cone rod dystrophies. Orphanet J Rare Dis. 2007 Feb 1; 2:7.

Hamman BD, Hendershot LM, Johnson AE. BiP maintains the permeability barrier of the ER membrane by sealing the lumenal end of the translocon pore before and early in translocation. Cell. 1998 Mar 20; 92 (6):747-58.

Hammes HP, Alt A, Niwa T, Clausen JT, Bretzel RG, Brownlee M, Schleicher ED. Differential accumulation of advanced glycation end products in the course of diabetic retinopathy. Diabetologia. 1999 Jun; 42 (6):728-36.

Handa JT, Verzijl N, Matsunaga H, Aotaki-Keen A, Lutty GA, te Koppele JM, Miyata T, Hjelmeland LM. Increase in the advanced glycation end product pentosidine in Bruch's membrane with age. Invest Ophthalmol Vis Sci. 1999 Mar; 40 (3):775-9.

Harada C, Mitamura Y, Harada T. The role of cytokines and trophic factors in epiretinal membranes: involvement of signal transduction in glial cells. Prog Retin Eye Res. 2006 Mar; 25 (2):149-64.

Harhaj NS, Antonetti DA. Regulation of tight junctions and loss of barrier function in pathophysiology. Int J Biochem Cell Biol. 2004 Jul; 36 (7):1206-37

Hartnett ME, Lappas A, Darland D, McColm JR, Lovejoy S, D'Amore PA. Retinal pigment epithelium and endothelial cell interaction causes retinal pigment epithelial barrier dysfunction via a soluble VEGF-dependent mechanism. Exp Eye Res. 2003 Nov; 77 (5):593-9.

He YL, Murby S, Warhurst G, Gifford L, Walker D, Ayrton J, Eastmond R, Rowland M. Species differences in size discrimination in the paracellular pathway reflected by oral bioavailability of poly(ethylene glycol) and D-peptides. J Pharm Sci. 1998 May; 87 (5):626-33.

Heller F, Florian P, Bojarski C, Richter J, Christ M, Hillenbrand B, Mankertz J, Gitter AH, Bürgel N, Fromm M, Zeitz M, Fuss I, Strober W, Schulzke JD. Interleukin-13 is the key effector Th2 cytokine in ulcerative colitis that affects epithelial tight junctions, apoptosis, and cell restitution. Gastroenterology. 2005 Aug; 129 (2):550-64.

Heller F, Fromm A, Gitter AH, Mankertz J, Schulzke JD. Epithelial apoptosis is a prominent feature of the epithelial barrier disturbance in intestinal inflammation: effect of pro-inflammatory interleukin-13 on epithelial cell function. Mucosal Immunol. 2008 Nov; 1 Suppl 1:S58-61.

Hering NA, Schulzke JD. Therapeutic options to modulate barrier defects in inflammatory bowel disease. Dig Dis. 2009; 27 (4):450-4.

Hervé JC, Bourmeyster N, Sarrouilhe D. Diversity in protein-protein interactions of connexins: emerging roles. Biochim Biophys Acta. 2004 Mar 23; 1662 (1-2):22-41.

Hicklin DJ, Ellis LM. Role of the vascular endothelial growth factor pathway in tumor growth and angiogenesis. J Clin Oncol. 2005 Feb 10; 23 (5):1011-27.

Hollborn M, Tenckhoff S, Seifert M, Köhler S, Wiedemann P, Bringmann A, Kohen L. Human retinal epithelium produces and responds to placenta growth factor. Graefes Arch Clin Exp Ophthalmol. 2006 Jun; 244 (6):732-41

Hollborn M, Kohen L, Wiedemann P, Enzmann V. The influence of pro-inflammatory cytokines on human retinal pigment epithelium cell receptors. Graefes Arch Clin Exp Ophthalmol. 2001 Apr; 239 (4):294-301

Holmes DI, Zachary I. The vascular endothelial growth factor (VEGF) family: angiogenic factors in health and disease. Genome Biol. 2005; 6 (2):209

Holtkamp GM, Kijlstra A, Peek R, de Vos AF. Retinal pigment epithelium-immune system interactions: cytokine production and cytokine-induced changes. Prog Retin Eye Res. 2001 Jan; 20 (1):29-48.

Hosoya K, Tomi M. Advances in the cell biology of transport via the inner blood-retinal barrier: establishment of cell lines and transport functions. Biol Pharm Bull. 2005 Jan; 28 (1):1-8.

Hosoya K, Tachikawa M. Inner blood-retinal barrier transporters: role of retinal drug delivery. Pharm Res. 2009 Sep; 26 (9):2055-65.

Ho TC, Yang YC, Cheng HC, Wu AC, Chen SL, Tsao YP. Pigment epithelium-derived factor protects retinal pigment epithelium from oxidant-mediated barrier dysfunction. Biochem Biophys Res Commun. 2006 Apr 7;342(2):372-8.

Humphries P, Farrar GJ, Kenna P, McWilliam P. Retinitis pigmentosa: genetic mapping in X-linked and autosomal forms of the disease. Clin Genet. 1990 Jul; 38 (1):1-13.

Humphries P, Cochet M, Krust A, Gerlinger P, Kourilsky P, Chambon P. Molecular cloning of extensive sequences of the in vitro synthesized chicken ovalbumin structural gene. Nucleic Acids Res. 1977 Jul; 4 (7):2389-406.

Ikenouchi J, Umeda K, Tsukita S, Furuse M, Tsukita S. Requirement of ZO-1 for the formation of belt-like adherens junctions during epithelial cell polarization. J Cell Biol. 2007 Mar 12; 176 (6):779-86.

Inoko A, Itoh M, Tamura A, Matsuda M, Furuse M, Tsukita S. Expression and distribution of ZO-3, a tight junction MAGUK protein, in mouse tissues. Genes Cells. 2003 Nov; 8 (11):837-45.

Irie S, Sezaki M, Kato Y. A faithful double stain of proteins in the polyacrylamide gels with Coomassie blue and silver. Anal Biochem. 1982 Nov 1; 126 (2):350-4.

Itoh M, Furuse M, Morita K, Kubota K, Saitou M, Tsukita S. Direct binding of three tight junction-associated MAGUKs, ZO-1, ZO-2, and ZO-3, with the COOH termini of claudins. J Cell Biol. 1999 Dec 13; 147 (6):1351-63.

Jentsch TJ, Stein V, Weinreich F, Zdebik AA. Molecular structure and physiological function of chloride channels. Physiol Rev. 2002 Apr; 82 (2):503-68.

Jin M, Barron E, He S, Ryan SJ, Hinton DR. Regulation of RPE intercellular junction integrity and function by hepatocyte growth factor. Invest Ophthalmol Vis Sci. 2002 Aug; 43 (8):2782-90.

Joussen AM, Poulaki V, Mitsiades N, Kirchhof B, Koizumi K, Döhmen S, Adamis AP. Nonsteroidal anti-inflammatory drugs prevent early diabetic retinopathy via TNF-alpha suppression. FASEB J. 2002 Mar; 16 (3):438-40.

Kannan R, Zhang N, Sreekumar PG, Spee CK, Rodriguez A, Barron E, Hinton DR. Stimulation of apical and basolateral VEGF-A and VEGF-C secretion by oxidative stress in polarized retinal pigment epithelial cells. Mol Vis. 2006 Dec 22; 12:1649-59.

Karim R, Tang B. Use of antivascular endothelial growth factor for diabetic macular edema. Clin Ophthalmol. 2010 May 25; 4:493-517.

Katoh M, Katoh M. CLDN23 gene, frequently down-regulated in intestinal-type gastric cancer, is a novel member of CLAUDIN gene family. Int J Mol Med. 2003 Jun; 11 (6):683-9.

Kauffmann DJ, van Meurs JC, Mertens DA, Peperkamp E, Master C, Gerritsen ME. Cytokines in vitreous humor: interleukin-6 is elevated in proliferative vitreoretinopathy. Invest Ophthalmol Vis Sci. 1994 Mar; 35 (3):900-6.

Kaur C, Foulds WS, Ling EA. Blood-retinal barrier in hypoxic ischaemic conditions: basic concepts, clinical features and management. Prog Retin Eye Res. 2008 Nov; 27 (6):622-47.

Kevany BM, Palczewski K. Phagocytosis of retinal rod and cone photoreceptors. Physiology (Bethesda). 2010 Feb; 25 (1):8-15.

Kevil CG, Payne DK, Mire E, Alexander JS. Vascular permeability factor/vascular endothelial cell growth factor-mediated permeability occurs through disorganization of endothelial junctional proteins. J Biol Chem. 1998 Jun 12; 273 (24):15099-103.

Klein R, Knudtson MD, Lee KE, Gangnon R, Klein BE. The Wisconsin Epidemiologic Study of Diabetic Retinopathy XXIII: the twenty-five-year incidence of macular edema in persons with type 1 diabetes. Ophthalmology. 2009 Mar; 116 (3):497-503.

Klein R, Peto T, Bird A, Vannewkirk MR. The epidemiology of age-related macular degeneration. Am J Ophthalmol. 2004 Mar; 137 (3):486-95.

Kociok N, Heppekausen H, Schraermeyer U, Esser P, Thumann G, Grisanti S, Heimann K. The mRNA expression of cytokines and their receptors in cultured iris pigment epithelial cells: a comparison with retinal pigment epithelial cells. Exp Eye Res. 1998 Aug; 67 (2):237-50.

Kojima S, Yamada T, Tamai M. Quantitative analysis of interleukin-6 in vitreous from patients with proliferative vitreoretinal diseases. Jpn J Ophthalmol. 2001 Jan-Feb; 45 (1):40-5.

Kowalczuk L, Touchard E, Omri S, Jonet L, Klein C, Valamanes F, Berdugo M, Bigey P, Massin P, Jeanny JC, Behar-Cohen F. Placental growth factor contributes to

micro-vascular abnormalization and blood-retinal barrier breakdown in diabetic retinopathy. PLoS One. 2011 Mar 7; 6 (3):e17462.

Krause G, Winkler L, Piehl C, Blasig I, Piontek J, Müller SL. Structure and function of extracellular claudin domains. Ann N Y Acad Sci. 2009 May; 1165:34-43.

Kurien BT, Scofield RH. A brief review of other notable protein detection methods on blots. Methods Mol Biol. 2009; 536:557-71.

Lal-Nag M, Morin PJ. The claudins. Genome Biol. 2009; 10 (8):235.

Leung KW, Barnstable CJ, Tombran-Tink J. Bacterial endotoxin activates retinal pigment epithelial cells and induces their degeneration through IL-6 and IL-8 autocrine signaling. Mol Immunol. 2009 Apr; 46(7):1374-86.

Li J, Ananthapanyasut W, Yu AS. Claudins in renal physiology and disease. Pediatr Nephrol. 2011 Mar 2

Limb GA, Chignell AH, Green W, LeRoy F, Dumonde DC. Distribution of TNF alpha and its reactive vascular adhesion molecules in fibrovascular membranes of proliferative diabetic retinopathy. Br J Ophthalmol. 1996 Feb; 80 (2):168-73.

Lopez PF, Grossniklaus HE, Lambert HM, Aaberg TM, Capone A Jr, Sternberg P Jr, L'Hernault N. Pathologic features of surgically excised subretinal neovascular membranes in age-related macular degeneration. Am J Ophthalmol. 1991 Dec 15; 112 (6):647-56.

Lu M, Kuroki M, Amano S, Tolentino M, Keough K, Kim I, Bucala R, Adamis AP. Advanced glycation end products increase retinal vascular endothelial growth factor expression. J Clin Invest. 1998 Mar 15; 101 (6):1219-24.

Luche S, Diemer H, Tastet C, Chevallet M, Van Dorsselaer A, Leize-Wagner E, Rabilloud T. About thiol derivatization and resolution of basic proteins in two-dimensional electrophoresis. Proteomics. 2004 Mar; 4 (3):551-61

Ma JX, Zhang SX, Wang JJ. Down-regulation of angiogenic inhibitors: a potential pathogenic mechanism for diabetic complications. Curr Diabetes Rev. 2005 May; 1 (2):183-96.

MacPhee DJ. Methodological considerations for improving Western blot analysis. J Pharmacol Toxicol. Methods. 2010 Mar-Apr; 61 (2):171-7.

Mark KS, Davis TP. Cerebral microvascular changes in permeability and tight junctions induced by hypoxia-reoxygenation. Am J Physiol Heart Circ Physiol. 2002 Apr; 282(4):H1485-94.

Mazzon E, Cuzzocrea S. Role of TNF-alpha in ileum tight junction alteration in mouse model of restraint stress. Am J Physiol Gastrointest Liver Physiol. 2008 May; 294 (5):G1268-80.

McCarthy KM, Skare IB, Stankewich MC, Furuse M, Tsukita S, Rogers RA, Lynch RD, Schneeberger EE. Occludin is a functional component of the tight junction. J Cell Sci. 1996 Sep; 109 (Pt 9):2287-98.

McNeil E, Capaldo CT, Macara IG. Zonula occludens-1 function in the assembly of tight junctions in Madin-Darby canine kidney epithelial cells. Mol Biol Cell. 2006 Apr; 17 (4):1922-32.

Medina R, Rahner C, Mitic LL, Anderson JM, Van Itallie CM. Occludin localization at the tight junction requires the second extracellular loop. J Membr Biol. 2000 Dec 1; 178 (3):235-47.

Meng W, Takeichi M. Adherens junction: molecular architecture and regulation. Cold Spring Harb Perspect Biol. 2009 Dec; 1 (6):a002899

Michlig S, Damak S, Le Coutre J. Claudin-based permeability barriers in taste buds. J Comp Neurol. 2007 Jun 20; 502 (6):1003-11.

Milatz S, Krug SM, Rosenthal R, Günzel D, Müller D, Schulzke JD, Amasheh S, Fromm M. Claudin-3 acts as a sealing component of the tight junction for ions of either charge and uncharged solutes. Biochim Biophys Acta. 2010 Nov; 1798 (11):2048-57.

Missotten, T., Baarsma, G., Vingerling, J., Martinez-Ciriano, J. and Van Hagen, P. (2007), Anti-TNF-alpha therapy for exudative ARMD. Acta Ophthalmologica Scandinavica, 85: 0. doi: 10.1111/j.1600-0420.2007.01063_3446.x

Mitamura Y, Harada C, Harada T. Role of cytokines and trophic factors in the pathogenesis of diabetic retinopathy. Curr Diabetes Rev. 2005 Feb; 1 (1):73-81.

Mitamura Y, Tashimo A, Nakamura Y, Tagawa H, Ohtsuka K, Mizue Y, Nishihira J. Vitreous levels of placenta growth factor and vascular endothelial growth factor in patients with proliferative diabetic retinopathy. Diabetes Care. 2002 Dec; 25 (12):2352.

Mitic LL, Anderson JM. Molecular architecture of tight junctions. Annu Rev Physiol. 1998; 60:121-42.

Mitic LL, Unger VM, Anderson JM. Expression, solubilization, and biochemical characterization of the tight junction transmembrane protein claudin-4. Protein Sci. 2003 Feb; 12 (2):218-27.

Miyamoto N, de Kozak Y, Normand N, Courtois Y, Jeanny JC, Benezra D, Behar-Cohen F. PlGF-1 and VEGFR-1 pathway regulation of the external epithelial hemato-ocular barrier A model for retinal edema. Ophthalmic Res. 2008; 40 (3-4):203-7.

Nagineni CN, Kommineni VK, William A, Detrick B, Hooks JJ. Regulation of VEGF expression in human retinal cells by cytokines: implications for the role of inflammation in age-related macular degeneration. J Cell Physiol. 2011 Mar 3

Nandrot EF, Kim Y, Brodie SE, Huang X, Sheppard D, Finnemann SC. Loss of synchronized retinal phagocytosis and age-related blindness in mice lacking alphavbeta5 integrin. J Exp Med. 2004 Dec 20; 200 (12):1539-45.

Noguchi M, Furuya S, Takeuchi T, Hirohashi S. Modified formalin and methanol fixation methods for molecular biological and morphological analyses. Pathol Int. 1997 Oct; 47 (10):685-91.

Oh H, Takagi H, Takagi C, Suzuma K, Otani A, Ishida K, Matsumura M, Ogura Y, Honda Y. The potential angiogenic role of macrophages in the formation of choroidal neovascular membranes. Invest Ophthalmol Vis Sci. 1999 Aug; 40 (9):1891-8.

Ohno-Matsui K, Yoshida T, Uetama T, Mochizuki M, Morita I. Vascular endothelial growth factor upregulates pigment epithelium-derived factor expression via VEGFR-1 in human retinal pigment epithelial cells. Biochem Biophys Res Commun. 2003 Apr 11; 303 (3):962-7.

Okamoto T, Yamagishi S, Inagaki Y, Amano S, Koga K, Abe R, Takeuchi M, Ohno S, Yoshimura A, Makita Z. Angiogenesis induced by advanced glycation end products and its prevention by cerivastatin. FASEB J. 2002 Dec; 16 (14):1928-30.

Overgaard CE, Daugherty BL, Mitchell LA, Koval M. Claudins: Control of Barrier Function and Regulation in Response to Oxidant Stress. Antioxid Redox Signal. 2011 May 9

Padden M, Leech S, craig B, Kirk J, Brankin B, McQuaid S. 2007. Differences in expression of junctional adhesion molecule-A and beta-catenin in multiple sclerosis brain tissue:increasing evidence for the role of tight junction pathology. Acta Neuropathol. 113(2):177-86.

Park JE, Chen HH, Winer J, Houck KA, Ferrara N. Placenta growth factor Potentiation of vascular endothelial growth factor bioactivity, in vitro and in vivo, and high affinity binding to Flt-1 but not to Flk-1/KDR. J Biol Chem. 1994 Oct 14; 269 (41):25646-54.

Patel JI, Saleh GM, Hykin PG, Gregor ZJ, Cree IA. Concentration of haemodynamic and inflammatory related cytokines in diabetic retinopathy. Eye (Lond). 2008 Feb; 22 (2):223-8.

Patel M, Chan CC. Immunopathological aspects of age-related macular degeneration. Semin Immunopathol. 2008 Apr; 30 (2):97-110.

Penfold PL, Wen L, Madigan MC, King NJ, Provis JM. Modulation of permeability and adhesion molecule expression by human choroidal endothelial cells. Invest Ophthalmol Vis Sci. 2002 Sep; 43 (9):3125-30.

Pournaras CJ, Rungger-Brändle E, Riva CE, Hardarson SH, Stefansson E. Regulation of retinal blood flow in health and disease. Prog Retin Eye Res. 2008 May; 27 (3):284-330.

Reddy VM, Zamora RL, Olk RJ. Quantitation of retinal ablation in proliferative diabetic retinopathy. Am J Ophthalmol. 1995 Jun; 119 (6):760-6.

Rizzolo LJ, Chen X, Weitzman M, Sun R, Zhang H. Analysis of the RPE transcriptome reveals dynamic changes during the development of the outer blood-retinal barrier. Mol Vis. 2007 Jul 23; 13:1259-73 (a).

Rizzolo LJ. Development and role of tight junctions in the retinal pigment epithelium. Int Rev Cytol. 2007; 258:195-234 (b).

Rosenthal R, Milatz S, Krug SM, Oelrich B, Schulzke JD, Amasheh S, Günzel D, Fromm M. Claudin-2, a component of the tight junction, forms a paracellular water channel. J Cell Sci. 2010 Jun 1; 123 (Pt 11):1913-21.

Rowland TJ, Buchholz DE, Clegg DO. Pluripotent human stem cells for the treatment of retinal disease. J Cell Physiol. 2011 Apr 25

Rozlomiy VL, Markov AG. Effect of interleukin-1β on the expression of tight junction proteins in the culture of HaCaT keratinocytes. Bull Exp Biol Med. 2010 Sep; 149 (3):280-3.

Sahel J, Bonnel S, Mrejen S, Paques M. Retinitis pigmentosa and other dystrophies. Dev Ophthalmol. 2010; 47:160-7.

Saitou M, Furuse M, Sasaki H, Schulzke JD, Fromm M, Takano H, Noda T, Tsukita S. Complex phenotype of mice lacking occludin, a component of tight junction strands. Mol Biol Cell. 2000 Dec; 11 (12):4131-42.

Saitou M, Fujimoto K, Doi Y, Itoh M, Fujimoto T, Furuse M, Takano H, Noda T, Tsukita S. Occludin-deficient embryonic stem cells can differentiate into polarized epithelial cells bearing tight junctions. J Cell Biol. 1998 Apr 20; 141 (2):397-408.

Schnaudigel O.V. Graefes Arch. Ophthalmol. (1913) 86, 93—105.

Schulzke JD, Gitter AH, Mankertz J, Spiegel S, Seidler U, Amasheh S, Saitou M, Tsukita S, Fromm M. Epithelial transport and barrier function in occludin-deficient mice. Biochim Biophys Acta. 2005 May 15; 1669 (1):34-42.

Seeliger MW, Biesalski HK, Wissinger B, Gollnick H, Gielen S, Frank J, Beck S, Zrenner E. Phenotype in retinol deficiency due to a hereditary defect in retinol binding protein synthesis. Invest Ophthalmol Vis Sci. 1999 Jan; 40 (1):3-11.

Shams N, Ianchulev T. Role of vascular endothelial growth factor in ocular angiogenesis. Ophthalmol Clin North Am. 2006 Sep; 19 (3):335-44

Shapiro L, Weis WI. Structure and biochemistry of cadherins and catenins. Cold Spring Harb Perspect Biol. 2009 Sep; 1 (3):a003053

Shi G, Maminishkis A, Banzon T, Jalickee S, Li R, Hammer J, Miller SS. Control of chemokine gradients by the retinal pigment epithelium. Invest Ophthalmol Vis Sci. 2008 Oct; 49 (10):4620-30.

Shin K, Margolis B. ZOning out tight junctions. Cell. 2006 Aug 25; 126 (4):647-9.

Simon DB, Lu Y, Choate KA, Velazquez H, Al-Sabban E, Praga M, Casari G, Bettinelli A, Colussi G, Rodriguez-Soriano J, McCredie D, Milford D, Sanjad S, Lifton RP. Paracellin-1, a renal tight junction protein required for paracellular Mg2+ resorption. Science. 1999 Jul 2; 285 (5424):103-6.

Steed E, Balda MS, Matter K. Dynamics and functions of tight junctions. Trends Cell Biol. 2010 Mar; 20 (3):142-9.

Stitt AW, Li YM, Gardiner TA, Bucala R, Archer DB, Vlassara H. Advanced glycation end products (AGEs) co-localize with AGE receptors in the retinal vasculature of diabetic and of AGE-infused rats. Am J Pathol. 1997 Feb; 150 (2):523-31.

Stitt AW. The role of advanced glycation in the pathogenesis of diabetic retinopathy. Exp Mol Pathol. 2003 Aug; 75 (1):95-108.

Strauss O. The retinal pigment epithelium in visual function. Physiol Rev. 2005 Jul; 85 (3):845-81.

Strunnikova NV, Maminishkis A, Barb JJ, Wang F, Zhi C, Sergeev Y, Chen W, Edwards AO, Stambolian D, Abecasis G, Swaroop A, Munson PJ, Miller SS. Transcriptome analysis and molecular signature of human retinal pigment epithelium. Hum Mol Genet. 2010 Jun 15; 19 (12):2468-86.

Takeuchi M, Takino J, Yamagishi S. Involvement of TAGE-RAGE System in the Pathogenesis of Diabetic Retinopathy. J Ophthalmol. 2010; 2010:170393.

Tanihara H, Yoshida M, Yoshimura N. Tumor necrosis factor-alpha gene is expressed in stimulated retinal pigment epithelial cells in culture. Biochem Biophys Res Commun. 1992 Sep 16; 187 (2):1029-34.

Tsukita S, Katsuno T, Yamazaki Y, Umeda K, Tamura A, Tsukita S. Roles of ZO-1 and ZO-2 in establishment of the belt-like adherens and tight junctions with paracellular permselective barrier function. Ann N Y Acad Sci. 2009 May; 1165:44-52.

Tsukita S, Furuse M, Itoh M. Molecular architecture of tight junctions: occludin and ZO-1. Soc Gen Physiol Ser. 1997; 52:69-76.

Tsukita S, Furuse M. Occludin and claudins in tight-junction strands: leading or supporting players?. Trends Cell Biol. 1999 Jul; 9 (7):268-73.

Tsukita S, Furuse M, Itoh M. Multifunctional strands in tight junctions. Nat Rev Mol Cell Biol. 2001 Apr; 2 (4):285-93.

Tsukita S, Furuse M. The structure and function of claudins, cell adhesion molecules at tight junctions. Ann N Y Acad Sci. 2000; 915:129-35.

Tsukita S, Furuse M. Overcoming barriers in the study of tight junction functions: from occludin to claudin. Genes Cells. 1998 Sep; 3 (9):569-73.

Turksen K, Troy TC. Junctions gone bad: Claudins and loss of the barrier in cancer. Biochim Biophys Acta. 2011 Apr 15

Turksen K, Troy TC. Barriers built on claudins. J Cell Sci. 2004 May 15; 117 (Pt 12):2435-47.

Umeda K, Ikenouchi J, Katahira-Tayama S, Furuse K, Sasaki H, Nakayama M, Matsui T, Tsukita S, Furuse M, Tsukita S. ZO-1 and ZO-2 independently determine where claudins are polymerized in tight-junction strand formation. Cell. 2006 Aug 25; 126 (4):741-54.

Umeda K, Matsui T, Nakayama M, Furuse K, Sasaki H, Furuse M, Tsukita S. Establishment and characterization of cultured epithelial cells lacking expression of ZO-1. J Biol Chem. 2004 Oct 22; 279 (43):44785-94.

Van Itallie CM, Anderson JM. Claudins and epithelial paracellular transport. Annu Rev Physiol. 2006; 68:403-29.

Van Itallie CM, Betts L, Smedley JG 3rd, McClane BA, Anderson JM. Structure of the claudin-binding domain of Clostridium perfringens enterotoxin. J Biol Chem. 2008 Jan 4; 283 (1):268-74.

Van Itallie CM, Holmes J, Bridges A, Gookin JL, Coccaro MR, Proctor W, Colegio OR, Anderson JM. The density of small tight junction pores varies among cell types and is increased by expression of claudin-2. J Cell Sci. 2008 Feb 1; 121 (Pt 3):298-305.

Van Itallie CM, Holmes J, Bridges A, Anderson JM. Claudin-2-dependent changes in noncharged solute flux are mediated by the extracellular domains and require attachment to the PDZ-scaffold. Ann N Y Acad Sci. 2009 May; 1165:82-7.

Van Itallie CM, Fanning AS, Holmes J, Anderson JM. Occludin is required for cytokine-induced regulation of tight junction barriers. J Cell Sci. 2010 Aug 15; 123 (Pt 16):2844-52.

Van Itallie CM, Fanning AS, Bridges A, Anderson JM. ZO-1 stabilizes the tight junction solute barrier through coupling to the perijunctional cytoskeleton. Mol Biol Cell. 2009 Sep; 20 (17):3930-40.

Van Itallie CM, Anderson JM. The molecular physiology of tight junction pores. Physiology (Bethesda). 2004 Dec; 19:331-8.

Van Itallie CM, Anderson JM. Occludin confers adhesiveness when expressed in fibroblasts. J Cell Sci. 1997 May; 110 (Pt 9):1113-21.

Van Itallie CM, Colegio OR, Anderson JM. The cytoplasmic tails of claudins can influence tight junction barrier properties through effects on protein stability. J Membr Biol. 2004 May 1; 199 (1):29-38.

Vinores SA, Küchle M, Derevjanik NL, Henderer JD, Mahlow J, Green WR, Campochiaro PA. Blood-retinal barrier breakdown in retinitis pigmentosa: light and electron microscopic immunolocalization. Histol Histopathol. 1995 Oct; 10 (4):913-23

Vinores SA, Derevjanik NL, Ozaki H, Okamoto N, Campochiaro PA. Cellular mechanisms of blood-retinal barrier dysfunction in macular edema. Doc Ophthalmol. 1999; 97 (3-4):217-28.

Wan L, Lin HJ, Tsai Y, Lee CC, Tsai CH, Tsai FJ, Tsai YY, Lin JM. Tumor necrosis factor-α gene polymorphisms in age-related macular degeneration. Retina. 2010 Nov-Dec; 30 (10):1595-600.

Wang Q, Chen Q, Zhao K, Wang L, Wang L, Traboulsi EI. Update on the molecular genetics of retinitis pigmentosa. Ophthalmic Genet. 2001 Sep; 22 (3):133-54.

Weber CR, Raleigh DR, Su L, Shen L, Sullivan EA, Wang Y, Turner JR. Epithelial myosin light chain kinase activation induces mucosal interleukin-13 expression to alter tight junction ion selectivity. J Biol Chem. 2010 Apr 16; 285 (16):12037-46.

Weber S, Schneider L, Peters M, Misselwitz J, Rönnefarth G, Böswald M, Bonzel KE, Seeman T, Suláková T, Kuwertz-Bröking E, Gregoric A, Palcoux JB, Tasic V, Manz F, Schärer K, Seyberth HW, Konrad M. Novel paracellin-1 mutations in 25 families with familial hypomagnesemia with hypercalciuria and nephrocalcinosis. J Am Soc Nephrol. 2001 Sep; 12 (9):1872-81.

Whitmire W, Al-Gayyar MM, Abdelsaid M, Yousufzai BK, El-Remessy AB. Alteration of growth factors and neuronal death in diabetic retinopathy: what we have learned so far. Mol Vis. 2011 Jan 28; 17:300-8.

Will C, Fromm M, Müller D. Claudin tight junction proteins: novel aspects in paracellular transport. Perit Dial Int. 2008 Nov-Dec; 28 (6):577-84.

Witmer AN, Vrensen GF, Van Noorden CJ, Schlingemann RO. Vascular endothelial growth factors and angiogenesis in eye disease. Prog Retin Eye Res. 2003 Jan; 22 (1):1-29.

Wolfensberger TJ, Gregor ZJ. Macular edema--rationale for therapy. Dev Ophthalmol. 2010; 47:49-58.

Yamada Y, Ishibashi K, Ishibashi K, Bhutto IA, Tian J, Lutty GA, Handa JT. The expression of advanced glycation endproduct receptors in rpe cells associated with basal deposits in human maculas. Exp Eye Res. 2006 May; 82 (5):840-8

Yang D, Elner SG, Bian ZM, Till GO, Petty HR, Elner VM. Pro-inflammatory cytokines increase reactive oxygen species through mitochondria and NADPH oxidase in cultured RPE cells. Exp Eye Res. 2007 Oct; 85 (4):462-72.

Yang W, Ahn H, Hinrichs M, Torry RJ, Torry DS. Evidence of a novel isoform of placenta growth factor (PlGF-4) expressed in human trophoblast and endothelial cells. J Reprod Immunol. 2003 Oct; 60 (1):53-60.

Yu AS. Molecular basis for cation selectivity in claudin-2-based pores. Ann N Y Acad Sci. 2009 May; 1165:53-7.

Yu H, Chen L, Jiang J. Administration of pigment epithelium-derived factor delivered by adeno-associated virus inhibits blood-retinal barrier breakdown in diabetic rats. Mol Vis. 2010 Nov 15;16:2384-94

Yuan X, Lin X, Manorek G, Kanatani I, Cheung LH, Rosenblum MG, Howell SB. Recombinant CPE fused to tumor necrosis factor targets human ovarian cancer cells expressing the claudin-3 and claudin-4 receptors. Mol Cancer Ther. 2009 Jul; 8 (7):1906-15.

Zeissig S, Bürgel N, Günzel D, Richter J, Mankertz J, Wahnschaffe U, Kroesen AJ, Zeitz M, Fromm M, Schulzke JD. Changes in expression and distribution of claudin 2, 5 and 8 lead to discontinuous tight junctions and barrier dysfunction in active Crohn's disease. Gut. 2007 Jan; 56 (1):61-72.

Zhou S, Bailey MJ, Dunn MJ, Preedy VR, Emery PW. A quantitative investigation into the losses of proteins at different stages of a two-dimensional gel electrophoresis procedure. Proteomics. 2005 Jul; 5 (11):2739-47.

Role of Vascular Endothelial Growth Factor, Placental Growth Factor and Cytokines on Blood Retinal Barrier function

Sukumaran S‡, Williams G‡, Ramaswamy G*, Wu B*, Brankin B‡

‡School of Biological Sciences, Dublin Institute of Technology, Dublin – 8
*School of Computing, Dublin Institute of Technology, Dublin 8

Fighting Blindness

Introduction:

The Blood Retinal Barrier (BRB) is composed of inner BRB (iBRB) and outer BRB (oBRB). The iBRB is formed by Retinal Microvascular Endothelial cells (RMEC). The Retinal Pigment Epithelium (RPE) forms the outer Blood Retinal Barrier (oBRB) and supports the function of the photoreceptor layer. The RPE layer provides a permeability barrier between the retina and the choroid. The integrity of oBRB is regulated by tight junctions in the RPE. Tight junctions act by regulating ion concentrations and water permeability. Tight junctions are formed by transmembrane protein Occludin, peripheral membrane protein Zo-1 and the Claudin family of proteins.

RPE damage may lead to degeneration of the neural retina, which occurs in the eye diseases – Retinitis Pigmentosa (RP) and Age Related Macular Degeneration (ARMD). ARMD studies have shown that drusen attract macrophages to the sub-epithelial space in the retina. Amyloid beta (Abeta) in drusen stimulates macrophages to produce Tumor Necrosis factor – alpha and Interleukin -1 beta.

We investigated the effect of growth factors – Vascular endothelial growth factor (VEGF) and Placental growth factor (PlGF), and cytokines Tumor Necrosis factor – alpha (TNF-α) and Interleukin -1 beta (IL-1β) on tight junction

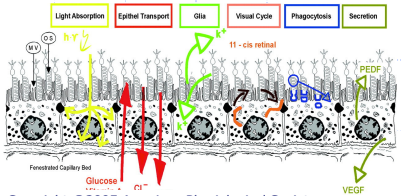

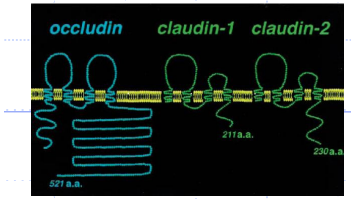

Tsukita & Furuse, 1998

Materials & Methods:

Cell culture

ARPE-19 cells were propagated in growth medium (DMEM) containing 10% bovine serum. Medium was stepped down to serum free medium, six hours prior to growth factor treatment. TNF-α and IL-1β was added at final concentrations of 1 and 10ng/ml and PlGF was added at final concentrations of 1, 10 and 100ng/ml. Untreated cells incubated in serum free medium was used as control. Cells were incubated for 24 hours, after which cells were washed 3x with PBS and harvested as required.

Western blot analysis

Confluent cell monolayer was scraped and homogenized in a cell extraction buffer containing 62.5mMTris, 2%w/v SDS, 10mMDTT, 10ul Protease inhibitor cocktail per 100ml. The homogenate was centrifuged at 14000g for 20 minutes at 4ºC. The supernatant was used for protein analysis. Equal amounts of protein was loaded to 12% SDS-PAGE gels. Proteins were separated using electrophoresis and transferred to nitrocellulose membrane for 2 hours using semi-dry blotting.

Enhanced chemiluminescence:

Post transfer, the nitrocellulose membrane was incubated in a blocking solution (5% Bovine Serum Albumin in TBS) for 2 hours. Membranes were washed quickly in TBS and incubated with the polyclonal rabbit anti-claudin2 or anti-claudin3 antibody (1:5000) overnight at 4ºC.

The membranes were washed 3x with 0.1%Tween20 in TBS and incubated with secondary anti-rabbit IgG with HRP-conjugate(1:5000) for 3 hours at room temperature. Immune complexes were detected using enhanced chemiluminescence. The film was scanned and densitometric analysis performed using Alpha Imager FC software.

Chromogenic detection:

Chromogenic detection of protein was done using Invitrogen Western-breeze Chromogenic kit – Anti mouse. Membrane blocking and wash steps were carried out as per instructions in the manual. The membrane was incubated overnight in mouse anti-occludin antibody (1:2500) at 4ºC then with the secondary antibody of mouse anti-IgG with alkaline phosphatase conjugate for 2 hours at room temperature. Final blot was scanned and densitometric analysis performed using Alpha Imager FC.

Viability assay

ARPE-19 cells were propagated in 6-well cell culture plates in 10% growth medium, until confluent. The medium was changed to serum free medium, 6 hours prior to growth factor treatment. Cells were incubated for 24 hours with growth factors as described earlier. The culture was then washed 3x with PBS and trypsinized. Trypsinisation was stopped by adding complete medium and the cells were centrifuged at 1000rpm. The pellet obtained was resuspended in 500µl DMEM. Equal amount of 0.4% Trypan Blue (Sigma Aldrich) and allowed to stand for 5 minutes. Number of viable and non-viable cells were counted under a microscope using a haemocytometer.

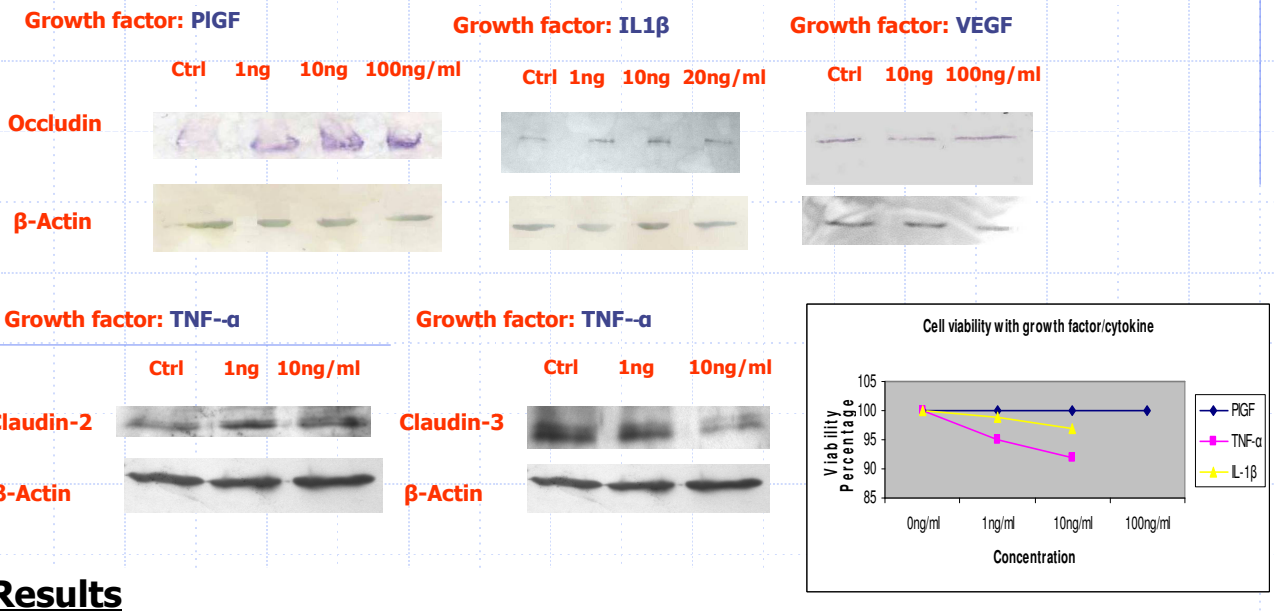

Results

Western blot analysis performed on RPE samples showed a significant increase in Occludin expression in samples treated with10ng/ml IL-1β ($P<0.05$). We found a significant upregulation of Occludin in samples treated with 10ng/ml PlGF ($P<0.05$) while VEGF did not cause a significant change in Occludin expression at concentrations of 10ng/ml and 100ng/ml ($P>0.05$).

Claudin-2 expression showed a significant increase for samples treated with 1ng/ml TNF-α ($P<0.05$). We did not find a significant change in the level of Claudin-3 for samples treated with 1ng/ml and 10ng/ml TNF-α.

Cell viability assay performed for cells treated with PlGF and VEGF for 24 hours showed no non-viable cells. Cell viability for samples treated with 1ng/ml and 10ng/ml TNF-α were found to be about 95% (57 viable out of 60cells) and 92% (40 viable out of 45cells) respectively, after 24 hours. Cells exposed to 1ng/ml and 10ng/ml IL-1β for 24 hours showed 99%(99 viable out of 100 cells) and 97% (68 viable out of 70 cells) viability respectively.

Conclusion

Placental Growth Factor and IL-1β significantly upregulates occludin expression in the RPE cells. TNF-α significantly upregulated Claudin-2 in RPE cells. There was no significant increase in either Claudin-3 or Claudin-4 expression in cells treated with TNF-α. We show a modulation of tight junction integrity by TNF-α, IL-1β and PlGF which may be of significance in retinal degeneration. Identification of intra vitreal factors that alter tight junction protein expression would be relevant in a further study of pathological conditions that induce BRB breakdown.

References

Brankin B, Campbell M, Canning P, Gardiner TA, Stitt AW., 2005. Endostatin modulates VEGF-mediated barrier dysfunction in the retinal microvascular endothelium. Exp Eye Res. 81(1):22-31

Campbell M, Humphries M, Kenna P, Humphries P, Brankin B., 2007. Altered expression and interaction of adherens junction proteins in the developing OLM of the Rho(-/-) mouse. Exp Eye Res. 85(5):714-20.

Research funded by DIT Strand 2 Scholarship & Fighting Blindness, Ireland